STRUCTURAL PROPERTIES OF AMINOSILICA MATERIALS FOR CO_2 CAPTURE

A Dissertation
Presented to
The Academic Faculty

by

Stephanie A. Didas

In Partial Fulfillment
of the Requirements for the Degree
Doctor of Philosophy in the
School of Chemical & Biomolecular Engineering

Georgia Institute of Technology
August 2014

STRUCTURAL PROPERTIES OF AMINOSILICA MATERIALS FOR CO_2 CAPTURE

Approved by:

Dr. Christopher W. Jones, Advisor
School of Chemical & Biomolecular Engineering
Georgia Institute of Technology

Dr. Ryan P. Lively
School of Chemical & Biomolecular Engineering
Georgia Institute of Technology

Dr. David S. Sholl
School of Chemical & Biomolecular Engineering
Georgia Institute of Technology

Dr. Krista S. Walton
School of Chemical & Biomolecular Engineering
Georgia Institute of Technology

Dr. Kim M. Cobb
School of Earth & Atmospheric Sciences
Georgia Institute of Technology

Date Approved: June 19, 2014

To My Family

ACKNOWLEDGEMENTS

The "graduate school experience" for me has been a time of self-discovery and growth, both academically as well as personally. There are many people who are responsible for this transformation. Some of whom I will undoubtedly overlook in this acknowledgement. Because I lack the words to truly express my feelings about these people and the impact they have made on me I will instead keep it simple and provide a list of all those to whom I would like to extend my deepest and most heartfelt thanks:

My advisor Dr. Jones

My committee members- Dr. Sholl, Dr. Walton, Dr. Lively and Dr. Cobb

Dr. Agrawal

Dr. Johannes Leisen and Dr. Leslie Gelbaum

My collaborators- Rongshun Zhu, Ambarish Kulkarni and Guo Shiou Foo

The Jones group (past and present), especially Nick Brunelli, Praveen Bollini, Miles Sakwa-Novak and Fateme Rezaei

My roommates- Katie Vermeersch, Aubrey Tiernan, Brian Setzler and Ismael Gomez

My Georgia Tech crew- Graham Wenz, Erin Redmond, Jonathan "T" Rubin, Ryan Clairmont and Justin Vaughn

And last but certainly not least, my family

Thank you all!

TABLE OF CONTENTS

LIST OF TABLES

LIST OF FIGURES

SUMMARY

Increased levels of carbon dioxide in the atmosphere are now widely attributed as a leading cause for global climate change. As such, research efforts into the capture and sequestration of CO_2 from large point sources (flue gas capture) as well as the ambient atmosphere (air capture) are gaining increased popularity and importance. Supported amine materials have emerged as a promising class of materials for these applications. However, more fundamental research is needed before these materials can be used in a practically relevant process. The following areas are considered critical research needs for these materials: (i) process design, (ii) material stability, (iii) kinetics of adsorption and desorption, (iv) improved sorbent adsorption efficiency and (v) understanding the effects of water on sorbent adsorption behaviour. The aim of the studies presented in this thesis is to further the scientific community's understanding of supported amine adsorbents with respect to stability, adsorption efficiency and adsorption behaviour with water.

The stability of primary amine functionalized silica adsorbents with differing alkyl linker length was investigated with respect to thermal, oxidative and CO_2-induced degradation to assess how differences in stability may result from different chain lengths. In conjunction with these studies, DFT calculations were used to assess CO_2 induced urea formation pathways, as well as to compare differences in stability between the varied alkyl chain lengths. Differences in stability were observed between the different materials. It was found that amine adsorbents with a methyl alkyl group between the amine and silicon atom have no thermal stability, and display a severe loss of amine

content upon heating. Adsorbents with ethyl and propyl alkyl chains demonstrated oxidative and thermal stability, but were prone to deactivation via urea formation in the presence of high concentration and high temperature, dry CO_2 for prolonged periods. A greater extent of deactivation was observed for materials with propyl alkyl chains, this was attributed to (i) the higher amine efficiency of propyl-based adsorbents compared to ethyl-based materials and (ii) the ability of propyl materials to interact with surface silanols. DFT calculations showed that the lowest energy route to urea formation was through an isocyanate intermediate, and also that amine or silanol assisted deactivation lower the energy barrier of deactivation.

A fundamental study on the adsorption properties of primary, secondary and tertiary amine materials was done to evaluate what amine type(s) are best suited for ultra-dilute CO_2 capture applications, specifically air capture. A series of comparable materials comprised of primary, secondary, or tertiary amines ligated to a mesoporous silica support via a propyl linker were used to systematically assess the role of amine type towards unary CO_2 and water adsorption. It was found that primary amines are the best candidates for CO_2 capture from air, as they possess both the highest amine efficiency for CO_2 adsorption as well as enhanced water affinity compared to other amine types.

Lastly, a study on the effect of low amounts of co-adsorbed water on CO_2 adsorption of primary amines was performed. Three materials were evaluated with amine surface coverages ranging from sub-monolayer to multi-layer. It was found that enhancement in CO_2 adsorption when co-adsorbing water was most pronounced for sub-monolayer amine adsorbents. *In-situ* FTIR suggested that one explanation for this observation could be due to a different adsorbed species in the presence of humidity for

this material. Whereas ammonium carbamate was the only species detected for humid adsorption in a material with multi-layer amine coverage, sub-monolayer materials were found to form bicarbonate at longer timescales upon contact with humid CO_2, in addition to the traditionally observed ammonium carbamate.

Overall, the results from these studies serve to further the fundamental understanding of supported amine adsorbents.

Chapter 1

AN INTRODUCTION TO SUPPORTED AMINE ADSORBENTS FOR CO_2 CAPTURE FROM FLUE GAS AND AMBIENT AIR

Parts of this chapter are adapted from 'Bollini, P.; Didas, S.A.; Jones, C.W. Amine-oxide Hybrid Materials for Acid Gas Separations. *J. Mater. Chem.* **2011**, *21*, 15100-15120.' with permission of The Royal Society of Chemistry, and from 'Bollini, P., Amine-oxide Adsorbents for Post-Combustion CO_2 Capture. *Dissertation, Georgia Institute of Technology*, **2013**.' with permission of Praveen Bollini.

1.1 Introduction & Motivation

The ever-increasing concentration of CO_2 in the atmosphere associated with fossil fuel combustion has been linked to significant global climate change over the course of the last century. As a result, a significant amount of recent research has focused on the development of materials and technologies that might be used to capture CO_2 from fossil emitting processes, especially from large point sources such as coal-fired power plants.[1,2] Additionally, there is a growing need to purify natural gas streams that contain CO_2, as many large methane reservoirs also contain vast volumes of CO_2.

For post-combustion CO_2 capture from large point sources, well-established absorption processes based on solutions of aqueous amines are considered the benchmark technology that is most likely to be widely implemented in the near future. This technology, which has been practiced commercially on various scales for a number of

years, is technologically feasible but carries with it high process costs, with the cost of regenerating the amine solution in the CO_2 stripping step being identified as a particularly expensive step. In the longer term, as a potentially lower cost option, many researchers have explored the use of solid adsorbents as potential alternatives to the use of amine solutions. An array of solid sorbents that selectively capture CO_2 from dilute gas streams are available.[3,4] These include materials that capture CO_2 via strong chemisorptive interactions and materials that weakly bind CO_2 via physisorptive interactions. Generally, the chemisorbents are more effective at adsorbing CO_2 from wet gas streams, such as flue gases as well as ultra-dilute gas streams, such as ambient air.

Among the array of available adsorbents, oxide-supported amine materials have recently emerged as a promising class of solids that can affectively adsorb CO_2 from humid gas streams at low temperature. The solids can then be regenerated using a variety of approaches, including use of a temperature swing (TSA), pressure or vacuum swing (PSA or VSA),[5] or perhaps even electric-field swing adsorption (ESA) methodologies.[6] Although oxide-supported amine materials have been used since 1992 to capture CO_2 from fluid streams, it was not until the last decade that significant activity on the design, synthesis and application of a variety of silica-supported amine materials significantly accelerated. In this chapter, a brief review is presented of the recent advances in the use of silica-supported amine materials for adsorption of CO_2 from dilute gas streams. Particular emphasis is placed on the significant research needs that exist in this still growing field. Detailed discussions of sorbent stability with respect to oxidation and urea formation, as well as air capture are avoided as they are discussed in greater detail in later chapters. At the end of this chapter, a summary of the critical research needs is presented.

1.2 Classes of Amine Adsorbent Materials

The array of silica-supported amine adsorbents has been previously categorized into three groups as shown in Figure 1.1.[5] While oxide-supported amine materials have been well-known for decades for use in chromatographic separations or for applications in catalysis, their use for the selective adsorption of CO_2 in separation applications was first reported by Tsuda in 1992.[7,8]

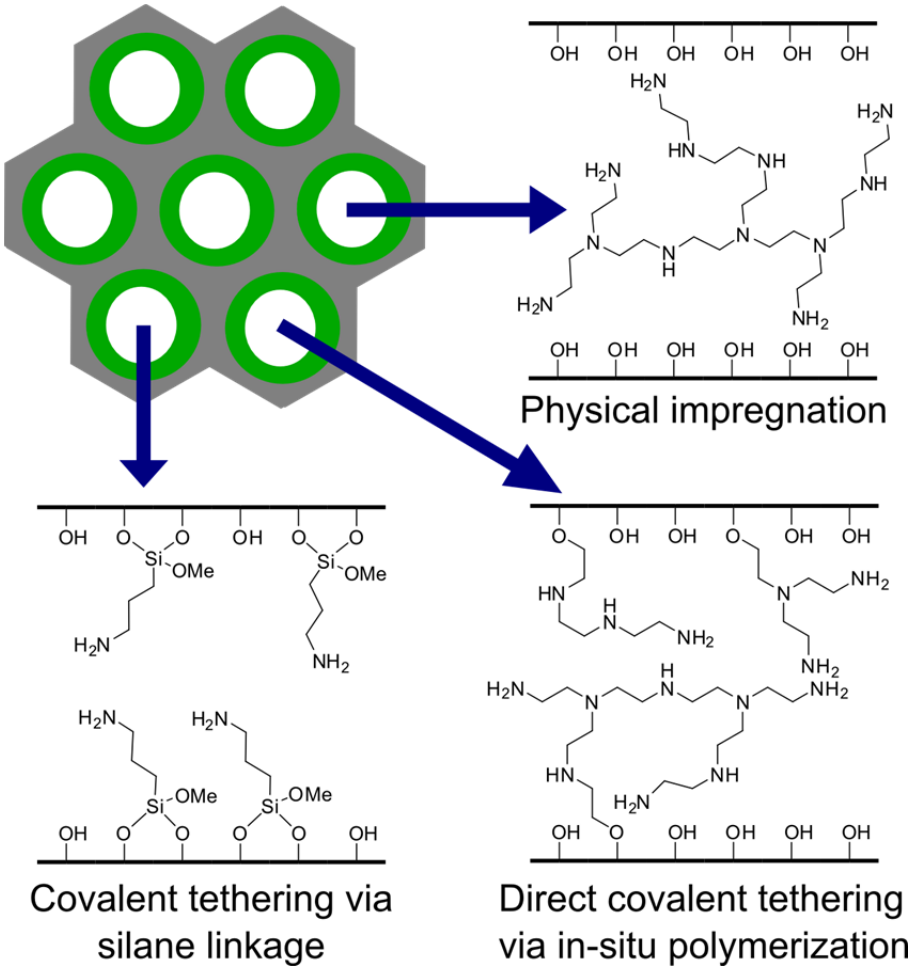

Figure 1.1. Porous silica supports can be incorporated with CO_2 adsorbing amines in three fashions: physical impregnation, covalent tethering and in situ polymerization within the pores.

Class 1 adsorbents are conceptually the easiest to prepare and may be the most practical for use on large scales in gas separation applications.[3] These materials are based on the physical combination of pre-synthesized amines and various silica supports. Typically, amine-containing polymers are used like those presented in Figure 1.2, as these have low volatility and the silica-polymer composites are more robust to a variety of treatment conditions. However, as noted below, amine-containing small molecules have also been used, including amine molecules that are well-studied in amine absorption applications. Typically, porous supports are impregnated with the amines, to give composite materials with the amines physically adsorbed onto or into the support. The introduction of this class of materials for applications in CO_2 capture was by Song in 2002,[9] and since then, numerous other groups have further explored this basic design.[9–21]

Class 2 adsorbents are based on the use of small amine-containing molecules, such as organosilanes, that can form covalent bonds to the silica support. Examples of well-studied aminosilanes include 3-aminopropyltrimethoxysilane (APS), 3-(trimethoxy-silyl)propylethylenediamine (diamine), and 3-[2-(2-aminoethylamino)ethylamino]propyl-trimethoxy-silane (triamine), yielding one two or three amine sites per molecule grafted to the silica surface. Some of the most common aminosilanes are presented in Figure 1.2. These materials have been most often prepared by grafting of the amines onto pre-formed silica supports, but they can also be prepared by co-condensation with silica sources and included within the oxide framework during the silica synthesis.[22] In the original application of this class of materials for CO_2 capture, Tsuda followed a co-condensation approach.[7,8]

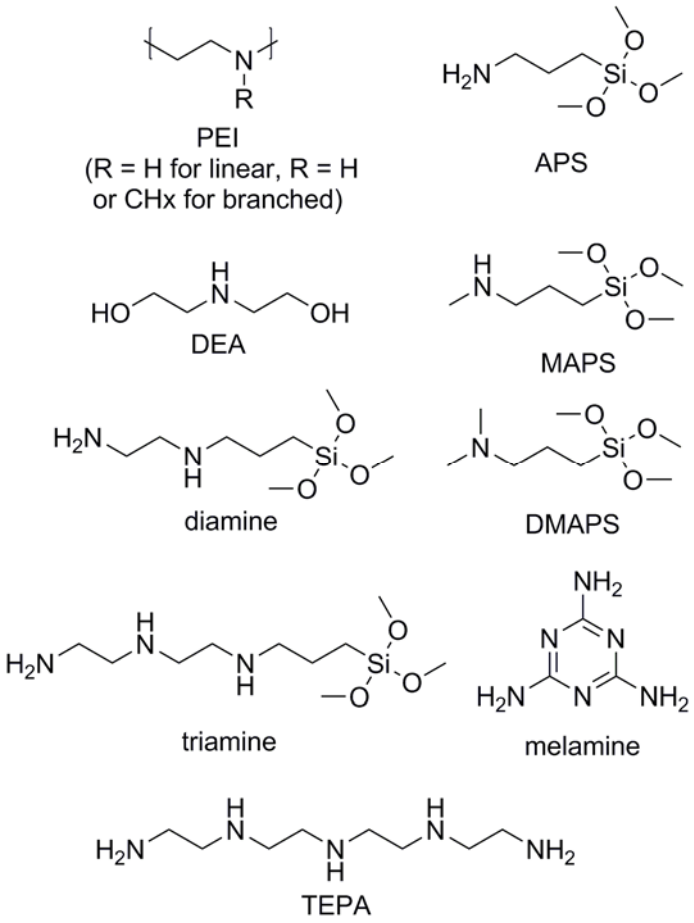

Figure 1.2. Common silanes and polymeric, amine-containing materials used for supported amine adsorbent synthesis.

The most recent class of silica-supported amine adsorbents, referred to as Class 3 adsorbents, are prepared by the in-situ polymerization of reactive amine monomers on and in the silica support. While in-situ polymerization of amine-containing monomers on porous silica supports has been reported a number of times, for example in the work of Shantz[23] and Rosenholm,[24] their application for CO_2 capture was first reported by our group in 2008.[25] Materials of this class can sometimes be considered a hybrid of class 1 and class 2 adsorbents, having the amine-silica covalent bonds of class 2 materials, and

the large site density of polymer amines commonly found in polymer-containing class 1 materials.

1.3 Adsorption of CO_2 with Supported Amine Adsorbents

Amine-oxide hybrid materials adsorb CO_2 by exploiting acid-base interactions between CO_2 and amine groups immobilized onto the external surface or within the pores of a solid material. These amines are typically primary, secondary or tertiary amines. Primary and secondary amines (including sterically hindered amines) react with CO_2 via the zwitterion mechanism, proposed by Caplow in 1968,[26] as shown in Figure 1.3. In this mechanism, an additional free base is needed, which is typically water, a hydroxyl ion or another amine. Thus, theoretically, in the absence of water, two moles of amine are required to capture one mole of CO_2 and in the presence of water only one mole of amine is required per mole of CO_2 captured. Water thus improves the amine efficiency of carbon capture, i.e. the number of moles of CO_2 adsorbed per mole of primary/secondary/sterically hindered amine.

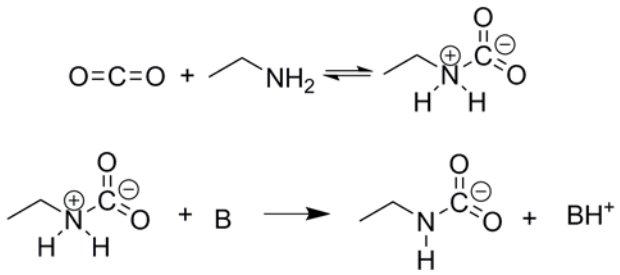

Figure 1.3. Zwitterion mechanism for CO_2 capture (valid for primary, secondary, and sterically hindered amines) in solution.

Tertiary amines capture CO_2 through a different mechanism, as shown in Figure 1.4. This mechanism was first proposed by Donaldson and co-workers in 1980.[27] This reaction mechanism is accessible to primary and secondary amines as well but the rate constants for this base catalyzed bicarbonate formation are typically smaller than those of the zwitterion mechanism described above. From the adsorption mechanism it can be noted that CO_2 capture by tertiary amines requires water, and under dry conditions supported amine adsorbents based on tertiary amines are not highly effective. Also note that the reaction mechanisms described above are based on mechanistic studies performed on CO_2 capture by aqueous amines.[26–28] Differences between the mechanism in solution versus on a solid surface, if any, are not well understood.

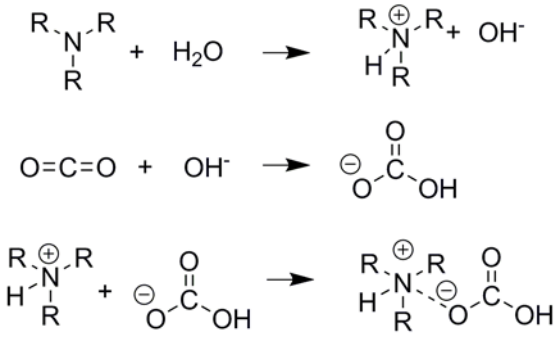

Figure 1.4. Mechanism for reaction of tertiary amines with CO_2 based on solution studies.

These adsorbents could potentially be used in a full-scale carbon capture process in a variety of configurations. Conventional packed bed configurations are routinely used for testing sorbents on the laboratory scale.[25,29] However, this configuration is not likely to be easily scalable for these materials due to the high heats of adsorption of CO_2 on amines and the intrinsic difficulty in managing heat transfer in packed bed reactors.

Potential commercial deployment configurations include fluidized-bed systems,[30–32] hollow fiber sorbents,[33–35] and monoliths.[36–38]

Regardless of the contactor configuration in which an adsorbent is used, it will be evaluated based on certain performance criteria. For an ultra-large-scale separation process like carbon capture from flue gas, these criteria include a large CO_2 adsorption capacity, rapid adsorption and desorption kinetics, selective adsorption of CO_2 over other flue gas components, and stability under a range of practical operating conditions. The criteria for a large-scale air capture process would be similar to that of flue gas capture without the restriction of ultra-fast adsorption kinetics since operating times can be longer. However, an additional constraint to consider for this process is the need for a process configuration that allows for the movement of massive amounts of gas volume with low pressure drop, without the aid of natural draft that is found in flue gas stacks.[39] Therefore, before being implemented in any type of full-scale carbon capture application, adsorbents must be evaluated based on the aforementioned criteria. In this as well as the next several sections, these performance metrics will be discussed in the context of amine-oxide hybrid materials for CO_2 capture.

1.3.1 CO_2 Adsorption Capacities

The CO_2 adsorption capacity is a measure of an adsorbent's potential to adsorb CO_2 and refers to the number of moles of carbon dioxide that a unit mass of an adsorbent is capable of adsorbing under (typically) equilibrium conditions. Adsorption capacities are dependent on both the partial pressure of CO_2 in the analysis gas and the temperature of operation and one must make sure that different materials are compared at the same temperature and CO_2 partial pressure. Furthermore, while some authors report

equilibrium capacities, other report working capacities after a specified adsorption time, capacities that do not represent a thermodynamic equilibrium.

In general, in the absence of transport limitations, the adsorption capacity should track approximately linearly with the number of amine sites present in the adsorbent under the partial pressure conditions typical of flue gas (P_{CO2} < 0.2 bar). As shown by Sayari and others,[40–43] at CO_2 partial pressures greater than 0.2 bar, this effect is complicated by the significant contribution of physisorption on the bare oxide surface. As more amine-containing organic functional groups are incorporated into the solid, this should thus increase the chemisorption capacity but decrease the physisorption capacity, which is associated with the bare silica surface. As expected, in the case of class 1 materials, it has been observed that the more polymer there is impregnated into the pores of the support, the higher the CO_2 adsorption capacity.[11,44] However, once the pores are filled, extra amine polymer deposits on the outer surface, giving a diffusion-inhibiting surface layer that slows adsorption kinetics and can reduce adsorption capacities.[9,16,45] The highest CO_2 adsorption capacity reported for class 1 materials is from Qi et al.[46] The TEPA impregnated mesoporous silica capsules in that study exhibited CO_2 adsorption capacities up to 7.9 mmol CO_2 g adsorbent^{-1}. The material was measured at 75°C using pre-humidified 10% CO_2 in argon as the test gas.

Apart from adsorption capacity, amine efficiency is another metric that can be used to assess CO_2 capture performance. The amine efficiency of an adsorbent is defined as the number of moles of carbon dioxide adsorbed per mole of amine functional groups and is expressed as a fraction. It is a measure of the fraction of amine groups present in an adsorbent that may actively participate in adsorbing CO_2 by chemisorption and was

first introduced into the literature by Yogo and co-workers who noted that water vapor had a favorable effect on the amine efficiency.[47] Note that the theoretical maximum value for amine efficiency under dry conditions is 50%, in the absence of significant physisorption at non-amine sites.

As described in a previous review,[3] adsorption isotherms of class 1 adsorbents show a plateau after a CO_2 partial pressure of 0.3 bar and a very high slope at low partial pressures, thus demonstrating significant promise as materials for CO_2 capture at low partial pressures (both capture from flue gas as well as direct capture of CO_2 from ambient air).[39] It is important to note that even though class 1 materials exhibit some of the highest CO_2 adsorption capacities reported in the literature, they sometimes have kinetic, stability and regenerability issues, as discussed in section 1.5.

Class 2 materials differ from class 1 materials in that there is an upper bound on the number of CO_2 capturing amine groups that can be present per unit mass of the adsorbent in the absence of silane polymerization (which better fills the support pores). This is because a monolayer or less of amine sites is prepared under most grafting and co-condensation syntheses. Therefore, the density of amine sites is directly related to the accessible surface area, unlike in the case of class 1 adsorbents, where support pore volumes dictate the maximum achievable amine loading for a given aminopolymer. On the other hand, because the formation of only a monolayer of sites on typical mesoporous silica supports occurs, class 2 materials tend to have more open porosity compared to class 1 and class 3 adsorbents, resulting in fewer diffusion limitations and potentially faster adsorption and desorption kinetics. Sayari and co-workers demonstrated that the limitation on the amine loading can be overcome partly by prehydrating the silica surface

by adding a small quantity of water to the reaction mixture prior to adding the silane coupling agent.[48] The presence of water molecules in the pores results in surface polymerization of aminosilanes, thus yielding much higher amine loadings than on previously reported class 2 materials, the highest being 8 mmol N/g silica. The optimally grafted material they developed showed a CO_2 capture capacity of 2.65 mmol g^{-1} at 25°C at a CO_2 partial pressure of 0.05 bar under dry adsorption conditions. Appropriate synthesis conditions can allow for significant amine loadings along with good residual sorbent porosity in class 2 materials.

Class 3 materials can combine the high CO_2 adsorption capacities of class 1 materials with the regenerative stability of class 2 materials. Our group was the first to report the application of these class of materials for the separation of CO_2 from flue gas.[25] Hyperbranched aminosilica (HAS) adsorbents were synthesized by the in-situ polymerization of aziridine molecules on and in a mesoporous SBA-15 silica support. The original HAS material, with an adsorption capacity of 3.1 mmol g^{-1}, exhibited almost ten times the adsorption capacity of a simple class 2 material synthesized on the same silica support. Further investigations into the structure and performance of these HAS materials revealed that during the functionalization of the SBA-15 silica support, polymerization of aziridine at the pore mouths occurred below a critical pore diameter of 5 nm, resulting in pore blockages.[29] Using supports with larger pore diameters was identified as a possible alternative to avoid these pore blocking effects, however high amine loadings could not be achieved with the more porous supports.[49] The HAS materials are promising candidates for CO_2 capture, based on CO_2 adsorption capacities, kinetics and selectivities. Nevertheless, more work is required to thoroughly understand

the synthesis of these materials and to be able to exercise control over the location and size of the polymer chains.

Overall, achieving high CO_2 capacity with hybrid aminosilica materials is best achieved developing material architectures that can allow for a large loading of highly accessible amine groups. For class 1 materials based on amine polymers, this generally implies large pore volumes. For class 2 materials, it appears that large surface areas are critical, in the absence of silane polymerization, as the grafting surface area dictates the overall amine loading. For class 3 materials, the critical role of porosity is not yet fully elucidated.

1.3.2 CO_2 Selectivity

For any adsorbent, to be considered a candidate for CO_2 separation it needs to be capable of adsorbing CO_2 selectively over all the other major components of the gas being processed. In the case of flue gas and air capture, these components are nitrogen, water vapor and oxygen. Amine-functionalized oxide materials selectively adsorb CO_2 over both oxygen and nitrogen, as demonstrated in a number of publications.[42,48,50] This is not surprising, as this is what nearly all nanoporous materials do,[51] but the CO_2-selective amines allow for exceptionally high selectivities. Also, as explained above, water improves the amine efficiency of CO_2 capture. The high selectivity of CO_2 over all the major components of flue gas combined with the promotion of amine efficiency due to the presence of water represents a major advantage for supported amine adsorbents over physisorbents like zeolite 13X, that do not have high enough selectivities for CO_2 over the other gas components such as water.[52] Other components of flue gas present at much lower concentrations, such as SO_x and NO_x, can adsorb strongly on supported

amine materials, as discussed below in section 1.5. Therefore, the flue gas stream will require significant scrubbing to lower the concentration of these contaminants to a level that makes the amine adsorbents stable for a sufficient number of cycles. Such gas clean-up is also required for the benchmark amine solution technology, which is already well established.

1.3.3 CO_2 Adsorption Kinetics

In a large scale carbon capture process adsorption cycles will likely be on the order of minutes for flue gas capture and 30 minutes for air capture. Therefore rates of adsorption are critical to process economics. These rates determine the amount of adsorbent a process requires and hence, the size of the equipment for the CO_2 capture process. Although there has been a tremendous number of studies measuring the equilibrium CO_2 adsorption capacities of oxide-supported amine materials,[3] providing valuable thermodynamic properties of the synthesized material, there has been very little work towards developing a quantitative understanding of the kinetics of CO_2 adsorption and desorption for silica-supported amine materials.

In a first-of-its-kind effort to study the kinetics of aminosilica adsorbents, Serna-Guerrero et al.[53] modeled breakthrough curves of a silica supported class 2 material using three different kinetic models: a pseudo-first order model, a pseudo-second order model and a fractional order kinetic model (Avrami's model). Of the three models used, Avrami's kinetic model applied with a fractional order of 1.4 was found to give the best fit with the experimental data, which indicates that a complex adsorption and transport mechanism was present. The major limiting assumption in this study was that the entire packed bed adsorption process was isothermal. This assumption, while reasonable in a

first study, likely does not hold in the case of a highly exothermic chemisorption processes like CO_2 reacting with amines. A later study from our group incorporated heat effects into the modelling of a combined breakthrough and modelling study for supported amine adsorbents and found two interesting conclusions: (i) heat effects were in fact negligible for lab scale conditions but would result in inaccurate predictions of breakthrough for large scale processes if they were neglected,[54] and (ii) adsorbents with high loadings of amines exhibited heterogeneous diffusive behaviour of CO_2 that led to depressed adsorption kinetics and premature column breakthrough.[55]

More recently, studies on the incorporation of silica-supported amines into hollow fibers have allowed for experimental and modelling studies on the adsorption and desorption kinetics of these materials in an industrially relevant setup.[35,56–58] Mathematical modelling of this system has demonstrated that supported amine hollow fiber sorbents can operate in rapid temperature swing adsorption (RTSA) processes with complete cycle times of 3 minutes.[58] Under non-optimized conditions it has been determined that CO_2 product purities of 90% and recoveries of 82% are possible. These results are very promising and indicate that supported amine adsorbents can allow for large quantities of CO_2 to be captured and concentrated within a reasonable time frame. Further optimization of this system will allow for higher purities and selectivities to be achieved.

1.3.4 Physical and Chemical Characteristics of Amine Adsorbents

Rationalizing the aforementioned performance criteria with respect to the physical and chemical properties of adsorbents is the key to developing new materials with improved CO_2 adsorption performance. All three steps of the adsorbent synthesis: the

synthesis of the oxide support, the choice of amine and the method used to incorporate amine groups into the pores of the support have an influence on the final material properties. The effect of the method used to incorporate amines (which in turn determines the class (1, 2 or 3) of adsorbent) on the properties of the adsorbent has been discussed throughout this article. In this section, the significance of the choice of support as well as the active amine on the physicochemical properties of the synthesized material is discussed.

1.3.4.1 Effect of the Oxide Support

The literature on amine-oxide hybrid materials for CO_2 capture focuses almost exclusively on silica-based mesoporous materials as supports for amine-based adsorbents. One of the reasons behind this is the fact that silica supports have been found to be sufficiently stable using the conditions under which they have been tested so far, with the exception of reports from our group which showed that exposure to steam resulted in the breakdown of the mesoporous structure.[18,59] This has prompted researchers working in the field to not only look at more stable silica supports but also non-silica based porous supports for CO_2 capture.

In fact, a few authors have started to study CO_2 adsorption properties of alumina based amine sorbents.[10,18,60–63] Chuang and co-workers compared otherwise similar amine-impregnated adsorbents based on three distinct porous supports: a silica, alumina and an aluminosilicate BEA zeolite.[10] Both the CO_2 adsorption performance as well as DRIFTS spectra of the TEPA impregnated materials (class 1) were assessed. The alumina-based adsorbents showed the lowest adsorption capacities in this study, which was attributed to the acidic nature of the alumina support. It was suggested that the

interactions between the acidic alumina surface and the basic amine groups, rendered the amine groups less reactive to the CO_2 molecules. In another study by our group, a basic mesoporous alumina was synthesized and compared to a mesoporous silica, both as prepared and impregnated with PEI.[18] The basic alumina had higher adsorption capacities at both flue gas and air capture conditions than the silica adsorbent. This material was also found to be stable in steaming environments as compared to the PEI-silica composite and therefore could be a good candidate for processes which use steam stripping for regeneration.

Llewellyn and co-workers[64] demonstrated through infrared spectroscopy and microcalorimetry measurements that the nature of the amine adsorption site is affected by the chemical nature of the support itself, supporting the hypothesis that attractive or repulsive interactions between the support and the amine groups can affect adsorption performance. This was further demonstrated by work from our group where varying amounts of metallic heteroatoms were incorporated into the silica matrix during synthesis (Al, Ti, Ze, Ce) and subsequently impregnated with PEI. It was found that different acid/base properties of the materials affected the PEI-oxide support interactions which thus altered CO_2 adsorption capacities as well as adsorption and desorption kinetics.[65,66]

Apart from the chemical composition of the support, the physical characteristics of the support such as the surface area, pore diameter and pore volume also have a significant impact on the adsorption performance. The pore size and connectivity in the support affect the rates of gas diffusion to the CO_2 adsorption sites, thus affecting the rates of the adsorption process. Son et al.[67] studied the CO_2 adsorption characteristics of 50 wt% PEI-impregnated adsorbents based on four different supports and found that the

adsorption capacities increased with increasing average pore diameters of the bare support. Also, the adsorption halftimes decreased with increasing support pore diameters, and this was suggested to be due to faster diffusion into the pores of the adsorbent. Also, three-dimensionally interconnected pores, as present in the case of MCM-48 and mesocellular foam silica (MCF) could provide better mass transfer properties compared to the (primarily) one-dimensional pore networks in the case of SBA-15 and MCM-41.

1.3.4.2 Effect of the Organic Group

A variety of different amines have been used as CO_2 adsorbents, with PEI being the main polymeric amine used in class 1 materials. A much wider array of amines have been used in class 2 materials, with some shown in Figure 1.2 and others described in reference 3**.** The fundamental difference between different amine moieties from the point of view of amine-CO_2 chemistry is the number of primary, secondary and tertiary amines they carry. Amine type can affect the performance of an adsorbent in two distinct ways. First, different amines have different basicities, which affects the strength of interaction between the CO_2 molecules and the amines. For example, aqueous solutions of MEA, which contains one primary amine, have been shown to have a higher heat of reaction with CO_2 (84 kJ mol^{-1}) compared to DEA (66 kJ mol^{-1}) and TEA (64 kJ mol^{-1}), which have one secondary and tertiary amine respectively. Amine type can also affect the amine efficiency depending on the level of humidity in the gas stream, as tertiary amines do not capture CO_2 in the absence of water.

Whereas the amine type influences the reaction chemistry, factors like the average size of the polymer chain and their degree of branching affects the accessibility of reactive amine groups to the incoming CO_2 molecules. The larger the length of a polymer

chain the more difficult it is for the chain to diffuse into the mesopores, which may result in immobilization of a smaller amount of amines in the bulk of the adsorbent particles. An increase in the degree of branching (which can occur when two amines are cross-linked by adsorbing CO_2 in a 2 N:1 CO_2 ratio) can also contribute to CO_2 transport limitations (discussed in section 1.3.1). It is important to understand that at this stage, the degree of understanding about amine distribution and morphology within hybrid adsorbents is still poorly developed, especially for materials that contain polymeric amines. Additional studies focused on understanding the physical structure of polymers located in the pores of the mesoporous supports are clearly needed.

1.4 Desorption of CO_2 from Supported Amine Adsorbents

Regeneration of supported-amine CO_2 adsorbents can be achieved via a temperature or CO_2 partial pressure swing, either alone or in combination. To date, regeneration of supported amine materials has, with few exceptions, been performed by temperature swing adsorption in a flow of inert purge gas (TSA/I). The focus of the community has been almost single minded in creating a material with the highest adsorption capacity, as noted above, and little attention has been given to practical regeneration processes for these materials. Using an inert gas such as nitrogen or argon to desorb CO_2 does not concentrate the CO_2, as required, before pipelining or sequestration. Thus, the majority of the papers in this field do not describe a technology that performs a useful separation. Other possible regeneration strategies include (i) temperature swing adsorption using a pure CO_2 stream as the sweep gas (TSA/CO_2), (ii) pressure swing adsorption (PSA), which includes the more often used vacuum swing adsorption (VSA), sometimes in combination with a temperature swing (T/VSA), and (iii) steam stripping.

There are advantages and disadvantages to each of these methods, and each method presents challenges for the material designer as discussed below.

1.4.1 Temperature Swing Adsorption with Inert Gas Purge (TSA/I)

Regeneration of the adsorbent is most commonly achieved by temperature swing with an inert purge gas such as helium or nitrogen to regenerate the adsorbent (TSA/I). TSA/I is a common regeneration technique, as the elevated temperatures are useful in supplying the energy needed to reverse the highly exothermic adsorption of CO_2 on amine sites while the inert purge gas provides a concentration driving force. Thus, higher temperatures result in larger desorption rates and an increased likelihood that all of the CO_2 will desorb, thereby returning the adsorbent ideally to its full capacity for the next adsorption cycle.

Of the three classes of materials, class 1 materials have generally exhibited the least stability in long term testing.[11,68–72] Specifically, the study by Tanthana et al. shows a significant loss of stability over 30 cycles at 115 °C for TEPA and TEPA modified with PEG on mesoporous silica. While the PEG modified material did exhibit a decrease in degradation rate, both materials exhibited a loss of greater than 50% capacity over the cycles.[68] However, Liu et al. report a capacity loss of only 5% for TEPA-impregnated into KIT-6 during 40 cycles of regeneration at 120 °C.[11] This is likely due to the fact that Tanthana tested regenerability in humid conditions while Liu performed adsorption in dry conditions and so the material may have leached amines due to water condensation and solublization, thus resulting in a decreased capacity.[11,68] In fact it has often been observed that class 1 materials lose significant capacity during cyclic testing in humid conditions due to the organic leaching out of the solids (section 1.5 explains this more fully along

with other modes of sorbent deactivation). However, Sayari et al. report the opposite trend in their humid adsorption/desorption study and observed that adsorption and desorption in humid gas streams improved stability for class 1 and 2 materials (PEI, APS and triamine on PE-MCM-41) as opposed to cyclic testing with dry gases.[73] It should be noted that the number of cycles tested for the class 1 material was about half that studied by Tanthana and so it is possible that with further cycling, leaching would be observed.[68,73] Sayari's findings from this study are discussed in more detail in the next section and in chapter 2.

1.4.2 Temperature Swing Adsorption with CO_2 Purge (TSA/CO_2)

Three studies have been reported using TSA with dry CO_2 as a sweep gas for adsorbent regeneration.[13,72,74] Although complete desorption is not possible with this method, as it lacks a significant partial pressure driving force for desorption, it does result in a high purity CO_2 product stream. The first study using this approach by Kim et al. considered both class 1 and 2 materials on MCM-48 (class 1: PEI; class 2: APS, polymerized APS and pyrrolidine), heating them to 120 °C in 1 atm of pure CO_2.[74] The amount of CO_2 adsorbed on all the materials started to decrease at temperatures below 50 °C. However, a weight gain was observed for the two polymeric materials (PEI and polymerized APS) once the temperature surpassed 62 °C. The authors attributed this behavior to an increased diffusivity at higher temperatures and thus greater accessibility to vacant sites in the polymer for these materials, leading to CO_2 adsorption. This is consistent with the behavior of other adsorbents containing polymeric amines. Both materials reverted to desorption upon a further increase of temperature between ca. 85 °C and 105 °C, depending on the material. Gray et al. used a temperature ramp with various

concentrations of CO_2 gas (from 10-80% CO_2 in inert) as a desorption technique for class 1 materials.[72] However, none of the CO_2 purge mixtures met the stated requirement of having a working capacity of at least 3 mmol g^{-1} adsorbent and so the method was ruled out in favor of a TSA/I process. Drage et al. also used pure CO_2 for desorption of a class 1 material (PEI on a mesoporous silica), but provided a larger thermal driving force by heating their materials up to 180 °C.[13] At temperatures above 135 °C, a weight gain was observed, which was attributed to formation of urea species observed by NMR and DRIFTS experiments. Attempts to regenerate the material by heating at elevated temperatures in inert proved futile and it was concluded that regeneration in flowing CO_2 gas irreversibly degraded the material and thus was not a viable option for adsorbent regeneration. Sayari et al. later showed that urea formation could be prevented by humidifying the gas stream.[73] These results are discussed in more detail in in chapter 2.

1.4.3 Steam Stripping

Steam stripping, like TSA with a CO_2 purge, represents a potentially practical regeneration method for supported amine adsorbents as it can result in a concentrated CO_2 stream. Like TSA/I, the temperature and composition of a gas stream provide both a thermal and partial pressure driving force for desorption of CO_2 from the amine. The CO_2 rich steam can then be compressed to produce liquid water and a high purity CO_2 gas stream that may be ready for a pipeline, sequestration, or other use. Additionally, low-grade steam (<110 °C) may generally be obtained at low cost from refineries and other facilities, as it is often unused and considered waste heat.

Thus far there have only been four studies reported on the regeneration of supported amines with saturated steam, the first of which was from our group.[5,75–77] In the

first study by Li et al.[5] saturated steam at 103 °C was used to regenerate class 1, 2 and 3 adsorbents (class 1: PEI on commercial silica; class 2: APS on commercial silica; class 3: HAS on mesocellular foam silica) over 3 successive adsorption cycles. It was found that steam effectively regenerated all three classes of adsorbents. Furthermore, quick regeneration times were observed, with essentially all the CO_2 desorbing in the first ten minutes, and 66 % within the first three minutes of steaming. However, 3 cycles is not enough to conclusively state that this regeneration method will work for these materials. In fact, follow up studies from our group showed that the stability of the silica support under prolonged steaming conditions may be problematic.[18,59] Under extensive, accelerated steaming conditions, it was shown that high pore volume, thin-walled supports such as mesocellular silica foams breakdown under many steaming conditions tested. A more recent study by Hammache et al. examined the stability of PEI impregnated in a commercial silica and found that there was no collapse of the support after 8 steam cycles. This could be due to the fact that the commercial support had a thicker wall and smaller pore volume of the support which could impart better stability to the composite adsorbent in the presence of steam. In that study, a slight loss of capacity was observed which was attributed to rearrangement of the polymer upon exposure to steam.[75]

From these studies it is still too early to make conclusions about the broader viability of steam-stripping for regeneration of supported amine CO_2 sorbents. Although the initial reports suggest that steam-stripping might be a viable option for regeneration, more extensive cycling is still needed to assess the impact that direct contact of steam will have on the stability of adsorbents. In addition, direct steam contact on the adsorbent

material will likely lead to condensed water within the pores of the solid, and its removal will incur an energy penalty to the capture process which may be too costly. Therefore further investigation of this regeneration strategy is still needed.

1.4.4 Pressure Swing Adsorption (PSA) and Derivatives

Pressure swing adsorption (PSA) is an alternative regeneration method that can provide a real separation of CO_2 from the adsorbent with no or minimal further purification downstream, unlike TSA/I. Pure PSA uses a partial pressure driving force to drive the CO_2 off of the material as opposed to a thermal driving force discussed above. This can be achieved in several ways: pulling vacuum (VSA),[78–80] operation at two different absolute pressures during adsorption and desorption (PSA),[81] or sweeping with an inert purge gas in the absence of heating (PSA/I).[9,67,73,82,83] PSA can also be used in conjunction with TSA to achieve desorption at lower temperatures with shorter generation times.[41,80,84–87] For example, many authors have combined vacuum and temperature swing (V/TSA).[42,80,85–89] It should be noted that on the large scales expected to be used for CO_2 capture from commercial coal plants, the cost and availability of vacuum equipment of appropriate size may be currently problematic.

Operation under VSA conditions results in a concentrated CO_2 purge stream that may require no additional downstream purification. However, longer desorption times are needed to recover capacity in comparison to TSA.[80] Sayari has reported numerous studies on regeneration conditions using VSA, PSA/I, TSA/I and V/TSA with class 1 and 2 materials on PE-MCM-41 (class 1: PEI; class 2: APS and triamine).[41,50,73,78,90,91] These studies have shown that at lower CO_2 concentration, such as 10% CO_2 in inert as opposed to pure CO_2, VSA can yield a capacity comparable to TSA when operating at 70 °C.[78]

Using V/TSA can also yield capacities comparable to TSA, with shorter times for desorption required.[78,80,90] However, in a statistical study by Sayari on the effect of various parameters on regeneration, it was determined that there was no benefit in terms of faster desorption or increased recovery when using vacuum at high desorption temperatures.[91] This does not take into account the added benefit of the more concentrated CO_2 stream that is recovered after desorption.

Overall, there are several regeneration methods that could be realistically used in an industrial application: (i) CO_2 purge, (ii) steam stripping and (iii) VSA or V/TSA. VSA or V/TSA can give a concentrated product stream and can allow for shorter desorption times when vacuum is applied with slight heating, with essentially complete regeneration.[78] Future regeneration studies should use methods such as these so that data relevant to practical desorption methods can be obtained. The field collectively needs to move away from TSA/I cycles that only give useful data on adsorption capacity and not desorption properties.

1.5 Stability of Supported Amine Adsorbents

As previously emphasized, capturing CO_2 effectively for flue gas or air capture requires that the adsorbent be sufficiently stable under capture and regeneration conditions. The solid adsorbent must demonstrate adequate performance over at least thousands and ideally many millions of cycles. Despite this, there are relatively few studies of aminosilica adsorbents that assess the stability of the adsorbent materials under realistic processing conditions, as most authors study adsorption/desorption cycles in the presence of CO_2, an inert gas, and in some cases, water vapor. Power plant flue gas typically contains 10-15% CO_2, 5-10% O_2, 4-5% water vapor, thousands of ppm of SO_x

(which must be reduced by scrubbing, in analogy to amine solution capture processes),[92,93] NO_x (which can be removed by selective catalytic reduction),[94] trace elements like Hg (each by definition less than 100 ppm in concentration) and the balance nitrogen. Ambient air contains approximately 21% O_2, 395 ppm CO_2, up to 4% water vapour and the balance nitrogen. Apart from nitrogen, which is an inert gas, the effect of all the components in flue gas and ambient air on adsorbent performance must be carefully evaluated. Any potential adsorbent degradation as a result of each of these components will depend on their partial pressure as well as the temperature at which they come in contact with the material. The body of knowledge that currently exists with respect to the effects of each of these components on amine-oxide hybrid material stability is discussed below.

1.5.1 Oxidative Degradation

In the aqueous amine absorption process, which is the benchmark process for CO_2 capture from power plant flue gas, oxidative degradation reactions are responsible for approximately half the overall amine makeup rate, which is about 2.2 kg MEA per tonne of CO_2 captured.[95–98] A number of reports discuss the oxidation of amines (especially monoethanolamine) in solution. In contrast, there is very little literature on the oxidative stability of supported amine adsorbents, and only recently have we begun to obtain some fundamental insight into the oxidation of supported amine adsorbents. These reports are discussed in detail in chapter 2.

1.5.2 Effect of Other Acid Gases: SO_x and NO_x

It has been reported that in the aqueous amine absorption process, the presence of SO_x (primarily SO_2) and NO_x (primarily NO) can result in significant amine losses via the formation of heat stable corrosive salts.[1,99] Flue gas desulfurization (FGD) scrubbers and selective catalytic NO_x reduction (SCR) equipment can reduce the concentrations of these acid gases to near 10 ppm, so as to limit these degradation losses. The literature on the effect of SO_x and NO_x on supported amines, though limited, indicates that the degradation issues observed in solution processes will also be present in adsorption processes using supported amines, thus necessitating significant sulfur and nitrogen oxide scrubbing prior to CO_2 capture, as noted above.

The first study on this subject was by Beckman and co-workers.[100,101] They studied the adsorption of all three acid gases: CO_2, SO_x and NO_x onto amine grafted polymeric adsorbents and reported that the thermal reversibility of the acid gas capture decreased in the order CO_2>SO_x>NO_x. Since then several other studies have looked at the effect of SO_x,[78,102] NO_x[103] or both gases[104,105] on supported amine adsorbents. The most comprehensive study to date came from our group which looked at silica impregnated with PEI (class 1) and silica functionalized with APS, MAPS and DMAPS (class 2) adsorbents that contained solely primary, secondary or tertiary amines.[105] This allowed for a systematic evaluation of the effect of structure type on stability to SO_2, NO_2 and NO gases. It was found that secondary amines adsorb the most SO_2, yet retain the highest percentage of CO_2 adsorption capacity after exposure to SO_2, implying the adsorption is reversible. All amine types were found to be resistant to significant NO adsorption. Additionally, all amine types were found to have large NO_2 adsorption capacities with a

corresponding drop in CO_2 uptake also, therefore implying this adsorption is irreversible and will deactivate materials for CO_2 adsorption. All studies to date show that SO_x and NO_x will likely have a detrimental effect on the supported amine adsorbent stability, even if ppm levels of SO_x and NO_x are present in the flue gas stream. However, mechanistic insights into the irreversible adsorption mechanism as well as the behaviour of these materials in a co-adsorption process are still unknown. Studies to elucidate such information are clearly needed.

1.5.3 Effect of Water Vapor

As discussed briefly in section 1.4, in the case of class 1 materials, water vapor has an adverse effect on leaching of organics. Leaching has been discussed in greater detail in section 1.5.5. In the literature, apart from increasing the degree of amine leaching, there are no other reported adverse effects of the presence of water vapor on either the support structure or the chemical stability of amines during the adsorption stage. In fact, in one study on the effect of co-presence of water vapor and CO_2 in the feed on amine-oxide stability, Sayari and co-workers reported that in addition to enhancing the CO_2 adsorption capacity of the adsorbent, water vapor also had a stabilizing effect on the amine groups,[73] as discussed in section 1.4.3,. Li et al.[59] evaluated the stability of sorbents to simulated steaming conditions and reported the appearance of carbonyl groups when all three classes of aminosilica adsorbents were exposed to steam in the co-presence of air. The only exception was aminopropyl functionalized silica, in which case carbonyl groups were not detected. Whether or not these carbonyl groups corresponded to urea linkages was not verified in that particular study. Apart from the adverse effects on the chemical structure of the organic groups,

structural collapse of the thin walled mesocellular foam silica support was also found to be partially responsible for the decrease in CO_2 adsorption performance in that work. Unlike oxidation effects, pore collapse was observed both in the co-presence of steam and air as well as steam and nitrogen.

1.5.4 Effect of Mercury and Other Trace Elements

The trace elements in flue gas include several heavy metals like mercury and some lighter elements like boron, beryllium and arsenic.[106,107] Because of the harmful effects these trace elements have on human health, electrostatic precipitators and fabric filters are used to further reduce their concentrations in the flue gas exhaust.[106,108] Parts per billion levels of mercury have been detected in absorption units when aqueous MEA was used as the sorbent, without any significant effects on the capture and regeneration performance.[109] It seems that the effect of oxidative degradation and degradation by acid gases apart from CO_2 may be more critical compared to irreversible damage caused by mercury and other trace elements. This is further supported by a report by Cui et al.,[110] in which a feasibility analysis was carried out for combined CO_2 and Hg capture using MEA. It was found that combined mercury and CO_2 capture using MEA was not feasible because of the low mercury absorption capacities. It is important to note that no degradation or adverse effect on the CO_2 capture performance of the MEA solution due to the co-presence of mercury was reported. Nonetheless, this topic requires significant further study from an environmental perspective, to assess the fate of these important trace elements in a process that includes post-combustion CO_2 capture using supported amine adsorbents.

Apart from the stability issues discussed above there are also some degradation mechanisms that occur under certain operating conditions for specific adsorbents that are not induced by reactive components in flue gas. These are relevant to both CO_2 capture from power plant flue gas as well as direct capture from ambient air and are discussed below.

1.5.5 Leaching of Organic Amines

An important potential degradation pathway for supported amine adsorbents is the leaching of organic groups from the solids, as noted in the above sections. Theoretically, this phenomenon should be more limited in class 2 and class 3 adsorbents due to the covalent bonding between the organic amines and the porous support. In general, this is what is observed experimentally. In contrast, it might be expected that class 1 adsorbents may be susceptible to leaching of organics since in their case, the amine containing molecules are physically impregnated into the pores without strong chemical bonding between amines and the support. Our group was the first to report leaching in class 1 materials for CO_2 capture applications.[25] It was observed during fixed bed runs that the adsorption column became clogged with leached species when PEI- impregnated SBA-15 was tested under humid flue gas conditions at both 25 ºC (RH = 99%) and 75 ºC (RH = 8%). Also, adsorption capacities of TEPA impregnated SBA-15 fell sharply after the first cycle and continued to drop in subsequent cycles when tested using humidified gases. Leaching was identified as the most likely cause of reduction in adsorption capacities, owing to the visible characterization of organic leaching from the solids in the glass reactors.

In the only report explicitly evaluating leaching of amines in class 2 CO_2 adsorbents, Langeroudi et al. reported that leaching did not occur during the actual adsorption-desorption cycles but did take place during an intermediate treatment step when the samples were immersed in water.[111] In that study, focused on assessing the stability of amine functionalized SBA-15 in water, the authors performed 24-hour immersion cycles in water at 40ºC and found that after the first few immersion cycles about 40% of the amines had leached out of the adsorbent. When the adsorbent was not exposed to liquid water, however, it exhibited highly reproducible CO_2 adsorption capacities over a limited number of cycles. In conclusion, class 2 and class 3 adsorbents have a significant advantage over class 1 adsorbents in that they are more resistant to amine leaching under capture and typical regeneration conditions, although more systematic studies of amine leaching from all classes of materials are needed.

1.6 Nature of the Adsorbed CO_2

As noted above, a fundamental difference between physisorbents and chemisorbents is the occurrence of a chemical reaction during the adsorption event in the latter materials. In the case of CO_2 capture by supported amines, the specific reactions are between CO_2 and the amine, as discussed in Section 1.3 for amine solutions. Although the species produced upon CO_2 absorption in solutions is well established, it is reasonable to expect that some differences in the structure of the adsorbed CO_2 may occur relative to these solution studies when using solid adsorbents. Depending on the nature of the supported amine, the amine site density, amine mobility, and other factors, one may hypothesize that a variety of amine-CO_2 interactions may occur during adsorption on supported amine adsorbents. A fundamental understanding of the reaction mechanisms

and the products formed is certainly critical to understanding the overall adsorption process. Also, since water vapor plays an important role in the surface reactions, it is necessary to understand the effect of humidity on the products formed. In this section, what is currently known about the chemical nature of the adsorbed CO_2 is discussed.

Fourier transform infrared spectroscopy (FTIR) has been the most widely used technique to investigate CO_2-amine interactions on solid adsorbents. A number of chemical structures have been identified using infrared spectroscopy and are shown in Figure 1.5. There are a few disagreements with respect to the peak assignments and therefore also the identification of the adsorbed species.[3] To gain a comprehensive understanding of the nature of the adsorbed species, it is necessary to know not only the chemical structures formed on the surface, but also determine under precisely what conditions they are formed, how strong/weak the bonds are, and the dependence of these structures on the types of amines and supports used.

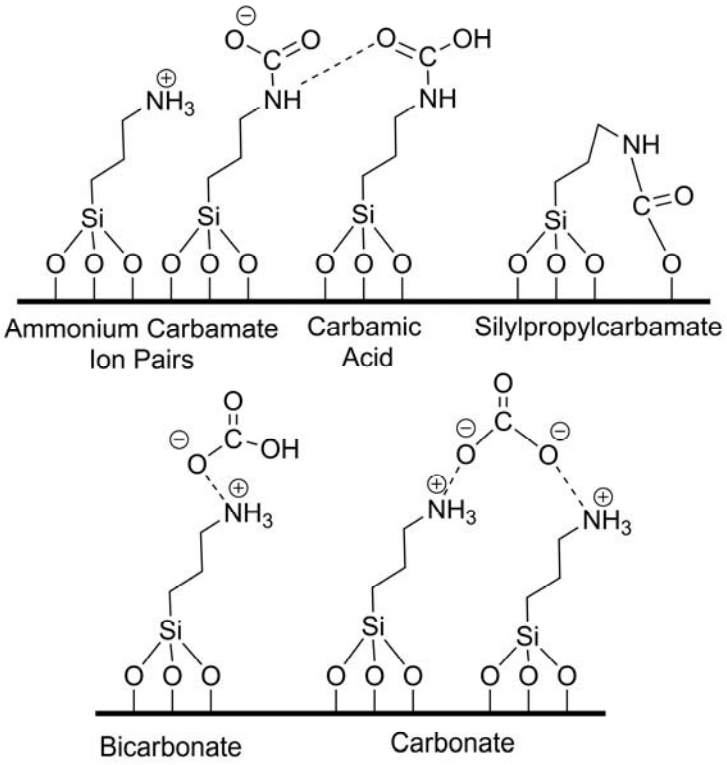

Figure 1.5. Most recent reported structures (top) and debated structures (bottom) of CO_2 supported amine adducts from FTIR studies.

When exposed to CO_2 under dry conditions, most studies report the formation of ammonium carbamate ion pairs, carbamic acid and/or surface bound carbamates.[64,69,112–115] Although these stretches are clearly observed in the IR spectra, it is not always straightforward to rigorously quantify the relative amounts of these two species based solely on the IR measurements, and the combination of solid state NMR data in conjunction with calorimetric measurements can help to quantitatively assess the relative amounts of carbamate and carbamic acid formed. Pinto and co-workers[116] performed a solid state NMR study of APS functionalized silica materials (class 2) before and after exposure to CO_2. Both CO_2 physically adsorbed onto the surface of the support (at about 125 ppm) as well as CO_2 chemically bound to the amines (at about 164 ppm) were

detected in the ^{13}C high power decoupling (HPDEC) NMR spectra. The peak at 164 ppm was assigned to carbamate; it also had a shoulder at 160 ppm that could be deconvoluted from the main peak that was assigned to carbamic acid. Correlating the NMR data with the adsorption capacity data, the amount of carbamate and carbamic acid species were calculated to be about 0.77 mmol g^{-1} and 0.29 mmol g^{-1} for samples tested at 1 bar CO_2 pressure. It was hypothesized that CO_2 can react with a primary amine to form a carbamic acid which then reacts with an amine in close proximity to yield an ammonium carbamate ion pair.

In the studies discussed so far, water vapor was absent from the gas feed. The presence of water vapor makes the interpretation of the structure of the adsorbed CO_2 using FTIR spectroscopy more complicated, but the characterization is more relevant to practical operating conditions. Recent studies using *in-situ* FTIR with humid CO_2 do not observe the formation of carbonates or bicarbonates, thereby refuting previous studies that had identified these products as adsorbed species in the presence of humid CO_2.[102,114,115,117] Instead it is found that more ammonium carbamate ions pairs form as well as carbamic acids that are hydrogen bonded to neighboring ammonium carbamate ion pairs.[114,115] From these studies, it is suggested that the presence of water improves amine efficiency by releasing amine groups that were previously unavailable to interact with CO_2, due to hydrogen bonding with the support.[114] However, there is still much to be explored within this realm. As one example, the degree of relative humidity can play a significant role in the type of adsorption that occurs since capillary condensation will create a quasi-aqueous amine environment. At this stage, the relative stabilities of the carbamates versus carbonates and bicarbonates on supported amine adsorbents is not well

established and there is limited understanding as to why certain products are formed under specific sets of conditions and not others. This concept is further discussed in chapter 5.

1.7 Flue Gas Capture vs. Direct Air Capture

Silica-supported amine CO_2 adsorbents were initially solely intended for and evaluated in hypothetical post-combustion CO_2 capture processes, as discussed previously. In these applications, large installations are envisioned whereby flue gas from major point sources, such as coal-fired power plants, would be contacted with the adsorbent for selective removal of the CO_2, while the remaining flue gases, primarily N_2, O_2 and H_2O, would continue out the plant stack. As a result, most studies of CO_2 adsorption using these materials have focused on gas streams with CO_2 concentrations between 5-20% by volume. However, amine-based adsorbent materials, having a relatively large heat of adsorption with CO_2, typically have steep adsorption isotherms at low pressures, allowing for large CO_2 capacities with low inlet CO_2 concentrations. Therefore, these materials can also prove useful in adsorbing CO_2 from ultra-dilute gas streams, such as for air purification in confined spaces like spacecraft and submarines.[118] However, the biggest potential impact is in the direct capture of CO_2 from the ambient air.[39,119] Today, the CO_2 concentration in ambient air is about 398 ppm and it continues to rise.

Air capture, unlike conventional CCS, can in principle account for all sources of anthropogenic carbon, including mobile sources such as cars, buses, and planes, if it were to be practiced on a sufficiently large scale.[119–121] In 1999, Lackner first introduced the idea of "air capture" as a way of reducing the global atmospheric CO_2 concentration.

However, technologies for the extraction of CO_2 from ambient air are still in their infancy, and the ultra-dilute conditions pose a significant challenge, one that might be met by only a few technologies, with supported amines being a promising class of adsorbent materials for this application.

In 2009, our group first reported the use of supported amine materials for CO_2 capture from gas streams simulating ambient air.[122] Specifically, class 3 HAS materials were reported to be effective adsorbents under simulated air capture conditions, efficiently extracting CO_2 from a source gas with CO_2 concentration of 400 ppm. Subsequently, Sayari demonstrated the use of his well-studied, class 2 materials (triamine) for adsorption of CO_2 from a 400 ppm CO_2 gas feed as well.[50] The adsorption isotherm from that communication is presented in Figure 1.6. It can be seen that the supported amine material, a strong chemisorbant for CO_2, has a great advantage for CO_2 capture at ultra-dilute concentrations, especially compared to a prototypical physisorbant, like zeolite 13X. Work by our group using class 1 and class 3 supported amine materials for CO_2 capture from simulated flue gas and ambient air showed that despite a 250 fold decrease in the CO_2 concentration, the adsorption capacity in some cases dropped by as little as a factor of 2.2, thus demonstrating the utility of the supported amine materials for CO_2 capture from ultra-dilute sources.[123]

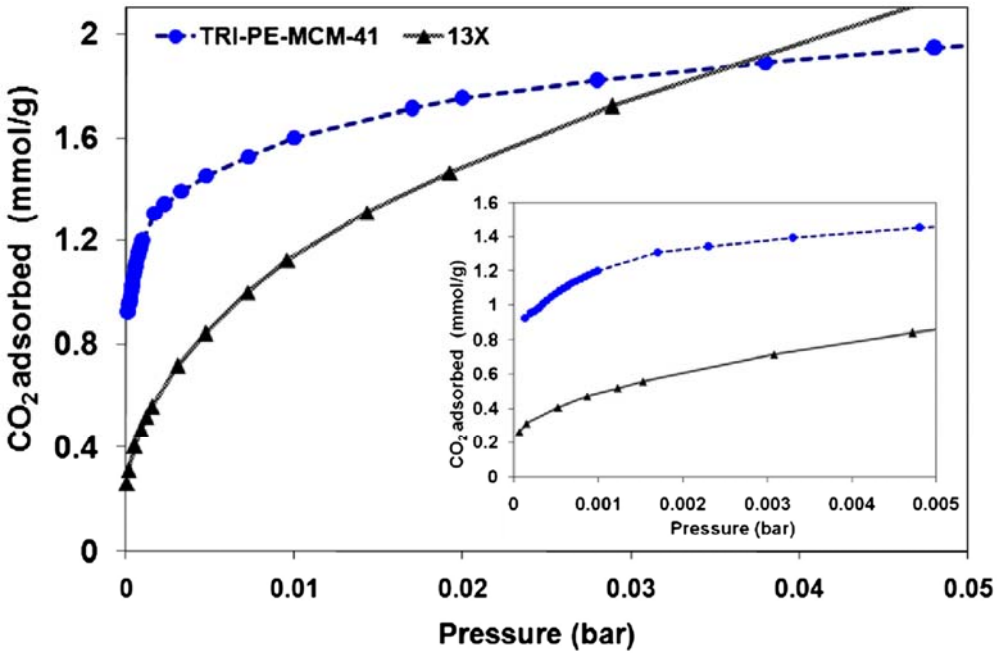

Figure 1.6. CO_2 adsorption isotherms for class 2 adsorbent, TRI-PE-MCM-41 at 298 K compared to zeolite 13X up to 0.05 bar; inset: close-up at very low pressure. Reprinted from reference 50 with permission from Elsevier.

Our group also recently reported the use of modified class 1 adsorbents for air capture.[124] In that work, two modifiers, APS and tetrapropyl orthotitanate (TPOT), were added to the PEI polymer during sorbent impregnation, with the goal of creating materials that are easy to prepare, like conventional class 1 adsorbents, but that are more robust over many thermal cycles. It was hypothesized that the amine groups in APS might self-assemble with the amines in PEI and that the Ti surface species created by TPOT would coordinate with the PEI to offer materials with enhanced stability. Physical characterization of the materials by TGA and FTIR spectroscopy suggested that the modifiers affect the structure of the composite materials. Characterization of the materials over multiple adsorption-desorption cycles using TSA/I under dry conditions showed the materials to have enhanced stability. Furthermore, these materials offer the highest

reported adsorption capacities to date for air capture, with a reported uptake of 2.36 mmol g^{-1}.[124] Since the time that air capture using supported amines was first proposed by our group in 2009, a significant amount of research has been put forth in the field.[18,50,65,66,88,89,123–141] This collection of work to date demonstrates supported amine materials are promising adsorbents for the direct extraction of CO_2 from ultra-dilute sources such as ambient air. However, more work is still needed in developing sorbents that combine fast adsorption kinetics, high working capacities, simple and scalable designs, and stability over many regeneration cycles.

1.8 Research Needs & Scope of Dissertation

Materials chemists have worked for the better part of a decade on the development of aminosilica hybird materials for CO_2 extraction from dilute gas streams. Over this period, several hundred studies have appeared, with most of them focused on developing hybrid materials with very large CO_2 capacities. At this stage, it can be argued that achieving adsorbents with ever larger CO_2 capacities represents minor, incremental advances, and the community must now turn its attention towards more pressing issues regarding the application of these materials in CO_2 capture scenarios. Specific areas that need further investigation are listed below:

1. Scalable adsorbent regeneration methods
2. Design of sorbents that are stable in their operating environment (CO_2, oxygen, SO_x, NO_x, steam)
3. Quantitative understanding of adsorption and desorption kinetics
4. Synthesis of more efficient adsorbent materials
5. Understanding the effects of water on adsorption performance

The work in this dissertation provides fundamental insight into supported amine adsorbents that directly contribute to needs 2, 4 and 5 listed above. A study on the structural contributions of amine adsorbents with respect to thermal, CO_2-induced and oxidative degradation are discussed in chapter 2. Chapter 3 describes a study on the effect of amine type on adsorption efficiency for air capture applications. Discussion on the design, building and validation of a volumetric system for binary (CO_2-H_2O) adsorption studies is presented in chapter 4. This system is used to explore the effect of amine surface coverage on the enhancement of CO_2 adsorption at ultra-dilute conditions imparted by the presence of water vapor in chapter 5.

1.9 References

(1) Aaron, D.; Tsouris, C. Separation of CO_2 from Flue Gas: A Review. *Sep. Sci. Technol.* **2005**, *40*, 321–348.

(2) Ebner, A. D.; Ritter, J. A. State-of-the-Art Adsorption and Membrane Separation Processes for Carbon Dioxide Production from Carbon Dioxide Emitting Industries. *Sep. Sci. Technol.* **2009**, *44*, 1273–1421.

(3) Choi, S.; Drese, J. H.; Jones, C. W. Adsorbent Materials for Carbon Dioxide Capture from Large Anthropogenic Point Sources. *ChemSusChem* **2009**, *2*, 796–854.

(4) Hedin, N.; Chen, L.; Laaksonen, A. Sorbents for CO_2 Capture from Flue Gas-Aspects from Materials and Theoretical Chemistry. *Nanoscale* **2010**, *2*, 1819–1841.

(5) Li, W.; Choi, S.; Drese, J. H.; Hornbostel, M.; Krishnan, G.; Eisenberger, P. M.; Jones, C. W. Steam-Stripping for Regeneration of Supported Amine-Based CO_2 Adsorbents. *ChemSusChem* **2010**, *3*, 899–903.

(6) Grande, C. A.; Ribeiro, R.; Rodrigues, A. E. Challenges of Electric Swing Adsorption for CO_2 Capture. *ChemSusChem* **2010**, *3*, 892–898.

(7) Tsuda, T.; Fujiwara, T. Polyethyleneimine and Macrocyclic Polyamine Silica Gels Acting as Carbon Dioxide Absorbents. *J. Chem. Soc.-Chem. Commun.* **1992**, 1659–1661.

(8) Tsuda, T.; Fujiwara, T.; Taketani, Y.; Saegusa, T. Amino Silica Gels Acting as a Carbon Dioxide Absorbent. *Chem. Lett.* **1992**, 2161–2164.

(9) Xu, X. C.; Song, C.; Andresen, J. M.; Miller, B. G.; Scaroni, A. W. Novel Polyethylenimine-Modified Mesoporous Molecular Sieve of MCM-41 Type as High-Capacity Adsorbent for CO_2 Capture. *Energy Fuels* **2002**, *16*, 1463–1469.

(10) Fisher, J. C.; Tanthana, J.; Chuang, S. S. C. Oxide-Supported Tetraethylenepentamine for CO_2 Capture. *Environ. Prog. Sustain. Energy* **2009**, *28*, 589–598.

(11) Liu, Y. M.; Shi, J. J.; Chen, J.; Ye, Q.; Pan, H.; Shao, Z. H.; Shi, Y. Dynamic Performance of CO_2 Adsorption with Tetraethylenepentamine-Loaded KIT-6. *Microporous Mesoporous Mater.* **2010**, *134*, 16–21.

(12) Chen, C.; Son, W. J.; You, K. S.; Ahn, J. W.; Ahn, W. S. Carbon Dioxide Capture Using Amine-Impregnated HMS Having Textural Mesoporosity. *Chem. Eng. J.* **2010**, *161*, 46–52.

(13) Drage, T. C.; Arenillas, A.; Smith, K. M.; Snape, C. E. Thermal Stability of Polyethylenimine Based Carbon Dioxide Adsorbents and Its Influence on Selection of Regeneration Strategies. *Microporous Mesoporous Mater.* **2008**, *116*, 504–512.

(14) Liu, S. H.; Wu, C. H.; Lee, H. K.; Liu, S. B. Highly Stable Amine-Modified Mesoporous Silica Materials for Efficient CO_2 Capture. *Top. Catal.* **2010**, *53*, 210–217.

(15) Yue, M. B.; Chun, Y.; Cao, Y.; Dong, X.; Zhu, J. H. CO_2 Capture by As-Prepared SBA-15 with an Occluded Organic Template. *Adv. Funct. Mater.* **2006**, *16*, 1717–1722.

(16) Franchi, R. S.; Harlick, P. J. E.; Sayari, A. Applications of Pore-Expanded Mesoporous Silica. 2. Development of a High-Capacity, Water-Tolerant Adsorbent for CO_2. *Ind. Eng. Chem. Res.* **2005**, *44*, 8007–8013.

(17) Wang, X.; Li, H.; Liu, H.; Hou, X. AS-Synthesized Mesoporous Silica MSU-1 Modified with Tetraethylenepentamine for CO_2 Adsorption. *Microporous Mesoporous Mater.* **2011**, *142*, 564–569.

(18) Chaikittisilp, W.; Kim, H.; Jones, C. W. Mesoporous Alumina-Supported Amines as Potential Steam-Stable Adsorbents for Capturing CO_2 from Simulated Flue Gas and Ambient Air. *Energy Fuels* **2011**, *25*, 5528–5537.

(19) Chen, Z.; Deng, S.; Wei, H.; Wang, B.; Huang, J.; Yu, G. Polyethylenimine-Impregnated Resin for High CO_2 Adsorption: An Efficient Adsorbent for CO_2 Capture from Simulated Flue Gas and Ambient Air. *ACS Appl. Mater. Interfaces* **2013**, *5*, 6937–6945.

(20) Zhao, W.; Zhang, Z.; Li, Z.; Cai, N. Investigation of Thermal Stability and Continuous CO_2 Capture from Flue Gases with Supported Amine Sorbent. *Ind. Eng. Chem. Res.* **2013**, *52*, 2084–2093.

(21) Subagyono, D. J. N.; Marshall, M.; Knowles, G. P.; Chaffee, A. L. CO_2 Adsorption by Amine Modified Siliceous Mesostructured Cellular Foam (MCF) in Humidified Gas. *Microporous Mesoporous Mater.* **2014**, *186*, 84–93.

(22) Kumar, P.; Guliants, V. V. Periodic Mesoporous Organic-Inorganic Hybrid Materials: Applications in Membrane Separations and Adsorption. *Microporous Mesoporous Mater.* **2010**, *132*, 1–14.

(23) Acosta, E. J.; Carr, C. S.; Simanek, E. E.; Shantz, D. F. Engineering Nanospaces: Iterative Synthesis of Melamine-Based Dendrimers on Amine-Functionalized SBA-15 Leading to Complex Hybrids with Controllable Chemistry and Porosity. *Adv. Mater.* **2004**, *16*, 985–989.

(24) Rosenholm, J. M.; Linde, M. Wet-Chemical Analysis of Surface Concentration of Accessible Groups on Different Amino-Functionalized Mesoporous SBA-15 Silicas. *Chem. Mater.* **2007**, *19*, 5023–5034.

(25) Hicks, J. C.; Drese, J. H.; Fauth, D. J.; Gray, M. L.; Qi, G. G.; Jones, C. W. Designing Adsorbents for CO2 Capture from Flue Gas-Hyperbranched Aminosilicas Capable of Capturing CO_2 Reversibly. *J. Am. Chem. Soc.* **2008**, *130*, 2902–2903.

(26) Caplow, M. Kinetics of Carbamate Formation and Breakdown. *J. Am. Chem. Soc.* **1968**, *90*, 6795–6803.

(27) Donaldson, T. L.; Nguyen, Y. N. Carbon Dioxide Reaction Kinetics and Transport in Aqueous Amine Membranes. *Ind. Eng. Chem. Fundam.* **1980**, *19*, 260–266.

(28) Vaidya, P. D.; Kenig, E. Y. CO_2-Alkanolamine Reaction Kinetics: A Review of Recent Studies. *Chem. Eng. Technol.* **2007**, *30*, 1467–1474.

(29) Drese, J. H.; Choi, S.; Lively, R. P.; Koros, W. J.; Fauth, D. J.; Gray, M. L.; Jones, C. W. Synthesis-Structure-Property Relationships for Hyperbranched Aminosilica CO_2 Adsorbents. *Adv. Func. Mater.* **2009**, *19*, 3821–3832.

(30) Yang, W.-C.; Hoffman, J. Exploratory Design Study on Reactor Configurations for Carbon Dioxide Capture from Conventional Power Plants Employing Regenerable Solid Sorbents. *Ind. Eng. Chem. Res.* **2009**, *48*, 341–351.

(31) Sjostrom, S.; Krutka, H. Evaluation of Solid Sorbents as a Retrofit Technology for CO_2 Capture. *Fuel* **2010**, *89*, 1298–1306.

(32) Monazam, E. R.; Spenik, J.; Shadle, L. J. Fluid Bed Adsorption of Carbon Dioxide on Immobilized Polyethylenimine (PEI): Kinetic Analysis and Breakthrough Behavior. *Chem. Eng. J.* **2013**, *223*, 795–805.

(33) Lively, R. P.; Leta, D. P.; DeRites, B. a.; Chance, R. R.; Koros, W. J. Hollow Fiber Adsorbents for CO_2 Capture: Kinetic Sorption Performance. *Chem. Eng. J.* **2011**, *171*, 801–810.

(34) Li, F. S.; Qiu, W.; Lively, R. P.; Lee, J. S.; Rownaghi, A. A.; Koros, W. J. Polyethyleneimine-Functionalized Polyamide Imide (Torlon) Hollow-Fiber Sorbents for Post-Combustion CO_2 Capture. *ChemSusChem* **2013**, *6*, 1216–1223.

(35) Rezaei, F.; Lively, R. P.; Labreche, Y.; Chen, G.; Fan, Y.; Koros, W. J.; Jones, C. W. Aminosilane-Grafted Polymer/silica Hollow Fiber Adsorbents for CO_2 Capture from Flue Gas. *ACS Appl. Mater. Interfaces* **2013**, *5*, 3921–3931.

(36) Chen, C.; Yang, S. T.; Ahn, W. S.; Ryoo, R. Amine-Impregnated Silica Monolith with a Hierarchical Pore Structure: Enhancement of CO_2 Capture Capacity. *Chem. Commun.* **2009**, 3627–3629.

(37) Wen, J. J.; Gu, F. N.; Wei, F.; Zhou, Y.; Lin, W. G.; Yang, J.; Yang, J. Y.; Wang, Y.; Zou, Z. G.; Zhu, J. H. One-Pot Synthesis of the Amine-Modified Meso-Structured Monolith CO_2 Adsorbent. *J. Mater. Chem.* **2010**, *20*, 2840–2846.

(38) Wang, J.; Long, D.; Zhou, H.; Chen, Q.; Liu, X.; Ling, L. Surfactant Promoted Solid Amine Sorbents for CO_2 Capture. *Energy Environ. Sci.* **2012**, *5*, 5742–5749.

(39) Jones, C. W. CO2 Capture from Dilute Gases as a Component of Modern Global Carbon Management. *Annu. Rev. Chem. Biomol. Eng.* **2011**, *2*, 31–52.

(40) Serna-Guerrero, R.; Da'na, E.; Sayari, A. New Insights into the Interactions of CO_2 with Amine-Functionalized Silica. *Ind. Eng. Chem. Res.* **2008**, *47*, 9406–9412.

(41) Belmabkhout, Y.; De Weireld, G.; Sayari, A. Amine-Bearing Mesoporous Silica for CO_2 and H_2S Removal from Natural Gas and Biogas. *Langmuir* **2009**, *25*, 13275–13278.

(42) Belmabkhout, Y.; Sayari, A. Effect of Pore Expansion and Amine Functionalization of Mesoporous Silica on CO_2 Adsorption over a Wide Range of Conditions. *Adsorption* **2009**, *15*, 318–328.

(43) Zhao, G.; Aziz, B.; Hedin, N. Carbon Dioxide Adsorption on Mesoporous Silica Surfaces Containing Amine-Like Motifs. *Appl. Energy* **2010**, *87*, 2907–2913.

(44) Xu, X. C.; Song, C.; Andresen, J. M.; Miller, B. G.; Scaroni, A. W. Preparation and Characterization of Novel CO_2 "Molecular Basket" Adsorbents Based on Polymer-Modified Mesoporous Molecular Sieve MCM-41. *Microporous Mesoporous Mater.* **2003**, *62*, 29–45.

(45) Kim, S. N.; Son, W. J.; Choi, J. S.; Ahn, W. S. CO_2 Adsorption Using Amine-Functionalized Mesoporous Silica Prepared via Anionic Surfactant-Mediated Synthesis. *Microporous Mesoporous Mater.* **2008**, *115*, 497–503.

(46) Qi, G.; Wang, Y.; Estevez, L.; Duan, X.; Anako, N.; Park, A.-H. A.; Li, W.; Jones, C. W.; Giannelis, E. P. High Efficiency Nanocomposite Sorbents for CO_2 Capture Based on Amine-Functionalized Mesoporous Capsules. *Energy Environ. Sci.* **2011**, *4*, 444–452.

(47) Hiyoshi, N.; Yogo, K.; Yashima, T. Adsorption of Carbon Dioxide on Amine Modified SBA-15 in the Presence of Water Vapor. *Chem. Lett.* **2004**, *33*, 510–511.

(48) Harlick, P. J. E.; Sayari, A. Applications of Pore-Expanded Mesoporous Silica. 5. Triamine Grafted Material with Exceptional CO_2 Dynamic and Equilibrium Adsorption Performance. *Ind. Eng. Chem. Res.* **2007**, *46*, 446–458.

(49) Drese, J. H.; Choi, S.; Didas, S. A.; Bollini, P.; Gray, M. L.; Jones, C. W. Effect of Support Structure on CO_2 Adsorption Properties of Pore-Expanded Hyperbranched Aminosilicas. *Microporous Mesoporous Mater.* **2012**, *151*, 231–240.

(50) Belmabkhout, Y.; Serna-Guerrero, R.; Sayari, A. Amine-Bearing Mesoporous Silica for CO_2 Removal from Dry and Humid Air. *Chem. Eng. Sci.* **2010**, *65*, 3695–3698.

(51) Keskin, S.; van Heest, T. M.; Sholl, D. S. Can Metal-Organic Framework Materials Play a Useful Role in Large-Scale Carbon Dioxide Separations? *ChemSusChem* **2010**, *3*, 879–891.

(52) Lively, R. P.; Chance, R. R.; Kelley, B. T.; Deckman, H. W.; Drese, J. H.; Jones, C. W.; Koros, W. J. Hollow Fiber Adsorbents for CO_2 Removal from Flue Gas. *Ind. Eng. Chem. Res.* **2009**, *48*, 7314–7324.

(53) Serna-Guerrero, R.; Sayari, A. Modeling Adsorption of CO_2 on Amine-Functionalized Mesoporous Silica. 2: Kinetics and Breakthrough Curves. *Chem. Eng. J.* **2010**, *161*, 182–190.

(54) Bollini, P.; Brunelli, N. A.; Didas, S. A.; Jones, C. W. Dynamics of CO_2 Adsorption on Amine Adsorbents. 1. Impact of Heat Effects. *Ind. Eng. Chem. Res.* **2012**, *51*, 15145–15152.

(55) Bollini, P.; Brunelli, N. A.; Didas, S. A.; Jones, C. W. Dynamics of CO_2 Adsorption on Amine Adsorbents. 2. Insights into Adsorbent Design. *Ind. Eng. Chem. Res.* **2012**, *51*, 15153–15162.

(56) Labreche, Y.; Lively, R. P.; Rezaei, F.; Chen, G.; Jones, C. W.; Koros, W. J. Post-Spinning Infusion of Poly(ethyleneimine) into Polymer/silica Hollow Fiber Sorbents for Carbon Dioxide Capture. *Chem. Eng. J.* **2013**, *221*, 166–175.

(57) Fan, Y.; Lively, R. P.; Labreche, Y.; Rezaei, F.; Koros, W. J.; Jones, C. W. Evaluation of CO_2 Adsorption Dynamics of Polymer/silica Supported Poly(ethylenimine) Hollow Fiber Sorbents in Rapid Temperature Swing Adsorption. *Int. J. Greenh. Gas Control* **2014**, *21*, 61–71.

(58) Rezaei, F.; Swernath, S.; Kalyanaraman, J.; Lively, R. P.; Kawajiri, Y.; Realff, M. J. Modeling of Rapid Temperature Swing Adsorption Using Hollow Fiber Sorbents. *Chem. Eng. Sci.* **2014**.

(59) Li, W.; Bollini, P.; Didas, S. A.; Choi, S.; Drese, J. H.; Jones, C. W. Structural Changes of Silica Mesocellular Foam Supported Amine-Functionalized CO_2 Adsorbents upon Exposure to Steam. *ACS Appl. Mater. Interfaces* **2010**, *2*, 3363–3372.

(60) Chen, C.; Ahn, W.-S. CO_2 Capture Using Mesoporous Alumina Prepared by a Sol–gel Process. *Chem. Eng. J.* **2011**, *166*, 646–651.

(61) Plaza, M. G.; Pevida, C.; Arias, B.; Fermoso, J.; Arenillas, a.; Rubiera, F.; Pis, J. J. Application of Thermogravimetric Analysis to the Evaluation of Aminated Solid Sorbents for CO_2 Capture. *J. Therm. Anal. Calorim.* **2008**, *92*, 601–606.

(62) Chaikittisilp, W.; Didas, S. A.; Kim, H.-J.; Jones, C. W. Vapor-Phase Transport as A Novel Route to Hyperbranched Polyamine-Oxide Hybrid Materials. *Chem. Mater.* **2013**, *25*, 613–622.

(63) Bali, S.; Chen, T. T.; Chaikittisilp, W.; Jones, C. W. Oxidative Stability of Amino Polymer–Alumina Hybrid Adsorbents for Carbon Dioxide Capture. *Energy Fuels* **2013**, *27*, 1547–1554.

(64) Knofel, C.; Martin, C.; Hornebecq, V.; Llewellyn, P. L. Study of Carbon Dioxide Adsorption on Mesoporous Aminopropylsilane-Functionalized Silica and Titania Combining Microcalorimetry and in Situ Infrared Spectroscopy. *J. Phys. Chem. C* **2009**, *113*, 21726–21734.

(65) Kuwahara, Y.; Kang, D.-Y.; Copeland, J. R.; Brunelli, N. A.; Didas, S. A.; Bollini, P.; Sievers, C.; Kamegawa, T.; Yamashita, H.; Jones, C. W. Dramatic Enhancement of CO_2 Uptake by Poly(ethyleneimine) Using Zirconosilicate Supports. *J. Am. Chem. Soc.* **2012**, *134*, 10757–10760.

(66) Kuwahara, Y.; Kang, D.-Y.; Copeland, J. R.; Bollini, P.; Sievers, C.; Kamegawa, T.; Yamashita, H.; Jones, C. W. Enhanced CO_2 Adsorption over Polymeric Amines Supported on Heteroatom-Incorporated SBA-15 Silica: Impact of Heteroatom Type and Loading on Sorbent Structure and Adsorption Performance. *Chem. Eur. J.* **2012**, *18*, 16649–16664.

(67) Son, W. J.; Choi, J. S.; Ahn, W. S. Adsorptive Removal of Carbon Dioxide Using Polyethyleneimine-Loaded Mesoporous Silica Materials. *Microporous Mesoporous Mater.* **2008**, *113*, 31–40.

(68) Tanthana, J.; Chuang, S. S. C. In Situ Infrared Study of the Role of PEG in Stabilizing Silica-Supported Amines for CO_2 Capture. *ChemSusChem* **2010**, *3*, 957–964.

(69) Wang, X. X.; Schwartz, V.; Clark, J. C.; Ma, X. L.; Overbury, S. H.; Xu, X. C.; Song, C. Infrared Study of CO_2 Sorption over "Molecular Basket" Sorbent Consisting of Polyethylenimine-Modified Mesoporous Molecular Sieve. *J. Phys. Chem. C* **2009**, *113*, 7260–7268.

(70) Lu, C. Y.; Bai, H. L.; Su, F. S.; Chen, W. F.; Hwang, J. F.; Lee, H. H. Adsorption of Carbon Dioxide from Gas Streams via Mesoporous Spherical-Silica Particles. *J. Air Waste Manage. Assoc.* **2010**, *60*, 489–496.

(71) Zheng, F.; Tran, D. N.; Busche, B. J.; Fryxell, G. E.; Addleman, R. S.; Zemanian, T. S.; Aardahl, C. L. Ethylenediamine-Modified SBA-15 as Regenerable CO_2 Sorbent. *Ind. Eng. Chem. Res.* **2005**, *44*, 3099–3105.

(72) Gray, M. L.; Hoffman, J. S.; Hreha, D. C.; Fauth, D. J.; Hedges, S. W.; Champagne, K. J.; Pennline, H. W. Parametric Study of Solid Amine Sorbents for the Capture of Carbon Dioxide. *Energy Fuels* **2009**, *23*, 4840–4844.

(73) Sayari, A.; Belmabkhout, Y. Stabilization of Amine-Containing CO_2 Adsorbents: Dramatic Effect of Water Vapor. *J. Am. Chem. Soc.* **2010**, *132*, 6312–6314.

(74) Kim, S.; Ida, J.; Guliants, V. V; Lin, J. Y. S. Tailoring Pore Properties of MCM-48 Silica for Selective Adsorption of CO_2. *J. Phys. Chem. B* **2005**, *109*, 6287–6293.

(75) Hammache, S.; Hoffman, J.; Gray, M. L.; Fauth, D.; Howard, B.; Pennline, H. Comprehensive Study of the Impact of Steam on Polyethyleneimine on Silica for CO_2 Capture. *Energy Fuels* **2013**, *27*, 6899–6905.

(76) Wang, Z.; Fang, M.; Pan, Y.; Yan, S.; Luo, Z. Amine-Based Absorbents Selection for CO_2 Membrane Vacuum Regeneration Technology by Combined Absorption–desorption Analysis. *Chem. Eng. Sci.* **2013**, *93*, 238–249.

(77) Sakwa-Novak, M. A.; Jones, C. W. Steam Induced Structural Changes of a Poly(ethyleneimine) Impregnated Gamma-Alumina Sorbent for CO_2 Extraction from Ambient Air. *ACS Appl. Mater. Interfaces* **2014**.

(78) Belmabkhout, Y.; Sayari, A. Isothermal versus Non-Isothermal Adsorption-Desorption Cycling of Triamine-Grafted Pore-Expanded MCM-41 Mesoporous Silica for CO_2 Capture from Flue Gas. *Energy Fuels* **2010**, *24*, 5273–5280.

(79) Chaffee, A. L.; Knowles, G. P.; Liang, Z.; Zhany, J.; Xiao, P.; Webley, P. A. CO_2 Capture by Adsorption: Materials and Process Development. *Int. J. Greenh. Gas Control* **2007**, *1*, 11–18.

(80) Lu, C. Y.; Su, F. S.; Hsu, S. C.; Chen, W. F.; Bai, H. L.; Hwang, J. F.; Lee, H. H. Thermodynamics and Regeneration of CO_2 Adsorption on Mesoporous Spherical-Silica Particles. *Fuel Process. Technol.* **2009**, *90*, 1543–1549.

(81) Liu, X. W.; Zhou, L.; Fu, X.; Sun, Y.; Su, W.; Zhou, Y. P. Adsorption and Regeneration Study of the Mesoporous Adsorbent SBA-15 Adapted to the Capture/separation of CO_2 and CH4. *Chem. Eng. Sci.* **2007**, *62*, 1101–1110.

(82) Knowles, G. P.; Graham, J. V; Delaney, S. W.; Chaffee, A. L. Aminopropyl-Functionalized Mesoporous Silicas as CO_2 Adsorbents. *Fuel Process. Technol.* **2005**, *86*, 1435–1448.

(83) Zelenak, V.; Halamova, D.; Gaberova, L.; Bloch, E.; Llewellyn, P. L. Amine-Modified SBA-12 Mesoporous Silica for Carbon Dioxide Capture: Effect of Amine Basicity on Sorption Properties. *Microporous Mesoporous Mater.* **2008**, *116*, 358–364.

(84) Liang, Z. J.; Fadhel, B.; Schneider, C. J.; Chaffee, A. L. Adsorption of CO_2 on Mesocellular Siliceous Foam Iteratively Functionalized with Dendrimers. *Adsorpt. Int. Adsorpt. Soc.* **2009**, *15*, 429–437.

(85) Wang, L. F.; Ma, L.; Wang, A. Q.; Liu, Q.; Mang, T. CO_2 Adsorption on SBA-15 Modified by Aminosilane. *Chinese J. Catal.* **2007**, *28*, 805–810.

(86) Bacsik, Z.; Atluri, R.; Garcia-Bennett, A. E.; Hedin, N. Temperature-Induced Uptake of CO_2 and Formation of Carbamates in Mesocaged Silica Modified with N-Propylamines. *Langmuir* **2010**, *26*, 10013–10024.

(87) Sanz, R.; Calleja, G.; Arencibia, A.; Sanz-Perez, E. S. CO_2 Adsorption on Branched Polyethyleneimine-Impregnated Mesoporous Silica SBA-15. *Appl. Surf. Sci.* **2010**, *256*, 5323–5328.

(88) Wurzbacher, J. A.; Gebald, C.; Steinfeld, A. Separation of CO_2 from Air by Temperature-Vacuum Swing Adsorption Using Diamine-Functionalized Silica Gel. *Energy Environ. Sci.* **2011**, *4*, 3584–3592.

(89) Wurzbacher, J. A.; Gebald, C.; Piatkowski, N.; Steinfeld, A. Concurrent Separation of CO_2 and H_2O from Air by a Temperature-Vacuum Swing Adsorption/Desorption Cycle. *Environ. Sci. Technol.* **2012**, *46*, 9191–9198.

(90) Serna-Guerrero, R.; Belmabkhout, Y.; Sayari, A. Further Investigations of CO_2 Capture Using Triamine-Grafted Pore-Expanded Mesoporous Silica. *Chem. Eng. J.* **2010**, *158*, 513–519.

(91) Serna-Guerrero, R.; Belmabkhout, Y.; Sayari, A. Influence of Regeneration Conditions on the Cyclic Performance of Amine- Grafted Mesoporous Silica for

CO_2 Capture: An Experimental and Statistical Study. *Chem. Eng. Sci.* **2010**, *65*, 4166–4172.

(92) Srivastava, R. K.; Jozewicz, W.; Singer, C. SO_2 Scrubbing Technologies: A Review. *Environ. Prog.* **2001**, *20*, 219–228.

(93) Rochelle, G. T.; King, C. J. The Effect of Additives on Mass Transfer in $CaCO_3$ or CaO Slurry Scrubbing of SO_2 from Waste Gases. *Ind. Eng. Chem. Fundam.* **1977**, *16*, 67–75.

(94) Valdessolis, T.; Marban, G.; Fuertes, A. B. Low-Temperature SCR of NO_x with NH_3 over Carbon-Ceramic Supported Catalysts. *Appl. Catal. B* **2003**, *46*, 261–271.

(95) Chi, S.; Rochelle, G. T. Oxidative Degradation of Monoethanolamine. *Ind. Eng. Chem. Res.* **2002**, *41*, 4178–4186.

(96) Strazisar, B. R.; Anderson, R. R.; White, C. M. Degradation Pathways for Monoethanolamine in a CO_2 Capture Facility. *Energy Fuels* **2003**, *17*, 1034–1039.

(97) Sexton, A. J. Amine Oxidation in CO_2 Capture Processes. *Dissertation*, University of Texas at Austin, 2008.

(98) Goff, G. S.; Rochelle, G. T. Oxidation Inhibitors for Copper and Iron Catalyzed Degradation of Monoethanolamine in CO_2 Capture Processes. *Ind. Eng. Chem. Res.* **2006**, *45*, 2513–2521.

(99) Yagi, T.; Shibuya, H.; Sasaki, T. Application of Chemical Absorption Process to CO_2 Recovery from Flue Gas Generated in Power Plants. *Energy Convers. Mgmt.* **1992**, *33*, 349–355.

(100) Diaf, A.; Garcia, J.; Beckman, E. Thermally Reversible Polymeric Sorbents for Acid Gases: CO_2, SO_2, and NO_x. *J. Appl. Polym. Sci.* **1994**, *53*, 857–875.

(101) Diaf, A.; Beckman, E. Thermally Reversible Polymeric Sorbents for Acid Gases . III . CO_2-Sorption Enhancement in Polymer-Anchored Amines. *React. Funct. Polym.* **1995**, *27*, 45–51.

(102) Khatri, R. A.; Chuang, S. S. C.; Soong, Y.; Gray, M. L. Thermal and Chemical Stability of Regenerable Solid Amine Sorbent for CO_2 Capture. *Energy Fuels* **2006**, *20*, 1514–1520.

(103) Xu, X. C.; Song, C.; Miller, B. G.; Scaroni, A. W. Adsorption Separation of Carbon Dioxide from Flue Gas of Natural Gas-Fired Boiler by a Novel Nanoporous “Molecular Basket” Adsorbent. *Fuel Process. Technol.* **2005**, *86*, 1457–1472.

(104) Liu, Y.; Ye, Q.; Shen, M.; Shi, J.; Chen, J.; Pan, H.; Shi, Y. Carbon Dioxide Capture by Functionalized Solid Amine Sorbents with Simulated Flue Gas Conditions. *Environ. Sci. Technol.* **2011**, *45*, 5710–5716.

(105) Rezaei, F.; Jones, C. W. Stability of Supported Amine Adsorbents to SO_2 and NO_x in Postcombustion CO_2 Capture. 1. Single-Component Adsorption. *Ind. Eng. Chem. Res.* **2013**, *52*, 12192–12201.

(106) Xu, M. H.; Yan, R.; Zheng, C. G.; Qiao, Y.; Han, J.; Sheng, C. D. Status of Trace Element Emission in a Coal Combustion Process: A Review. *Fuel Process. Technol.* **2004**, *85*, 215–237.

(107) Hatanpaa, E.; Kajander, K.; Laitinen, T. G.; Piepponen, S.; Revitzer, H. A Study of Trace Element Behavior in Two Modern Coal-Fired Power Plants I. Development and Optimization of Trace Element Analysis Using Reference Materials. *Fuel Process. Technol.* **1997**, *51*, 205–217.

(108) Pavlish, J. H.; Sondreal, E. A.; Mann, M. D.; Olson, E. S.; Galbreath, K. C.; Laudal, D. L.; Benson, S. A. Status Review of Mercury Control Options for Coal-Fired Power Plants. *Fuel Process. Technol.* **2003**, *82*, 89–165.

(109) Strazisar, B. R.; Anderson, R. R.; White, C. M. Degradation Pathways for Monoethanolamine in a CO_2 Capture Facility. *Energy Fuels* **2003**, *17*, 1034–1039.

(110) Cui, Z.; Aroonwilas, A.; Veawab, A. Simultaneous Capture of Mercury and CO_2 in Amine-Based CO_2 Absorption Process. *Ind. Eng. Chem. Res.* **2010**, *49*, 12576–12586.

(111) Langeroudi, E. G.; Kleitz, F.; Iliuta, M. C. Grafted Amine/CO_2 Interactions in Gas-Liquid-Solid Adsorption/Absorption Equilibria. *J. Phys. Chem. C* **2009**, *113*.

(112) Ma, X. L.; Wang, X. X.; Song, C. "Molecular Basket" Sorbents for Separation of CO_2 and H_2S from Various Gas Streams. *J. Am. Chem. Soc.* **2009**, *131*, 5777–5783.

(113) Danon, A.; Stair, P. C.; Weitz, E. FTIR Study of CO_2 Adsorption on Amine-Grafted SBA-15: Elucidation of Adsorbed Species. *J. Phys. Chem. C* **2011**, *115*, 11540–11549.

(114) Bacsik, Z.; Ahlsten, N.; Ziadi, A.; Zhao, G.; Garcia-Bennett, A. E.; Martín-Matute, B.; Hedin, N. Mechanisms and Kinetics for Sorption of CO_2 on Bicontinuous Mesoporous Silica Modified with N-Propylamine. *Langmuir* **2011**, *27*, 11118–11128.

(115) Aziz, B.; Hedin, N.; Bacsik, Z. Quantification of Chemisorption and Physisorption of Carbon Dioxide on Porous Silica Modified by Propylamines : Effect of Amine Density. *Microporous Mesoporous Mater.* **2012**, *159*, 42–49.

(116) Pinto, M.; Mafra, L.; Guil, J.; Pires, J.; Rocha, J. Adsorption and Activation of CO_2 by Amine-Modified Nanoporous Materials Studied by Solid-State NMR and $^{13}CO_2$ Adsorption. *Chem. Mater.* **2011**, *23*, 1387–1395.

(117) Chang, A. C. C.; Chuang, S. S. C.; Gray, M. L.; Soong, Y. In-Situ Infrared Study of CO_2 Adsorption on SBA-15 Grafted with Gamma-(aminopropyl)triethoxysilane. *Energy Fuels* **2003**, *17*, 468–473.

(118) Satyapal, S.; Filburn, T.; Trela, J.; Strange, J. Performance and Properties of a Solid Amine Sorbent for Carbon Dioxide Removal in Space Life Support Applications. *Energy Fuels* **2001**, *15*, 250–255.

(119) Lackner, K. S.; Ziock, H.; Grimes, P. Carbon Dioxide Extraction from Air: Is It an Option? In *24th International Conference on Coal Utilization & Fuel Systems*; Clearwater, FL, 1999.

(120) Lackner, K. S.; Brennan, S. Envisioning Carbon Capture and Storage: Expanded Possibilities due to Air Capture, Leakage Insurance, and C-14 Monitoring. *Clim. Change* **2009**, *96*, 357–378.

(121) Eisenberger, P. M.; Cohen, R. W.; Chichilnisky, G.; Eisenberger, N. M.; Chance, R. R.; Jones, C. W. Global Warming and Carbon-Negative Technology: Prospects for a Lower-Cost Route to a Lower-Risk Atmosphere. *Energy Environ.* **2009**, *20*, 973–984.

(122) Choi, S.; Drese, J. H.; Eisenberger, P. M.; Jones, C. W. A New Paradigm of Anthropogenic CO2 Reduction: Adsorptive Fixation of CO_2 from the Ambient Air as a Carbon Negative Technology. In *AIChE Annual Meeting*; Nashville, 2009.

(123) Choi, S.; Drese, J. H.; Eisenberger, P. M.; Jones, C. W. Application of Amine-Tethered Solid Sorbents for Direct CO_2 Capture from the Ambient Air. *Environ. Sci. Technol.* **2011**, *45*, 2420–2427.

(124) Choi, S.; Gray, M. L.; Jones, C. W. Amine-Tethered Solid Adsorbents Coupling High Adsorption Capacity and Regenerability for CO_2 Capture from Ambient Air. *ChemSusChem* **2011**, *4*, 628–635.

(125) Chaikittisilp, W.; Khunsupat, R.; Chen, T. T.; Jones, C. W. Poly(allylamine)-Mesoporous Silica Composite Materials for CO_2 Capture from Simulated Flue Gas or Ambient Air. *Ind. Eng. Chem. Res.* **2011**, *50*, 14203–14210.

(126) Chaikittisilp, W.; Lunn, J. D.; Shantz, D. F.; Jones, C. W. Poly(L-Lysine) Brush-Mesoporous Silica Hybrid Material as a Biomolecule-Based Adsorbent for CO_2 Capture from Simulated Flue Gas and Air. *Chem. Eur. J.* **2011**, *17*, 10556–10561.

(127) Stuckert, N. R.; Yang, R. T. CO_2 Capture from the Atmosphere and Simultaneous Concentration Using Zeolites and Amine-Grafted SBA-15. *Environ. Sci. Technol.* **2011**, *45*, 10257–10264.

(128) Gebald, C.; Wurzbacher, J. A.; Tingaut, P.; Zimmermann, T.; Steinfeld, A. Amine-Based Nanofibrillated Cellulose as Adsorbent for CO_2 Capture from Air. *Environ. Sci. Technol.* **2011**, *45*, 9101–9208.

(129) Goeppert, A.; Czaun, M.; May, R. B.; Prakash, G. K. S.; Olah, G. A.; Narayanan, S. R. Carbon Dioxide Capture from the Air Using a Polyamine Based Regenerable Solid Adsorbent. *J. Am. Chem. Soc.* **2011**,*133,* 20164-20167.

(130) Wang, X.; Ma, X.; Schwartz, V.; Clark, J. C.; Overbury, S. H.; Zhao, S.; Xu, X.; Song, C. A Solid Molecular Basket Sorbent for CO2 Capture from Gas Streams with Low CO_2 Concentration under Ambient Conditions. *Phys. Chem. Chem. Phys.* **2012**, *14*, 1485–1492.

(131) Didas, S. A.; Kulkarni, A. R.; Sholl, D. S.; Jones, C. W. Role of Amine Structure on Carbon Dioxide Adsorption from Ultradilute Gas Streams such as Ambient Air. *ChemSusChem* **2012**, *5*, 2058–2064.

(132) He, L.; Fan, M.; Dutcher, B.; Cui, S.; Shen, X.; Kong, Y.; Russell, A. G.; McCurdy, P. Dynamic Separation of Ultradilute CO_2 with a Nanoporous Amine-Based Sorbent. *Chem. Eng. J.* **2012**, *189-190*, 13–23.

(133) Kulkarni, A. R.; Sholl, D. S. Analysis of Equilibrium-Based TSA Processes for Direct Capture of CO_2 from Air. *Ind. Eng. Chem. Res.* **2012**, *51*, 8631–8645.

(134) Rahaman, M. S. A.; Zhang, L.; Cheng, L.-H.; Xu, X.-H.; Chen, H.-L. Capturing Carbon Dioxide from Air Using a Fixed Carrier Facilitated Transport Membrane. *RSC Adv.* **2012**, *2*, 9165–9172.

(135) Goldberg, D. S.; Lackner, K. S.; Han, P.; Slagle, A. L.; Wang, T. Co-Location of Air Capture, Subseafloor CO_2 Sequestration, and Energy Production on the Kerguelen Plateau. *Environ. Sci. Technol.* **2013**, *47*, 7521–7529.

(136) Gebald, C.; Wurzbacher, J. A.; Tingaut, P.; Steinfeld, A. Stability of Amine-Functionalized Cellulose during Temperature-Vacuum-Swing Cycling for CO_2 Capture from Air. *Environ. Sci. Technol.* **2013**, *47*, 10063–10070.

(137) Lu, W.; Sculley, J. P.; Yuan, D.; Krishna, R.; Zhou, H.-C. Carbon Dioxide Capture from Air Using Amine-Grafted Porous Polymer Networks. *J. Phys. Chem. C* **2013**, *117*, 4057–4061.

(138) He, H.; Zhong, M.; Konkolewicz, D.; Yacatto, K.; Rappold, T.; Sugar, G.; David, N. E.; Matyjaszewski, K. Carbon Black Functionalized with Hyperbranched Polymers: Synthesis, Characterization, and Application in Reversible CO_2 Capture. *J. Mater. Chem. A* **2013**, *1*, 6810–6821.

(139) He, H.; Li, W.; Zhong, M.; Konkolewicz, D.; Wu, D.; Yaccato, K.; Rappold, T.; Sugar, G.; David, N. E.; Matyjaszewski, K. Reversible CO_2 Capture with Porous Polymers Using the Humidity Swing. *Energy Environ. Sci.* **2013**, *6*, 488–493.

(140) Wörmeyer, K.; Smirnova, I. Adsorption of CO_2, Moisture and Ethanol at Low Partial Pressure Using Aminofunctionalised Silica Aerogels. *Chem. Eng. J.* **2013**, *225*, 350–357.

(141) Gebald, C.; Wurzbacher, J. a; Borgschulte, A.; Zimmermann, T.; Steinfeld, A. Single-Component and Binary CO_2 and H_2O Adsorption of Amine-Functionalized Cellulose. *Environ. Sci. Technol.* **2014**, *48*, 2497–2504.

Chapter 2

THERMAL, OXIDATIVE AND CO_2 INDUCED DEGRADATION OF PRIMARY AMINES: EFFECT OF ALKYL LINKER ON STABILITY

Parts of this chapter are reproduced from 'Didas, S.A.; Zhu, R.; Brunelli, N.A.; Sholl, D.S.; Jones, C.W. Thermal, Oxidative and CO_2 Induced Degradation of Primary Amines Used for CO_2 Capture: Effect of Alkyl Linker. *J. Phys. Chem. C.* **2014**, *118*, 12302-12311.'

2.1 Background

As mentioned in chapter 1, increased levels of carbon dioxide in the atmosphere have prompted research efforts into the capture and sequestration of CO_2. Supported amine adsorbent materials have emerged as promising materials for both flue gas as well as air capture processes due to the materials' high equilibrium adsorption capacities, ease of regeneration, fast adsorption kinetics and improved efficiency under humid conditions.[1–4]

Today, the majority of research on supported amine adsorbents still focuses on incremental adsorption capacity improvements.[2] However, increasingly, researchers are starting to look at practical issues that will affect the eventual implementation of these materials by investigating other critical aspects such as kinetics,[5–11] contactor design,[12–19] regeneration conditions[6,20–35] and material stability.[21,24,27,33,35–50] The topic of material stability is especially important as it can affect the adsorbent lifetime and therefore the

operating costs of the process. The presence of gaseous species in both flue gas and ambient air such as oxygen, steam, SO_x, NO_x and CO_2 itself make it possible for side reactions to occur that can deactivate the adsorbent and thus decrease its adsorption capabilities. Therefore, before these materials can be used in any practical application, it is essential that the possibility of sorbent deactivation be examined and addressed.

Most of the studies on sorbent stability so far have been with respect to oxidative degradation.[36–43] In 2011, Bollini et al.[36] and Heydari-Gorji et al.[37] independently reported the effects of oxidation on primary, secondary and tertiary monoamines as well as primary-secondary mixed amines as a function of temperature. Both studies reported that primary and tertiary amines possess oxidative stability while secondary and mixed amines that include a secondary amine are unstable at temperatures above 80 °C. Interestingly, the mixed amine materials that contained a primary amine underwent complete deactivation, suggesting that the degradation products or intermediates associated with the secondary amine reacted with the primary amine to deactivate all of the adsorption sites. In 2012 Heydari-Gorji et al. evaluated the stability of branched and linear PEI impregnated sorbents, which contain primary, secondary and tertiary amines, with respect to air, simulated flue gas and $CO_2/O_2/N_2$ gas mixtures, thereby evaluating thermal, oxidative and CO_2 induced degradation of the adsorbents.[39] Control experiments carried out in pure nitrogen with temperatures ranging from 75-150 °C showed that all materials possessed thermal stability. A slight loss in organic content was observed for the lowest molecular weight PEI but this was attributed to evaporation of TEPA, which was also present in the polymer mixture. Deactivation from CO_2 via urea formation was observed under dry conditions; however this could be avoided with humidified gas

streams. Mixtures of $CO_2/O_2/N_2$ showed that the presence of CO_2, when humidified, can stabilize the material towards oxidative degradation due to the faster reaction of CO_2 with the amine as compared to O_2. In 2013, Bali et al. investigated the oxidative stability of impregnated PAA, an all primary aminopolymer, as well as branched PEI on an alumina support.[42] They showed that PAA, while not fully stable as in the case of grafted primary amine sorbents, possessed dramatically increased stability towards oxidative degradation compared to PEI. A loss of 10% in adsorption capacity was observed for the most extreme treatment condition of 21% O_2 at 105 °C, whereas the PEI based material lost 70% of its capacity. However, it was hypothesized that thermal as opposed to oxidative degradation may have played a role in the loss of PAA's adsorption performance as indications of oxidation (imines, amides) could not be confirmed spectroscopically for this material.

CO_2-induced deactivation of supported amine adsorbents was first noted by Drage et al.[21] in 2008 and since then has predominantly been investigated by Sayari's group.[27,35,39,44,45] Drage et al. found that when regenerating silica supported PEI adsorbents at elevated temperatures of 110-140 °C in pure CO_2 that a weight gain occurred, coupled with deactivation of the sorbent's capacity upon repeated adsorption cycles.[21] This was attributed to chemical reaction of CO_2 with the amines at high temperatures to form irreversible urea linkages. Similar thermal stability studies at high temperatures in pure nitrogen showed that the materials were thermally stable. In 2010 Sayari et al. looked at different temperature swing desorption parameters using pure CO_2 for grafted primary monoamine and (primary-secondary containing) triamine materials as well as PEI impregnated silica.[27] It was found that under dry adsorption-desorption

conditions the primary amine material lost adsorption capacity due to formation of urea, which was verified via solid state NMR. It was also found that humidity prevented the deactivation from occurring. In 2012, Sayari subsequently presented two studies of CO_2-induced deactivation of amine supported materials. The first considered solely grafted amines, specifically a primary, secondary and tertiary monoamine along with a primary-secondary triamine.[44] It was found that the primary amine material was the only monoamine to deactivate due to urea formation and that the primary-secondary triamine also deactivated. Therefore it was proposed that isocyanate was a reaction intermediate to urea formation, which only a primary amine can form.

Later in 2012 Sayari et al. published a more comprehensive study looking at the grafted amines previously studied as well as the silica supported polymeric amines branched PEI, linear PEI and PAA.[45] All materials were subject to dry adsorption-desorption cycling in pure CO_2 with adsorption temperatures of 50 and 100 ºC and desorption temperatures ranging from 130-160 ºC. The treated materials were then analyzed via DRIFT and ^{13}C CP MAS NMR spectroscopy. All the materials except for the secondary monoamine material were found to be unstable under mild conditions and prone to deactivation via the formation of open chain and/or cyclic ureas, which was confirmed spectroscopically. Based on the observed degradation products, two deactivation mechanisms were proposed for the formation of open chain and cyclic ureas, as depicted in Figure 2.1. The first pathway consisted of dehydration of a carbamic acid to an isocyanate intermediate that could then go on to form urea. The second route was conversion of carbamic acid to ammonium carbamate that then dehydrated to form urea; this is the only possible pathway to urea formation for all secondary amine containing

materials. The isocyanate pathway must be initiated with a primary amine, but can proceed in the second step with primary or secondary amine, which would explain why polymeric amines and triamines deactivate as well. While this seems to be the most likely pathway for urea formation to occur, the alternative route whereby urea is formed from ammonium carbamate could not be ruled out for primary amine containing materials.

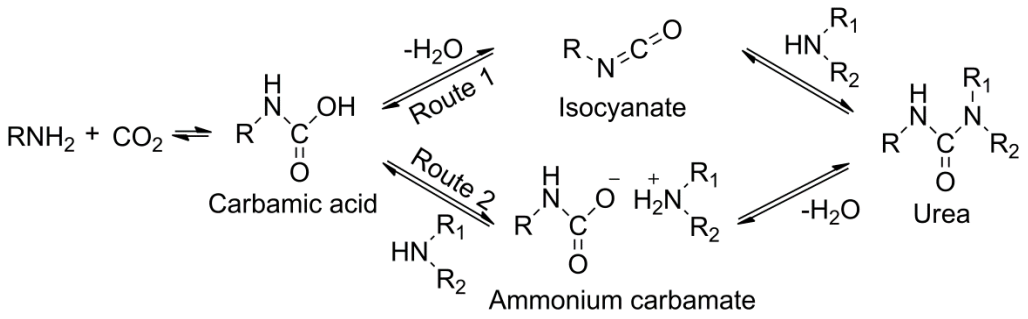

Figure 2.1. Reaction pathways proposed by Sayari for the deactivation of amines through open chain urea formation.[45]

Based on the results of previous studies with respect to stability, primary amines have emerged as a favorable amine type for CO_2 capture processes as they are the most oxidatively stable and because CO_2-induced deactivation can be avoided with humid gas streams. Additionally, primary amines have been found to be the most efficient amine type for adsorbing CO_2 at flue gas as well as air capture conditions, as will be discussed in chapter 3. More recently, a new set of primary aminosilane grafted materials have been developed in our group, with methyl and ethyl alkyl chains on the organosilane.[51] These materials can be used to tailor the interactions between the amines and the surface both for catalytic applications as well as CO_2 capture. Additionally, they can be implemented into supports with smaller pore sizes due to the smaller size of the aminosilane molecule.

One example of this is the report by Kang et al., whereby single-walled aminoaluminosilicate nanotubes were synthesized for the first time using aminomethylsilane to incorporate amine functionalities into the nanotubes.[52] These nanotubes showed improved adsorption selectivity for CO_2/CH_4 and CO_2/N_2 separations as compared to the bare nanotube. With the promising oxidative results of PAA aminopolymer and grafted propylamine based adsorbents, and the emerging use of new smaller linker primary aminosilanes, it is worthwhile to investigate the stability of these new aminosilanes as it pertains to CO_2, O_2 and thermal induced deactivation to elucidate how they compare to their propylamine counterparts. Thus, the objective of this work is to examine the stability of different alkyl chain length primary amines supported on silica to thermal, oxidative and CO_2 induced degradation using prolonged isothermal conditions to accelerate the effects of degradation. In addition to degradation experiments, DFT calculations were also performed to examine the effects of different alkyl chain lengths on CO_2 induced deactivation using the proposed routes by Sayari et al. A definitive pathway for deactivation is proposed.

2.2 Experiments

2.2.1 Materials Synthesis

SBA-15 was the silica support used for this study and was synthesized using methods previously reported in literature.[51] Briefly, 24 g of Pluronic 123 was dissolved in 120 mL of concentrated hydrochloric acid and 636 mL distilled water. Next 46.26 g of tetraethylorthosilicate (TEOS) was added to the mixture and stirred at 40 ºC for 20 h after which the stir bar was removed and heating continued for 24 h at 100 ºC. The reaction was quenched with distilled water, the solids were then filtered and washed with copious

amounts of distilled water and then dried overnight in a 75 °C oven. The surfactant was removed via calcination in flowing air with the following protocol: ramp to 200 °C at 1.2 °C min^{-1} and hold for 1 h, ramp to 550 °C at 1.2 °C min^{-1} and soak for 6 h then cool to ambient temperature at 10 °C min^{-1}.

Silanes that were not commercially available (aminomethyltriethoxysilane and 2-aminoethyltrimethoxysilane) were synthesized using previously reported methods.[51] A brief description of the synthesis is as follows: 10 g of the terminally halogenated alkyltri(m)ethoxysilane was added to a 50 mL Parr reactor. Helium was passed through the reactor to remove air before closing the outlet valve. Ammonia was then condensed inside the reactor via cooling with liquid nitrogen while stirring the reactor. Once a sufficient amount of ammonia was inside the reactor, the inlet valve was closed and the reactor was heated to 100 ° for 5 h under stirring with the reactor pressure reaching 900-1000 psi. The reactor was then cooled to room temperature and excess ammonia was exhausted and purged with helium steam. Next the reactor was opened in a fume hood and 20 mL of anhydrous pentane was added to precipitate the ammonium chloride salt. The mixture was then filtered and purified using a rotovap followed by vacuum distillation. Proton NMR characterization was used to confirm the synthesis of the organosilanes.

Amine-functionalized materials were prepared by first drying 0.5 g calcined SBA-15 on a Schlenk line overnight at 110 °C. The round bottom was then capped with a rubber septum and degassed with UHP nitrogen for 30 min. Next 12.5 mL dry toluene mixed with a 2x excess of the desired molar amount of aminosilane with respect to the amount of silica was injected into the round bottom containing the silica with stirring.

The mixture was stirred at room temperature for 24 h, after which 10 uL distilled water was added and the solution was heated to 80 °C to react for another 24 h. The resulting solid was then cooled, filtered and washed with copious amounts of toluene, hexane and ethanol. It was then dried overnight at reduced pressure (10 mTorr) and 100 ºC.

2.2.2 Materials Characterization

Elemental analysis (Atlantic Microlabs, Norcross, GA, USA) was used to determine nitrogen content of synthesized and CO_2 treated materials. Nitrogen physisorption measurements were obtained using a Micromeritics Tristar II. Isotherms were measured at 77 K and the resulting data was used to determine surface areas and pore volume. The Brunauer-Emmett-Teller (BET) model was used to estimate surface area while the BdB-FHH method was used to determine pore size distribution and pore volume. ^{13}C CP-MAS solid state NMR was used to evaluate the materials before and after degradation treatments. Measurements were taken on a Bruker DSX-300 spectrometer. Samples were spun at a frequency of 10 kHz. A TA Instruments Q500 TGA was used to evaluate dry adsorption capacities of materials before and after degradation experiments. A typical adsorption run consisted of pretreating the material with pure He gas at 120 ºC for 3 h and then cooling to 30 °C before switching to a gas mixture of 10% CO_2 in He for 3 h of adsorption.

2.2.3 Degradation Experiments

To evaluate the stability of materials to various types of degradation, packed bed experiments were performed whereby 80 mg of sample was loaded into a 1 cm diameter Pyrex tube with a frit in the middle to hold the material in place. Samples were first

pretreated by heating to 120 ºC in flowing nitrogen gas at 20 mL min^{-1} for 3 h to remove preadsorbed water or CO_2. The temperature was then increased to 135 ºC and the gas was either switched to pure CO_2 or O_2 or maintained with N_2 for thermal degradation experiments. For CO_2 and thermal degradation, gas was flowed at 135 ºC for 4 d. The CO_2 treatment was designed to simulate the prolonged CO_2 exposure associated with multiple adsorption-desorption cycles. For the oxidative degradation experiments, 20 h of reaction time was used, as this timescale has been shown in the past to be sufficient to produce significant degradation for materials that are not stable.[36] The material was then recovered for post-treatment analysis.

2.3 Modeling

All calculations were carried out using the Gaussian 09 program.[53] The geometric parameters of the reactants, products, intermediates and transition states along reaction pathways were optimized at the B3LYP level of theory (i.e., Becke's three-parameter nonlocal exchange functional[54] with the non-local correlation functional of Lee, Yang, and Parr[55]) using the 6-311+G** basis set. All the stationary points have been identified for local minima and transition states by vibrational analysis. Intrinsic reaction coordinate analyses[56] have been performed to confirm the connection between transition states and designated reactants, products or intermediates. On the basis of the optimized geometries, single-point energies of the stationary points for the lowest-energy pathways were refined using the coupled-cluster theory with single, double, and noniterative triple excitations (CCSD(T)) combined with the 6-311+G** basis set. Energy values were corrected with zero-point vibrational energies (ZPE) calculated at the B3LYP level.

2.4 Results & Discussion

2.4.1 Materials Synthesis & Characterization

Adsorbent materials were synthesized using primary aminosilanes with an alkyl chain length varying from methyl to propyl, as represented in Figure 2.2. These silanes were grafted onto a well-defined SBA-15 mesoporous silica support. Some difficulties were encountered in getting appreciably high amine loadings with the aminomethylsilane grafting procedure, even when adding catalytic agents such as ethylene diamine.[57] Therefore, only a low amine loading methyl material was prepared while ethyl and propyl materials were synthesized with low and high loadings. This way, a comparison could be made directly to the methyl material for the low loading adsorbents, while the higher loading materials allowed the observation of (i) how increased loading affects stability and (ii) what degradation behavior would look like for a practical adsorbent with a higher amine content. Material properties along with descriptions and nomenclature are presented in Table 2.1.

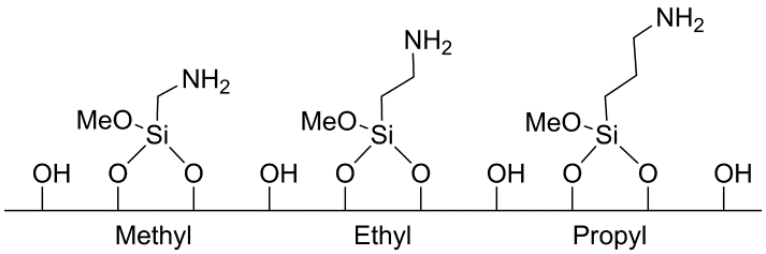

Figure 2.2. Aminosilanes grafted onto silica SBA-15 with one (methyl), two (ethyl), and three (propyl) carbon alkyl chains.

Table 2.1. Physical properties of bare support and amine functionalized materials.

Material	Material Abbreviation	BET SA (m^2 g_{SiO2}^{-1})	Amine Loading (mmol N g^{-1})
Bare silica support	SBA	675	--
Silica with methyl linker, low loading	SBA-Methyl-low	356	0.76
Silica with ethyl linker, low loading	SBA-Ethyl-low	340	0.85
Silica with ethyl linker	SBA-Ethyl	269	1.80
Silica with propyl linker, low loading	SBA-Propyl-low	347	0.74
Silica with propyl linker	SBA-Propyl	314	1.43

Previous work has been done in our group with this range of materials investigating their effect on acid-base cooperativity in catalysis as well as CO_2 capture performance as a function of the flexibility of the alkyl chain length. It was shown that for SBA-15 silica supports, three carbons was the critical chain length required to reach optimized catalytic as well as adsorption efficiency.[51] This was due to the fact that the shorter chains had a limited range of flexibility and could not interact with surface silanols. Work by Danon et al. using FTIR spectroscopy to observe the nature of adsorbed CO_2 on grafted aminosilicas suggests that amine-silanol interactions are another route for CO_2 to adsorb onto the surface in dry conditions, as opposed to the more commonly discussed pathway of two amines adsorbing CO_2 to form a carbamate.[58] A schematic description of the potential interactions that can occur between amines and silanols based on alkyl chain length is shown in Figure 2.3. Based on these findings we

can assume that methyl and ethyl linker materials will only have interactions with neighboring amines while amines with propyl linkers can interact with surface silanols in addition to neighboring amines. In this study it will be possible to see if these interactions play a significant role in deactivation pathways for primary amine materials.

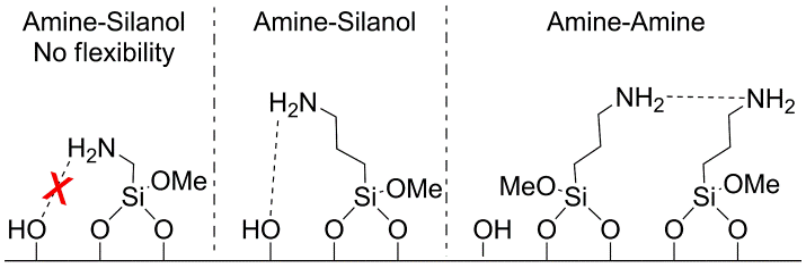

Figure 2.3. Proposed amine interactions with the surface and neighboring amines that can occur based on alkyl chain length. Amines with short alkyl chains have no ability (methyl) or very limited ability (ethyl) to interact with the silanols on the surface.

2.4.2 Degradation Experiments

2.4.2.1 Stability of Organic Content

Materials were evaluated for stability with respect to high temperature carbon dioxide and oxygen exposure conditions. Additionally, thermal stability was evaluated both as a control to the other experiments as well as to observe effects of prolonged high temperature exposure on the materials. Elemental analysis of the materials was obtained both before and after degradation experiments to see if there was any effect to the nitrogen content of the materials. The nitrogen content of the materials after degradation experiments at 135 ºC normalized to the fresh loading are presented in Figure 2.4. The results suggest that SBA-Methyl-low is thermally unstable, as it loses a considerable

amount of its nitrogen content after heating in any gas. A loss of approximately 80% of the organic content is observed even after heating in an inert gas. The lesser degree of deactivation for the oxygen treated material can be attributed to the fact that the material was thermally treated for a shorter period of time than in the inert gas case. The loss of amines from high temperature CO_2 and O_2 treatment of SBA-Methyl-low cannot be conclusively attributed to anything other than thermal cleavage due to the fact that the inert gas experiment gave similar results. The rest of the materials showed no appreciable loss of nitrogen from thermal, oxidative or CO_2 degradative conditions. The slight disparities in normalized loading for these materials fall within the expected variation of elemental analyses.[59] It is unclear what would cause the instability of a methyl alkyl chain vs. an ethyl or propyl alkyl between the amine and silicon atom. However, it is clear that aminomethyl functionalized materials may not be suitable for higher temperature applications as compared to their ethyl and propyl counterparts.

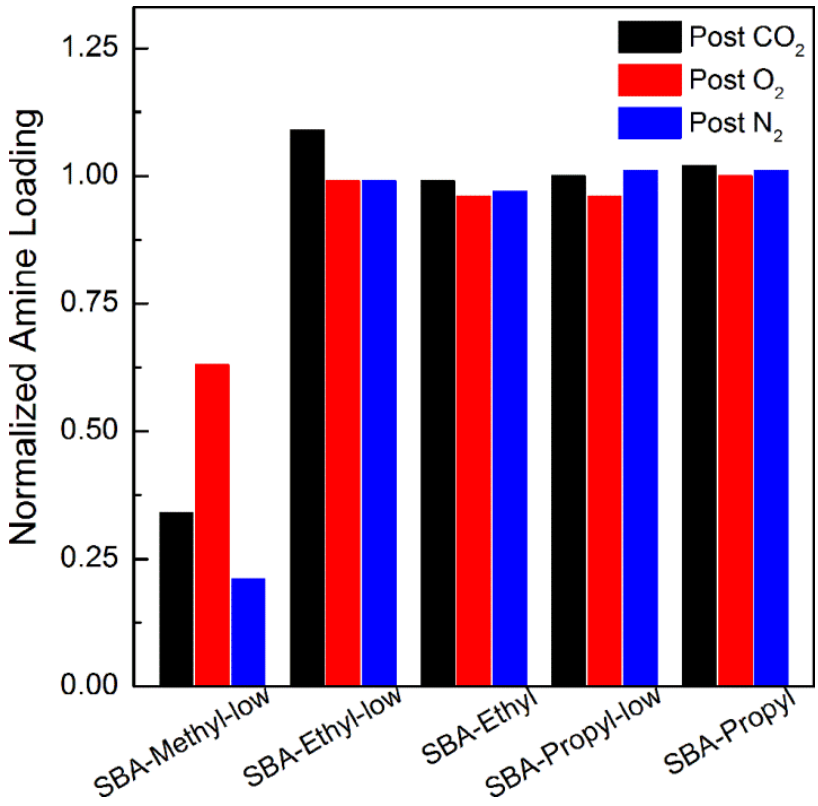

Figure 2.4. Nitrogen content of silica SBA-15 amine functionalized materials determined from elemental analysis after degradation at 135 ºC. Values are normalized to the initial nitrogen loading before degradation experiments.

2.4.2.2 Adsorption Capacity Measurements

Carbon dioxide adsorption capacities were evaluated for materials before and after degradation experiments to evaluate if there was any deactivation of the material's adsorptive performance. Due to the loss of amine content of SBA-Methyl-low, adsorption comparisons cannot be made for this material and so they are excluded in this part of the analysis. Normalized CO_2 adsorption capacities are presented in Figure 2.5 for the remaining four materials. From comparing post-oxidation to post-nitrogen treatment experiments it can be seen that any decrease in capacity can be attributed to thermal effects alone, and to some degree natural variability in TGA measurements. Therefore it

can be concluded that oxidative stability holds for all materials and that the length of the alkyl chain for primary amines as well as amine loading does not change its stability for ethyl and propyl linked materials. This result was expected for the propyl material due to previous research,[36,37] but here it is confirmed that a primary amine connected to an ethyl alkyl chain also does not undergo oxidative degradation under these conditions.

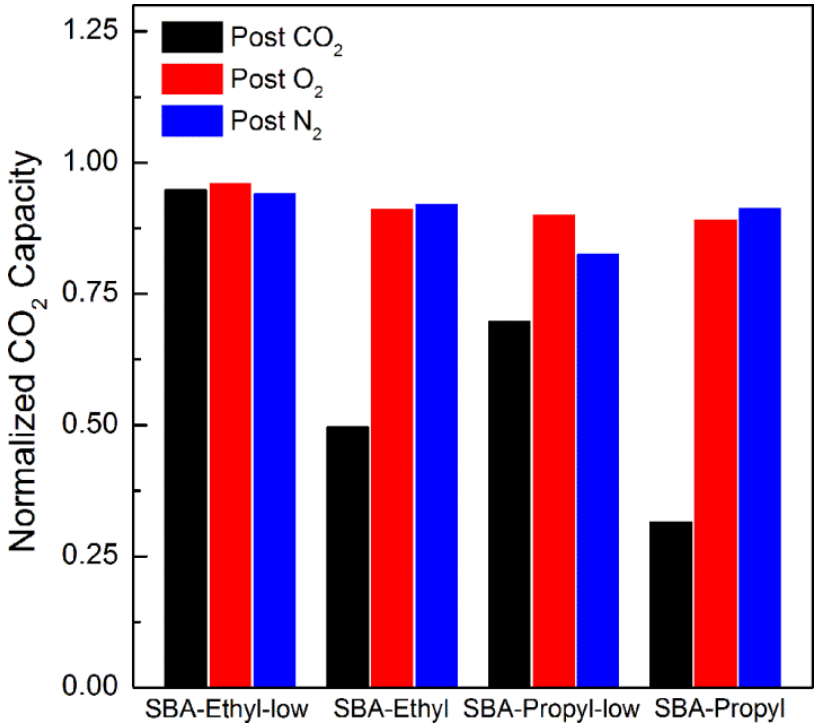

Figure 2.5. CO_2 adsorption capacities of silica SBA-15 amine functionalized adsorbents treated at 135 °C in flowing CO_2, O_2 or N_2. Values are normalized to the materials' original CO_2 adsorption capacity before degradation.

Differences in stability with these materials can most drastically be seen in the results from CO_2 induced degradation. It appears that SBA-Propyl has the greatest degree of deactivation from CO_2, followed by SBA-Ethyl, SBA-Propyl-low and finally SBA-Ethyl-low, which appears to undergo no deactivation at all. The stability of SBA-Ethyl-

low is likely due to the fact that the low surface coverage yields limited interactions with neighboring amines as well as the inability of the amine to interact with surface silanols due to the shortened alkyl chain. This is demonstrated by the lower amine efficiency of SBA-Ethyl-low compared to SBA-Propyl-low, with values of 0.13 vs. 0.17 respectively, as shown in Table 2.2. Deactivation is observed for SBA-Ethyl however, due to the fact that there is a high enough density of proximal amines that sufficient interaction and therefore urea formation can now readily occur. A small degree of deactivation is observed for SBA-Propyl-low. This suggests that there is either a greater clustering of amines on the surface[60,61] as compared to SBA-Ethyl-low, which facilitates amine interaction and urea formation, or that an improved ability to interact with surface silanols can propagate urea formation. This hypothesis is tested in the modeling portion of this work, below. A final observation from these data is that there is a greater degree of deactivation observed in SBA-Propyl as compared to SBA-Ethyl, which loses roughly 70% of its capacity versus roughly 50% for the latter. Considering the data in Table 2.2, it can be seen that the amine efficiencies for these materials initially are quite different, with values of 0.24 and 0.13, respectively. It is likely that the greater deactivation observed for SBA-Propyl is due to the increased amine efficiency of this material, as a greater extent of amine utilization for CO_2 capture translates to a greater degree being deactivated upon heating.

Table 2.2. Amine adsorption efficiencies of fresh materials compared to degraded materials in pure CO_2 at 135 °C.

	Amine Efficiency (mol CO_2 mol N^{-1})	
Sample	Fresh	Post CO_2 Treatment
SBA-Ethyl-low	0.13	0.13
SBA-Ethyl	0.13	0.07
SBA-Propyl-low	0.17	0.12
SBA-Propyl	0.24	0.07

2.4.2.3 Solid-State NMR Spectroscopy

^{13}C CP MAS NMR was used to analyze materials before and after degradation experiments to assess if any changes to the carbon chains in the material occurred. Given the observed trends from the CO_2 adsorption capacity data, it was mainly expected that structural changes would be seen in the SBA-Ethyl and SBA-Propyl(-low) spectra due to urea formation. Previous studies of amine degradation via urea formation in an aminopropylsilane functionalized silica material have reported the appearance of peaks at 160.5[27] and 159.6 ppm[45] corresponding to urea. The NMR spectra for these materials are presented in Figure 2.6-Figure 2.8. The spectrum for SBA-Methyl-low is shown in Figure 2.6. Shifts at 59.3, 25.7 and 16.3 ppm correspond to the two carbons from dangling ethoxy groups and the methyl group between the silicon atom and the amine. A severe reduction in the methyl carbon signal at 25.7 ppm, as the intensity of the signal is not much higher than the noise in the baseline. This correlates with the elemental analysis results and implies that the cleavage is not just the nitrogen being lost from the alkyl chain as ammonia but rather via loss of methylamine species.

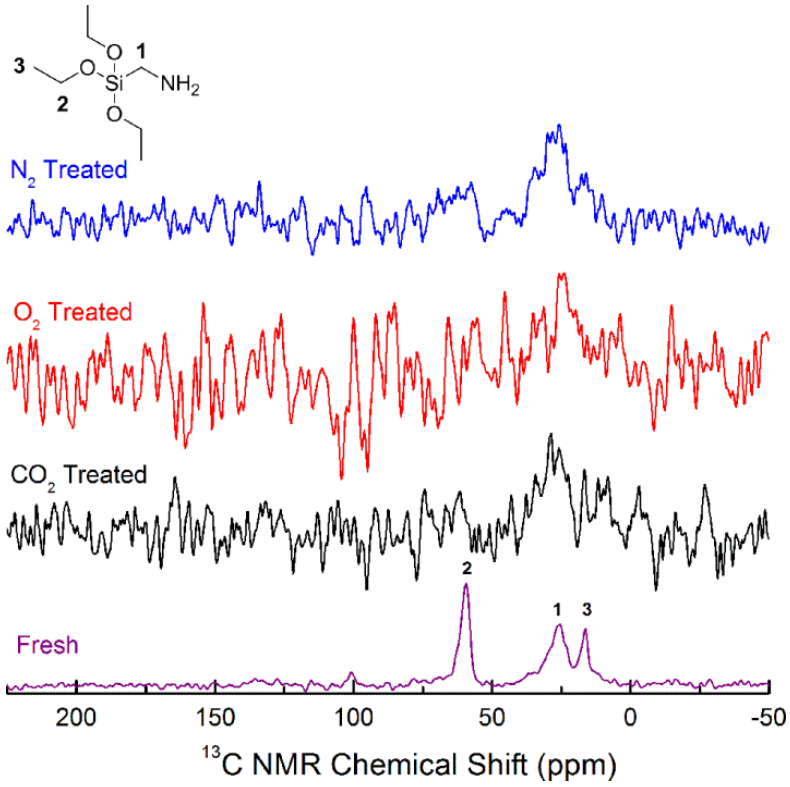

Figure 2.6. ^{13}C CP MAS NMR spectra for SBA-Methyl-low before and after degradation experiments at 135 ºC. All spectra were obtained under the same conditions.

The spectra for SBA-Ethyl-low and SBA-Propyl-low are shown in Figure 2.7a,b, respectively. Shifts are observed at 60, 36.3 and 13.4 ppm for fresh SBA-Ethyl-low and 59.5, 43.9, 25.4, 16.6 and 8.5 ppm for fresh SBA-Propyl-low, corresponding to the ethyl/propyl carbons and dangling methoxy/ethoxy groups, respectively. The spectra do not show any significant changes to the material apart from cleavage of the (m)ethoxy groups upon heating. The lack of a urea peak for SBA-Propyl-low, despite the observed reduction in CO_2 adsorption capacity, could be due to the combination of a lesser extent of deactivation of the material coupled with a smaller abundance of carbon from the lower surface coverage. If urea formation occurred, the signal would be extremely weak and lie within the baseline noise of these experiments. Spectra for the higher loading

materials are shown in Figure 2.8a,b. Shifts for these materials are observed at 60, 36.7 and 16.6 ppm for fresh SBA-Ethyl and 57.3, 43.5, 23 and 10.1 ppm for fresh SBA-Propyl. The appearance of a urea peak is observed for the higher loading materials at 161.4 ppm after CO_2 degradation experiments. This peak is similar to that previously reported by Sayari and is outside of the range where one would expect to see adsorbed CO_2 from ambient air in the form of a carbamate signal, which occurs between 164.5-165.5 ppm.[36,62]

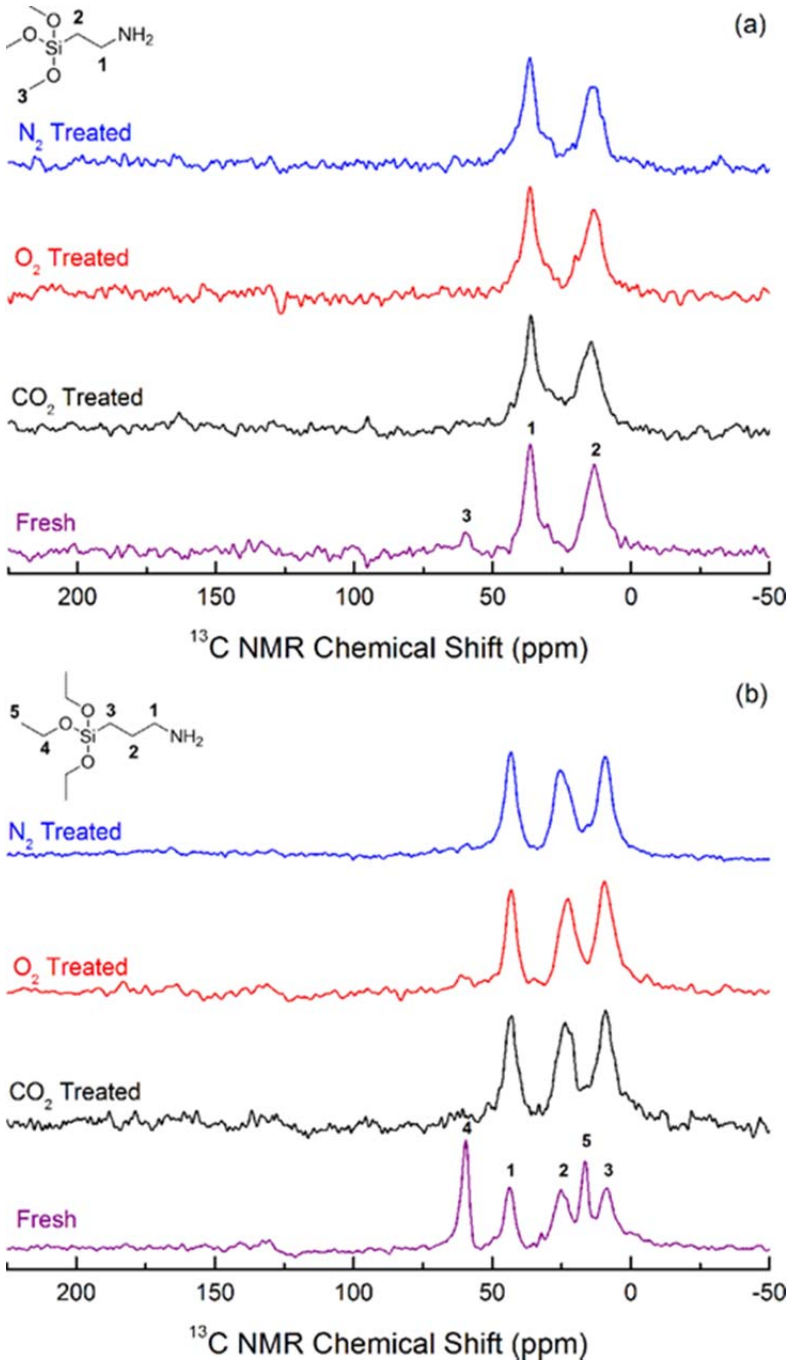

Figure 2.7. ^{13}C CP MAS NMR spectra for (a) SBA-Ethyl-low and (b) SBA-Propyl-low before and after degradation experiments at 135 ºC. All spectra were obtained under the same conditions.

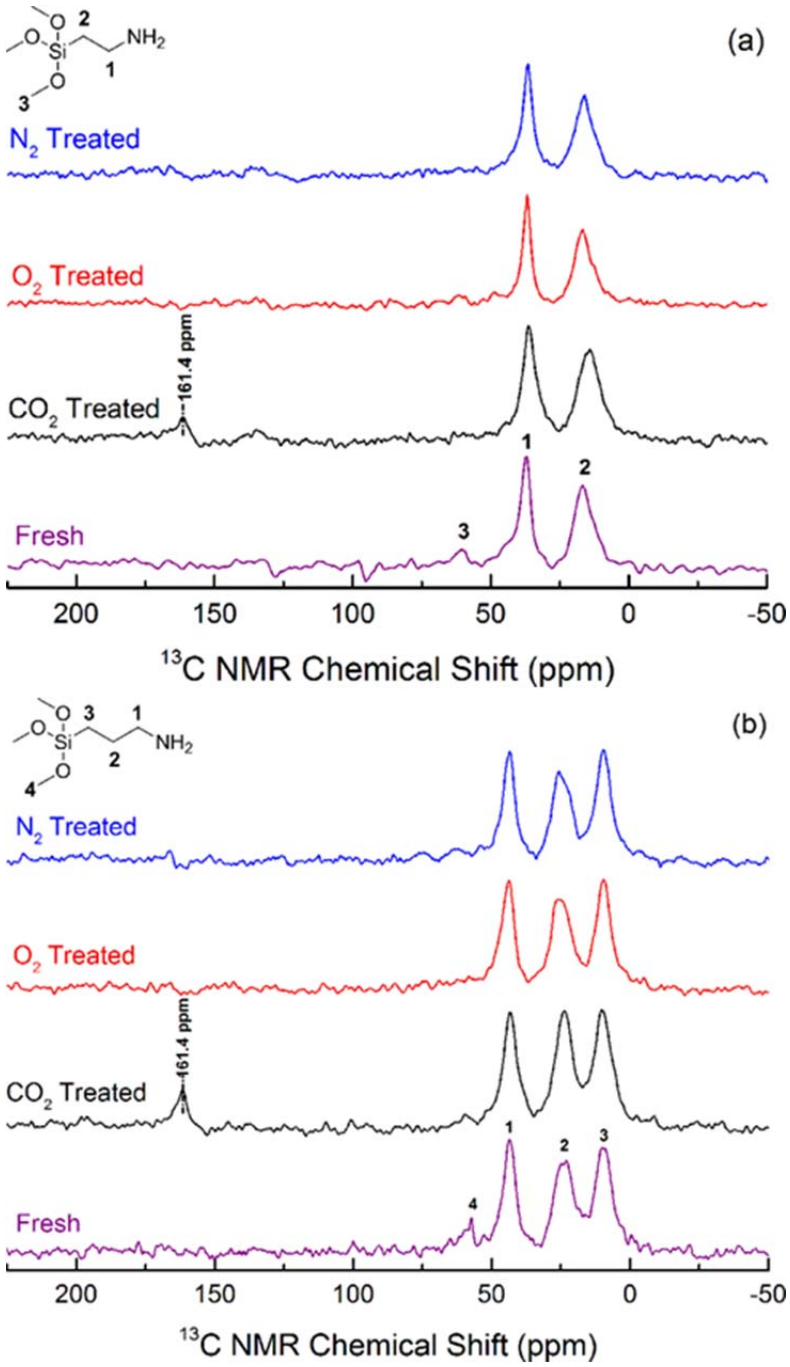

Figure 2.8. ^{13}C CP MAS NMR spectra for (a) SBA-Ethyl and (b) SBA-Propyl before and after degradation experiments at 135 ºC. All spectra were obtained under the same conditions.

2.4.3 DFT Calculations Assessing Urea Formation Pathways

The experimental results in the previous sections indicate that SBA-Ethyl and SBA-Propyl with higher amine loadings have severe deactivation from high temperature CO_2 environments. To explain the CO_2 induced deactivation phenomena, the possible reaction pathways of CO_2 with RNH_2 in the gas phase have been explored using density functional theory (DFT) calculations based on the deactivation pathways proposed by Sayari et al., as shown in Figure 2.1. The results are presented in the following sections.

2.4.3.1 Carbamic acid formation from CO_2 with RNH_2

For the formation of carbamic acid, two scenarios were examined as shown in reactions (1) and (2). The barrier for the first process, where one $CH_3CH_2NH_2$ molecule reacts with CO_2, is 39.7 kcal mol^{-1}, as shown in Table 2.3. However, if the reaction is assisted by a second $CH_3CH_2NH_2$ molecule (see reaction 2), the barrier is dramatically reduced to 15.9 kcal mol^{-1}, indicating an additional molecule is required to catalyze the reaction.

$$RNH_2 + CO_2 \leftrightarrow RNHCOOH \text{ (carbamic acid)} \quad (1)$$

$$2RNH_2 + CO_2 \leftrightarrow RNHCOOH \text{ (carbamic acid)} + RNH_2 \quad (2)$$

Based on this information, we propose that the second amine or a protic molecule (such as a neighboring amine or surface silanol) can efficiently catalyze the reaction of RNH_2 with CO_2 to form carbamic acid. Several reactions were used to test the effect of alkyl chain length as well as amine-amine versus amine-silanol interactions on the energy barrier for carbamic acid formation, as displayed in Table 2.3. The transition state

structures are shown in appendix A. Gas molecules terminated with CH_2 groups and trimethoxysilyl groups were examined and showed a variation of 4.9 kcal mol^{-1} (Table 2.3b,e). The energy barrier for a silica functionalized amine is therefore likely to fall within this range. The values in Table 2.3 indicate that by lengthening the alkyl chain by the addition of one CH_2 group, the barrier for carbamic acid formation can decrease between 0.6- 2.7 kcal mol^{-1} for different linkers. Additionally, amine and silanol assisted (self-catalyzed versus silanol catalyzed) reactions have similar energy barriers, meaning that either can contribute to the reaction pathway.

Table 2.3. The first step (carbamic acid formation) energy barriers (kcal mol^{-1}) for the degradation of different primary amines from CO_2, calculated at the B3LYP/6-311+G** level. Barriers are relative to the separated reactants with ZPE corrections. The transition state structures of TS (a) to TS (g) are displayed in appendix A.

Reactions	Barrier (kcal mol^{-1})
One Step Mechanism	
(a) $CH_3CH_2NH_2 + CO_2 \rightarrow CH_3CH_2NHCOOH$	39.7, TS(a)
Self-catalyzed	
(b) $2CH_3CH_2NH_2 + CO_2 \rightarrow CH_3CH_2NHCOOH + CH_3CH_2NH_2$	15.9, TS(b)
(c) $2CH_3CH_2CH_2NH_2 + CO_2 \rightarrow CH_3CH_2CH_2NHCOOH + CH_3CH_2CH_2NH_2$	15.3, TS(c)
(d) $2(CH_3O)_3\text{-}SiCH_2NH_2 + CO_2 \rightarrow (CH_3O)_3\text{-}SiCH_2NHCOOH + (CH_3O)_3\text{-}SiCH_2NH_2$	13.7, TS(d)
(e) $2(CH_3O)_3\text{-}SiCH_2CH_2NH_2 + CO_2 \rightarrow (CH_3O)_3\text{-}SiCH_2CH_2NHCOOH + (CH_3O)_3\text{-}SiCH_2CH_2NH_2$	11.0, TS(e)
Silanol catalyzed	
(f) $CH_3CH_2NH_2 + (CH_3O)_3\text{-}SiCH_2OH + CO_2 \rightarrow CH_3CH_2NHCOOH + (CH_3O)_3\text{-}SiCH_2OH$	14.9, TS(f)
(g) $CH_3CH_2CH_2NH_2 + (CH_3O)_3\text{-}SiCH_2OH + CO_2 \rightarrow CH_3CH_2CH_2NHCOOH + (CH_3O)_3\text{-}SiCH_2OH$	14.3, TS(g)

Although the barriers for carbamic acid formation vary slightly for different alkyl chain lengths in the primary amine, the mechanism for deactivation of any alkyl chain length should be similar since the first step for the interaction of CO_2 with RNH_2 takes place between a nonbonding electron pair at the amine nitrogen atom and an antibonding empty orbital in CO_2. Therefore in the following calculations only the ethyl molecule, $CH_3CH_2NH_2$, was used to calculate the subsequent pathways shown in Figure 2.9 as it can be inferred that energies will be similar for all structures.

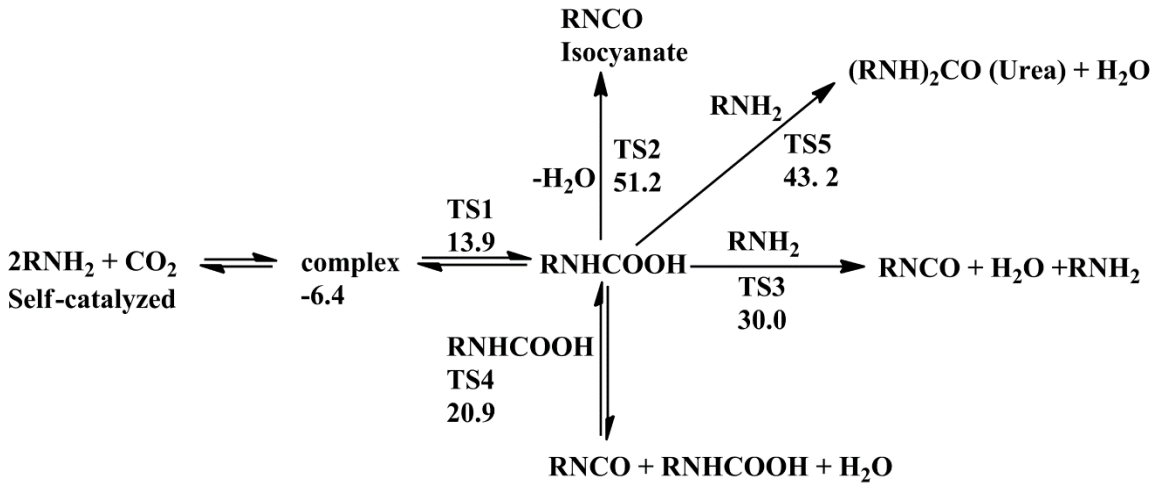

Figure 2.9. Reaction pathways for the formation of carbamic acid and isocyanate, R = CH_3CH_2. Values in kcal mol^{-1}, calculated at the B3LYP/6-311+G** level with ZPE corrections.

2.4.3.2 Isocyanate formation

Once carbamic acid has been formed via TS1 (see Figure 2.9), several pathways for the formation of isocyanate were examined, as well as a direct route to urea via dehydration of ammonium carbamate. Direct dehydration of carbamic acid produces isocyanate via TS2 with a rather high barrier (51.2 kcal mol^{-1}), indicating it is a kinetically unfavorable pathway. However, if a newly formed carbamic acid is assisted catalytically by a neighboring amine or carbamic acid (via TS3 or TS4) to form isocyanate, the barrier is reduced to 30.0 and 20.9 kcal mol^{-1}, respectively. The ammonium carbamate route for urea formation discussed by Sayari is shown in TS5 where a carbamic acid reacts with a second amine and dehydrates into urea. The energy barrier for this is quite high, with a value of 43.2 kcal mol^{-1}. From these calculations it can be seen that the most energetically favored route to urea formation is through an

isocyanate intermediate, and more specifically from a self-assisted reaction of two carbamic acids.

2.4.3.3 Urea formation

Three pathways were investigated for the formation of urea from isocyanate as shown in Figure 2.10. If isocyanate reacts with a neighboring amine and dehydrates via TS6, the energy barrier is 27.2 kcal mol^{-1}. If an additional amine is involved to act as a catalyst via TS7 it can be seen that the energy barrier is reduced to 8.0 kcal mol^{-1}. The final pathway would take advantage of water produced from previous dehydration reactions which could now be associated with amines, whereby if an amine and water molecule reacts with isocyanate, the energy barrier is lowered even further to 1.5 kcal mol^{-1} with a larger exothermicity of -18.9 kcal mol^{-1}. Once again, it can be seen that an additional protic molecule such as a neighboring amine or surface silanol can dramatically reduce the energetic barrier to urea formation.

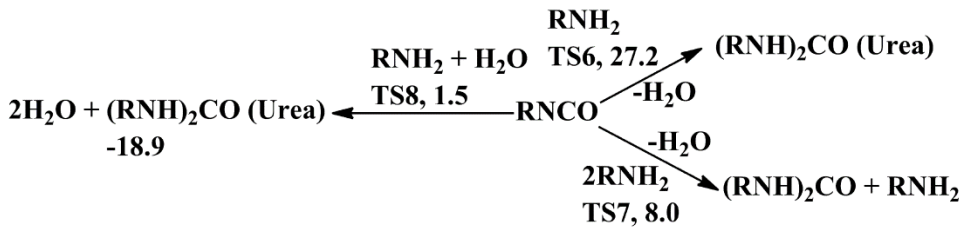

Figure 2.10. Urea formation channels, R = CH_3CH_2. Values in kcal mol^{-1}, calculated at the B3LYP/6-311+G** level with ZPEs correction.

Combining the mechanisms from Figure 2.9 and Figure 2.10 it can be seen that isocyanate formation is the most energetically favored route to urea formation and that the pathways to urea from isocyanate have an exothermic release and are thus feasible.

The lowest energy route to urea formation is shown in Figure 2.11. The fact that assisted reactions, by means of a neighboring amine or silanols, have lower energy barriers help to support the observation that degradation increases with increased amine loading, as there are more proximal amines to interact and initiate the deactivation mechanism. Furthermore, the lesser extent of deactivation observed for SBA-Ethyl as compared to SBA-Propyl could be partly due to the inability of these materials to interact with surface silanols, as that has been shown with these calculations to be another route to catalyzing the deactivation pathway.

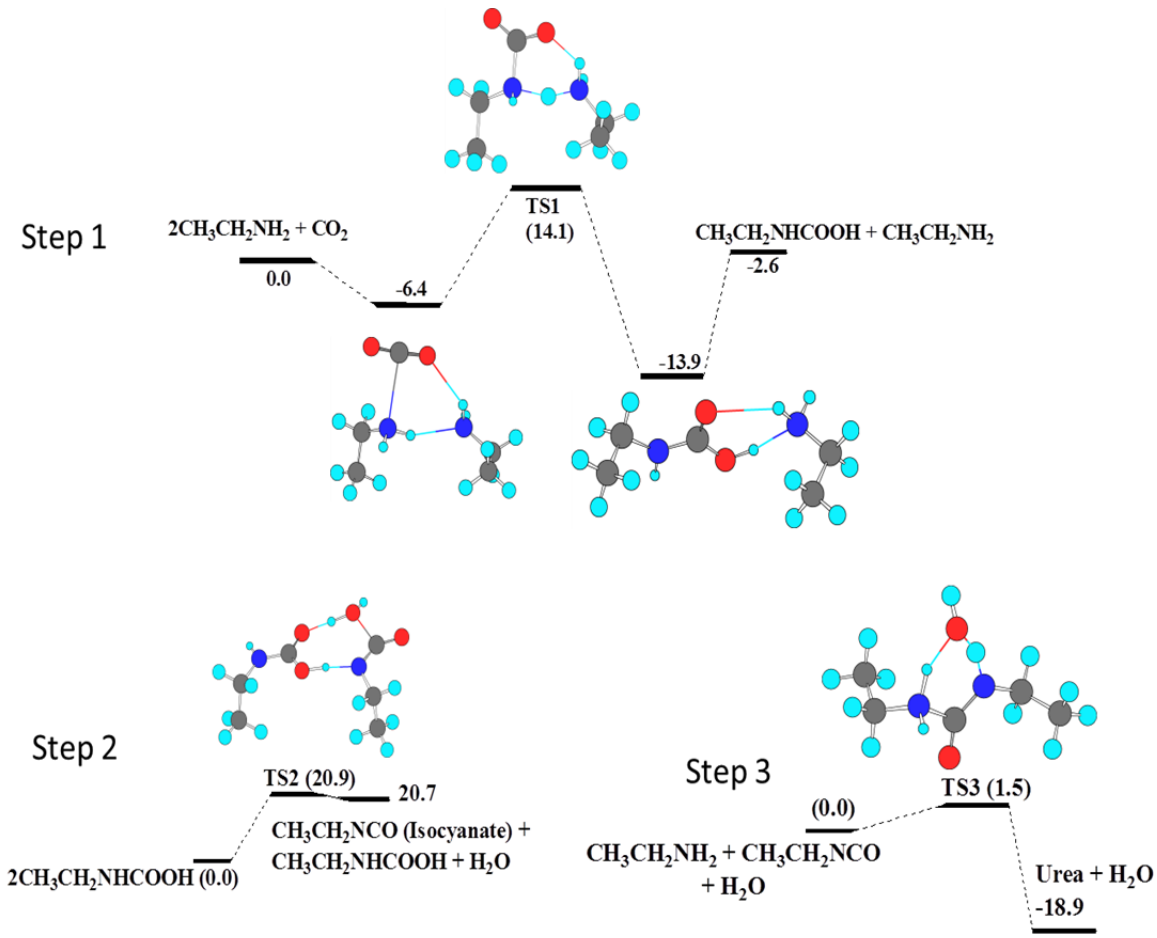

Figure 2.11. The lowest energy pathways (in kcal mol^{-1}) for deactivation of $CH_3CH_2NH_2$ from CO_2 via urea formation. Calculated at the CCSD (T)/6-311+G**//B3LYP/6-311+G** level.

2.5 Conclusions

The effect of alkyl chain length for primary aminosilanes was investigated with respect to thermal, oxidative and CO_2 induced degradation. It was found that materials with methyl amine functionality possessed thermal instability and were prone to loss of organic content upon heating at elevated temperatures. Therefore moderately high temperature applications for materials with methylamine functionality are not possible and should instead use ethyl or propyl organosilanes. Materials with ethyl and propyl amine functionality possessed thermal and oxidative stability, but were susceptible to

deactivation via urea formation in dry, high temperature CO_2 environments. Propyl amine materials had a greater extent of CO_2 adsorption capacity loss as compared to ethyl based sorbents. It is believed that this is due to the higher amine efficiency of propyl based adsorbents along with the ability of the material to interact with surface silanols, as findings from DFT calculations suggest that this increased efficiency could contribute to the greater deactivation through self-catalyzed reaction pathways that lead to isocyanate and urea formation. DFT calculations showed that there was no significant difference in stability for the different alkyl chain materials, and also confirmed the lowest energy route to urea formation is through an isocyanate intermediate, thus ruling out the ammonium carbamate route and explaining why primary amines are required for urea formation. These calculations also showed that assisted deactivation through neighboring amine or silanol interactions greatly lowered the energy for reaction, and therefore explain why the higher amine loading materials experienced a greater degree of deactivation in dry high temperature CO_2 environments.

2.6 References

(1) Choi, S.; Drese, J. H.; Jones, C. W. Adsorbent Materials for Carbon Dioxide Capture from Large Anthropogenic Point Sources. *ChemSusChem* **2009**, *2*, 796–854.

(2) Bollini, P.; Didas, S. A.; Jones, C. W. Amine-Oxide Hybrid Materials for Acid Gas Separations. *J. Mater. Chem.* **2011**, *21*, 15100–15120.

(3) Sayari, A.; Belmabkhout, Y.; Serna-Guerrero, R. Flue Gas Treatment via CO_2 Adsorption. *Chem. Eng. J.* **2011**, *171*, 760–774.

(4) Hedin, N.; Andersson, L.; Bergström, L.; Yan, J. Adsorbents for the Post-Combustion Capture of CO_2 Using Rapid Temperature Swing or Vacuum Swing Adsorption. *Appl. Energy* **2013**, *104*, 418–433.

(5) Serna-Guerrero, R.; Sayari, A. Modeling Adsorption of CO_2 on Amine-Functionalized Mesoporous Silica. 2: Kinetics and Breakthrough Curves. *Chem. Eng. J.* **2010**, *161*, 182–190.

(6) Stuckert, N. R.; Yang, R. T. CO_2 Capture from the Atmosphere and Simultaneous Concentration Using Zeolites and Amine-Grafted SBA-15. *Environ. Sci. Technol.* **2011**, *45*, 10257–10264.

(7) Bollini, P.; Brunelli, N. A.; Didas, S. A.; Jones, C. W. Dynamics of CO_2 Adsorption on Amine Adsorbents. 1. Impact of Heat Effects. *Ind. Eng. Chem. Res.* **2012**, *51*, 15145–15152.

(8) Bollini, P.; Brunelli, N. A.; Didas, S. A.; Jones, C. W. Dynamics of CO_2 Adsorption on Amine Adsorbents. 2. Insights into Adsorbent Design. *Ind. Eng. Chem. Res.* **2012**, *51*, 15153–15162.

(9) Monazam, E. R.; Spenik, J.; Shadle, L. J. Fluid Bed Adsorption of Carbon Dioxide on Immobilized Polyethylenimine (PEI): Kinetic Analysis and Breakthrough Behavior. *Chem. Eng. J.* **2013**, *223*, 795–805.

(10) Monazam, E. R.; Shadle, L.; Miller, D.; Pennline, H.; Fauth, D.; Hoffman, J.; Gray, M. L. Equilibrium and Kinetics Analysis of Carbon Dioxide Capture Using Immobilized Amine on a Mesoporous Silica. *AIChE J.* **2013**, *59*, 923–935.

(11) Monazam, E. R.; Shadle, L.; Siriwardane, R. Equilibrium and Absorption Kinetics of Carbon Dioxide by Solid Supported Amine Sorbent. *AIChE J.* **2011**, *57*, 3153–3159.

(12) Chen, C.; Yang, S. T.; Ahn, W. S.; Ryoo, R. Amine-Impregnated Silica Monolith with a Hierarchical Pore Structure: Enhancement of CO_2 Capture Capacity. *Chem. Commun.* **2009**, 3627–3629.

(13) Wen, J. J.; Gu, F. N.; Wei, F.; Zhou, Y.; Lin, W. G.; Yang, J.; Yang, J. Y.; Wang, Y.; Zou, Z. G.; Zhu, J. H. One-Pot Synthesis of the Amine-Modified Meso-Structured Monolith CO_2 Adsorbent. *J. Mater. Chem.* **2010**, *20*, 2840–2846.

(14) Wang, J.; Long, D.; Zhou, H.; Chen, Q.; Liu, X.; Ling, L. Surfactant Promoted Solid Amine Sorbents for CO_2 Capture. *Energy Environ. Sci.* **2012**, *5*, 5742–5749.

(15) Li, F. S.; Qiu, W.; Lively, R. P.; Lee, J. S.; Rownaghi, A. A.; Koros, W. J. Polyethyleneimine-Functionalized Polyamide Imide (Torlon) Hollow-Fiber Sorbents for Post-Combustion CO_2 Capture. *ChemSusChem* **2013**, *6*, 1216–1223.

(16) Li, F. S.; Labreche, Y.; Lively, R. P.; Lee, J. S.; Jones, C. W.; Koros, W. J. Poly (ethyleneimine) Infused and Functionalized Torlon-Silica Hollow Fiber Sorbents for Post-Combustion CO_2 Capture. *Polymer* **2013**, *55*, 1341–1346.

(17) Labreche, Y.; Lively, R. P.; Rezaei, F.; Chen, G.; Jones, C. W.; Koros, W. J. Post-Spinning Infusion of Poly(ethyleneimine) into Polymer/silica Hollow Fiber Sorbents for Carbon Dioxide Capture. *Chem. Eng. J.* **2013**, *221*, 166–175.

(18) Rezaei, F.; Lively, R. P.; Labreche, Y.; Chen, G.; Fan, Y.; Koros, W. J.; Jones, C. W. Aminosilane-Grafted Polymer/silica Hollow Fiber Adsorbents for CO_2 Capture from Flue Gas. *ACS Appl. Mater. Interfaces* **2013**, *5*, 3921–3931.

(19) Fan, Y.; Lively, R. P.; Labreche, Y.; Rezaei, F.; Koros, W. J.; Jones, C. W. Evaluation of CO_2 Adsorption Dynamics of Polymer/silica Supported Poly(ethylenimine) Hollow Fiber Sorbents in Rapid Temperature Swing Adsorption. *Int. J. Greenh. Gas Control* **2014**, *21*, 61–71.

(20) Chaffee, A. L.; Knowles, G. P.; Liang, Z.; Zhany, J.; Xiao, P.; Webley, P. A. CO_2 Capture by Adsorption: Materials and Process Development. *Int. J. Greenh. Gas Control* **2007**, *1*, 11–18.

(21) Drage, T. C.; Arenillas, A.; Smith, K. M.; Snape, C. E. Thermal Stability of Polyethylenimine Based Carbon Dioxide Adsorbents and Its Influence on Selection of Regeneration Strategies. *Microporous Mesoporous Mater.* **2008**, *116*, 504–512.

(22) Liu, X. W.; Zhou, L.; Fu, X.; Sun, Y.; Su, W.; Zhou, Y. P. Adsorption and Regeneration Study of the Mesoporous Adsorbent SBA-15 Adapted to the Capture/separation of CO_2 and CH_4. *Chem. Eng. Sci.* **2007**, *62*, 1101–1110.

(23) Lu, C. Y.; Su, F. S.; Hsu, S. C.; Chen, W. F.; Bai, H. L.; Hwang, J. F.; Lee, H. H. Thermodynamics and Regeneration of CO_2 Adsorption on Mesoporous Spherical-Silica Particles. *Fuel Process. Technol.* **2009**, *90*, 1543–1549.

(24) Li, W.; Bollini, P.; Didas, S. A.; Choi, S.; Drese, J. H.; Jones, C. W. Structural Changes of Silica Mesocellular Foam Supported Amine-Functionalized CO_2 Adsorbents upon Exposure to Steam. *ACS Appl. Mater. Interfaces* **2010**, *2*, 3363–3372.

(25) Belmabkhout, Y.; Sayari, A. Isothermal versus Non-Isothermal Adsorption-Desorption Cycling of Triamine-Grafted Pore-Expanded MCM-41 Mesoporous Silica for CO_2 Capture from Flue Gas. *Energy Fuels* **2010**, *24*, 5273–5280.

(26) Serna-Guerrero, R.; Belmabkhout, Y.; Sayari, A. Influence of Regeneration Conditions on the Cyclic Performance of Amine- Grafted Mesoporous Silica for CO_2 Capture: An Experimental and Statistical Study. *Chem. Eng. Sci.* **2010**, *65*, 4166–4172.

(27) Sayari, A.; Belmabkhout, Y. Stabilization of Amine-Containing CO_2 Adsorbents: Dramatic Effect of Water Vapor. *J. Am. Chem. Soc.* **2010**, *132*, 6312–6314.

(28) Sanz, R.; Calleja, G.; Arencibia, A.; Sanz-Perez, E. S. CO_2 Adsorption on Branched Polyethyleneimine-Impregnated Mesoporous Silica SBA-15. *Appl. Surf. Sci.* **2010**, *256*, 5323–5328.

(29) Ebner, A.; Gray, M. L.; Chisholm, N.; Black, Q.; Mumford, D.; Nicholson, M.; Ritter, J. Suitability of a Solid Amine Sorbent for CO_2 Capture by Pressure Swing Adsorption. *Ind. Eng. Chem. Res.* **2011**, *50*, 5634–5641.

(30) Wurzbacher, J. A.; Gebald, C.; Steinfeld, A. Separation of CO_2 from Air by Temperature-Vacuum Swing Adsorption Using Diamine-Functionalized Silica Gel. *Energy Environ. Sci.* **2011**, *4*, 3584–3592.

(31) Wurzbacher, J. A.; Gebald, C.; Piatkowski, N.; Steinfeld, A. Concurrent Separation of CO_2 and H_2O from Air by a Temperature-Vacuum Swing Adsorption/Desorption Cycle. *Environ. Sci. Technol.* **2012**, *46*, 9191–9198.

(32) Gebald, C.; Wurzbacher, J. A.; Tingaut, P.; Steinfeld, A. Stability of Amine-Functionalized Cellulose during Temperature-Vacuum-Swing Cycling for CO_2 Capture from Air. *Environ. Sci. Technol.* **2013**, *47*, 10063–10070.

(33) Zhao, W.; Zhang, Z.; Li, Z.; Cai, N. Investigation of Thermal Stability and Continuous CO_2 Capture from Flue Gases with Supported Amine Sorbent. *Ind. Eng. Chem. Res.* **2013**, *52*, 2084–2093.

(34) Hammache, S.; Hoffman, J.; Gray, M. L.; Fauth, D.; Howard, B.; Pennline, H. Comprehensive Study of the Impact of Steam on Polyethyleneimine on Silica for CO_2 Capture. *Energy Fuels* **2013**, *27*, 6899–6905.

(35) Subagyono, D. J. N.; Marshall, M.; Knowles, G. P.; Chaffee, A. L. CO_2 Adsorption by Amine Modified Siliceous Mesostructured Cellular Foam (MCF) in Humidified Gas. *Microporous Mesoporous Mater.* **2014**, *186*, 84–93.

(36) Bollini, P.; Choi, S.; Drese, J. H.; Jones, C. W. Oxidative Degradation of Aminosilica Adsorbents Relevant to Post-Combustion CO_2 Capture. *Energy Fuels* **2011**, *25*, 2416–2425.

(37) Heydari-Gorji, A.; Belmabkhout, Y.; Sayari, A. Degradation of Amine-Supported CO_2 Adsorbents in the Presence of Oxygen-Containing Gases. *Microporous Mesoporous Mater.* **2011**, *145*, 146–149.

(38) Calleja, G.; Sanz, R.; Arencibia, A.; Sanz-Pérez, E. S. Influence of Drying Conditions on Amine-Functionalized SBA-15 as Adsorbent of CO_2. *Top. Catal.* **2011**, *54*, 135–145.

(39) Heydari-gorji, A.; Sayari, A. Thermal , Oxidative , and CO_2 -Induced Degradation of Supported Polyethylenimine Adsorbents. *Ind. Eng. Chem. Res.* **2012**, *51*, 6887–6894.

(40) Srikanth, C. S.; Chuang, S. S. C. Spectroscopic Investigation into Oxidative Degradation of Silica-Supported Amine Sorbents for CO_2 Capture. *ChemSusChem* **2012**, *5*, 1435–1442.

(41) Ahmadalinezhad, A.; Tailor, R.; Sayari, A. Molecular-Level Insights into the Oxidative Degradation of Grafted Amines. *Chem. Eur. J.* **2013**, *19*, 10543–10550.

(42) Bali, S.; Chen, T. T.; Chaikittisilp, W.; Jones, C. W. Oxidative Stability of Amino Polymer–Alumina Hybrid Adsorbents for Carbon Dioxide Capture. *Energy Fuels* **2013**, *27*, 1547–1554.

(43) Ahmadalinezhad, A.; Sayari, A. Oxidative Degradation of Silica-Supported Polyethylenimine for CO_2 Adsorption: Insights into the Nature of Deactivated Species. *Phys. Chem. Chem. Phys.* **2014**, *16*, 1529–1535.

(44) Sayari, A.; Belmabkhout, Y.; Da'na, E. CO_2 Deactivation of Supported Amines: Does the Nature of Amine Matter? *Langmuir* **2012**, *28*, 4241–4247.

(45) Sayari, A.; Heydari-Gorji, A.; Yang, Y. CO_2-Induced Degradation of Amine-Containing Adsorbents: Reaction Products and Pathways. *J. Am. Chem. Soc.* **2012**, *134*, 13834–13842.

(46) Chaikittisilp, W.; Kim, H.; Jones, C. W. Mesoporous Alumina-Supported Amines as Potential Steam-Stable Adsorbents for Capturing CO_2 from Simulated Flue Gas and Ambient Air. *Energy Fuels* **2011**, *25*, 5528–5537.

(47) Khatri, R. A.; Chuang, S. S. C.; Soong, Y.; Gray, M. L. Thermal and Chemical Stability of Regenerable Solid Amine Sorbent for CO_2 Capture. *Energy Fuels* **2006**, *20*, 1514–1520.

(48) Xu, X. C.; Song, C.; Miller, B. G.; Scaroni, A. W. Adsorption Separation of Carbon Dioxide from Flue Gas of Natural Gas-Fired Boiler by a Novel Nanoporous "Molecular Basket" Adsorbent. *Fuel Process. Technol.* **2005**, *86*, 1457–1472.

(49) Rezaei, F.; Jones, C. W. Stability of Supported Amine Adsorbents to SO_2 and NO_x in Postcombustion CO_2 Capture. 1. Single-Component Adsorption. *Ind. Eng. Chem. Res.* **2013**, *52*, 12192–12201.

(50) Lin, K.; Petit, C.; Park, A. Effect of SO_2 on CO_2 Capture Using Liquid-like Nanoparticle Organic Hybrid Materials. *Energy Fuels* **2013**, *27*, 4167–4174.

(51) Brunelli, N. A.; Didas, S. A.; Venkatasubbaiah, K.; Jones, C. W. Tuning Cooperativity by Controlling the Linker Length of Silica-Supported Amines in Catalysis and CO_2 Capture. *J. Am. Chem. Soc.* **2012**, *134*, 13950–13953.

(52) Kang, D.-Y.; Brunelli, N. A.; Yucelen, G. I.; Venkatasubramanian, A.; Zang, J.; Leisen, J.; Hesketh, P. J.; Jones, C. W.; Nair, S. Direct Synthesis of Single-Walled Aminoaluminosilicate Nanotubes with Enhanced Molecular Adsorption Selectivity. *Nat. Commun.* **2014**, *5*, 3342–3350.

(53) Frisch, M.; Trucks, G.; Schlegel, H.; Scuseria, G.; Robb, M.; Cheeseman, J.; Scalmani, J.; Barone, V.; Mennucci, B.; Petersson, G.; et al. Gaussian 09, Revision D.01, 2009.

(54) Becke, A. D. Density-Functional Thermochemistry. III. The Role of Exact Exchange. *J. Chem. Phys.* **1993**, *98*, 5648–5652.

(55) Lee, C.; Yang, W.; Parr, R. Development of the Colle-Salvetti Correlation-Energy Formula into a Functional of the Electron Density. *Phys. Rev. B* **1988**, *37*, 785–789.

(56) Hratchian, H. P.; Schlegel, H. B. Accurate Reaction Paths Using a Hessian Based Predictor-Corrector Integrator. *J. Chem. Phys.* **2004**, *120*, 9918–9924.

(57) Kanan, S. M.; Tze, W. T. Y.; Tripp, C. P. Method to Double the Surface Concentration and Control the Orientation of Adsorbed (3-Aminopropyl)

Dimethylethoxysilane on Silica Powders and Glass Slides. *Langmuir* **2002**, *18*, 6623–6627.

(58) Danon, A.; Stair, P. C.; Weitz, E. FTIR Study of CO_2 Adsorption on Amine-Grafted SBA-15: Elucidation of Adsorbed Species. *J. Phys. Chem. C* **2011**, *115*, 11540–11549.

(59) Brunelli, N. A.; Venkatasubbaiah, K.; Jones, C. W. Cooperative Catalysis with Acid–Base Bifunctional Mesoporous Silica: Impact of Grafting and Co-Condensation Synthesis Methods on Material Structure and Catalytic Properties. *Chem. Mater.* **2012**, *24*, 2433–2442.

(60) Hicks, J. C.; Dabestani, R.; Buchanan, A. I.; Jones, C. W. Spacing and Site Isolation of Amine Groups in 3-Aminopropyl-Grafted Silica Materials: The Role of Protecting Groups. *Chem. Mater.* **2006**, *18*, 5022–5032.

(61) Hicks, J. C.; Jones, C. W. Controlling the Density of Amine Sites on Silica Surfaces Using Benzyl Spacers. *Langmuir* **2006**, *22*, 2676–2681.

(62) Didas, S. A.; Kulkarni, A. R.; Sholl, D. S.; Jones, C. W. Role of Amine Structure on Carbon Dioxide Adsorption from Ultradilute Gas Streams such as Ambient Air. *ChemSusChem* **2012**, *5*, 2058–2064.

Chapter 3

ROLE OF AMINE TYPE ON SINGLE COMPONENT CO_2 AND WATER ADSORPTION FOR APPLICATIONS IN AIR CAPTURE

Parts of this chapter are reproduced from 'Didas, S.A.; Kulkarni, A.; Sholl, D.S.; Jones, C.W. Role of Amine Structure on Carbon Dioxide Adsorption from Ultra-Dilute Gas Streams Such as Ambient Air. *ChemSusChem*. **2012**, *5*, 2058-2064.'

3.1 Background

In chapter 1 air capture was discussed as a complementary technique for carbon dioxide removal from the atmosphere. One key technical challenge to air capture over flue gas capture is the fact that the process occurs at ambient conditions with ultra-dilute CO_2 concentrations in the range of 400 ppm. As a result of different operating conditions and process requirements, adsorbents deemed acceptable for flue gas applications will not necessarily be useful air capture materials.

Several methods for air capture have been reported to date. After air capture was raised as a means to address increasing anthropogenic CO_2 emissions,[1] CO_2 absorption from ambient air using aqueous alkaline solutions was heavily investigated, as this technique had been developed over 50 years ago for dilute and ultra-dilute CO_2 separation applications.[2–11] However, the energy penalty for regenerating aqueous alkali is quite high due to the significant heating that is required to overcome the binding energy of CO_2 with the material and to heat the large volume of water, so solid adsorbents such as solid alkali hydroxides,[12,13] quaternary ammonium resins,[14,15] and

supported amines[16–37] have more recently been investigated for air capture. So far the majority of research with supported amine adsorbents has focused on class 1 and class 2 materials, with several examples of class 3 materials as well. These initial studies have each largely focused on a representative supported amine material that is typically a mixture of different types of amines (either primary, secondary and tertiary or primary and secondary). In contrast, this study focuses on studying a series of class 2 adsorbents in the propyl-silane family to systematically determine the utility of the different types of amine sites for CO_2 capture from ambient air. Adsorbents based on 3-aminopropyl-trimethoxysilane, (N-methylaminopropyl)-trimethoxysilane, and (N,N-dimethylaminopropyl)-trimethoxysilane grafted to mesocellular foam are evaluated for their CO_2 and water adsorption properties to assess the utility of different types of amines for air capture applications.

3.2 Experiments

3.2.1 Materials Synthesis

Mesocellular foam (MCF) was used as the silica support for these studies and was synthesized based on previously reported literature methods.[40] Briefly, 16.0 g of P123 block copolymer was dissolved in a solution 47.4 g concentrated HCl and 260 g of DI water at room temperature. Next 16.0 g of TMB was added to the solution and stirred vigorously at 40 °C for 2 hours, after which 34.6 g TEOS was added to the solution and stirred for an additional 5 min. The solution was then left quiescent for 20 h in an oven at 40 °C. A solution of 184 mg NH_4F and 20 mL DI water was added and the resulting solution was briefly swirled before aging at 100 °C for 24 hours. The resulting solid was filtered, washed with copious amounts of DI water, dried overnight at 75 °C and then

calcined in air at 550 °C with a 1 °C min^{-1} ramp. Approximately 9.5 g of MCF was collected with this method.

Aminosilicas were prepared using an adapted procedure reported by Harlick and Sayari.[41] First, calcined MCF silica was dried overnight at 110 °C on a Schlenk line under a pressure of 20 mTorr. The silica was then stirred with toluene for 30 minutes after which 0.30 g of DI water was added per gram of silica. The solution was then equilibrated at room temperature for 2 hours. Next 2.0 g aminosilane per gram of silica was added to the mixture that was then heated at 85 °C for 16 hours. The product was then filtered and washed with copious amounts of toluene, hexane and methanol. Finally, the recovered material was dried overnight at 75 °C on a Schlenk line under a pressure of 20 mTorr.

3.2.2 Materials Characterization

Nitrogen physisorption measurements were taken with a Micromeritics Tristar II at 77K. Surface area and pore volume were calculated from the isotherm data using the Brunauer-Emmett-Teller[42] and BdB-FHH method's,[43] respectively. Elemental analysis was used to determine the nitrogen content and subsequent amine loading of the materials. Analyses were performed by Atlantic Microlabs (Norcross, GA, USA). ^{13}C CP-MAS solid state NMR were performed on a Bruker DSX-300 spectrometer. The samples spun at a frequency of 4 kHz. FT-IR spectroscopy using KBr pellets were obtained on a Bruker Vertex 80v optical bench.

3.2.3 Adsorption Measurements

A TA Instruments Q500 TGA was used to measure dry CO_2 adsorption capacities. A typical adsorption run consisted of pretreating the material for three hours at 120 °C in flowing helium to remove any pre-adsorbed CO_2 and water, followed by cooling to the desired temperature for adsorption measurement and then adsorbing the test gas for twelve hours. Single component water vapor isotherms were measured using a Hiden IGASorp. A typical experiment consisted of pretreating the material at 100 °C for five hours in flowing nitrogen, followed by cooling to the desired temperature and adsorption of water vapor in flowing nitrogen gas. Adsorption is monitored at each relative humidity until a 95% equilibrium value is reached as determined by the equipment software.

3.3 Results & Discussion

As discussed in chapter 1, there are two mechanisms by which supported amine materials can adsorb CO_2 based on aqueous amine literature. From these mechanisms the maximum amine efficiencies can be determined. Therefore, in dry conditions the theoretical maximum efficiency for supported amines in the absence of water is 0.5 moles CO_2 captured: 1 mole (primary and/or secondary) amine and improves to 1 mole CO_2:1 mole (primary, secondary or tertiary) amine in the presence of water. These amine efficiencies are important metrics for evaluating CO_2 adsorbents, and will be used extensively in the discussion that follows in this chapter.

3.3.1 Materials Synthesis & Characterization

Primary, secondary and tertiary amines were functionalized onto a mesoporous silica foam support (mesocellular foam (MCF)). This support has a large surface area, large pore diameter and 3D pore network, which reduces diffusive resistance of the adsorbates. The silanes used and the corresponding nomenclature for the adsorbent samples are presented in Figure 3.1 and Table 3.1. The structure of all of these aminosilanes is similar, consisting of an amine group connected to a trimethoxysilane group via a propyl chain. Thus, all the amines are structurally similar, allowing for systematic comparison of the reactivity of the different types of amine sites. This approach has been used previously both by our group and others for examining differences of structural effects to oxidation and CO_2 desorption kinetics.[44–47]

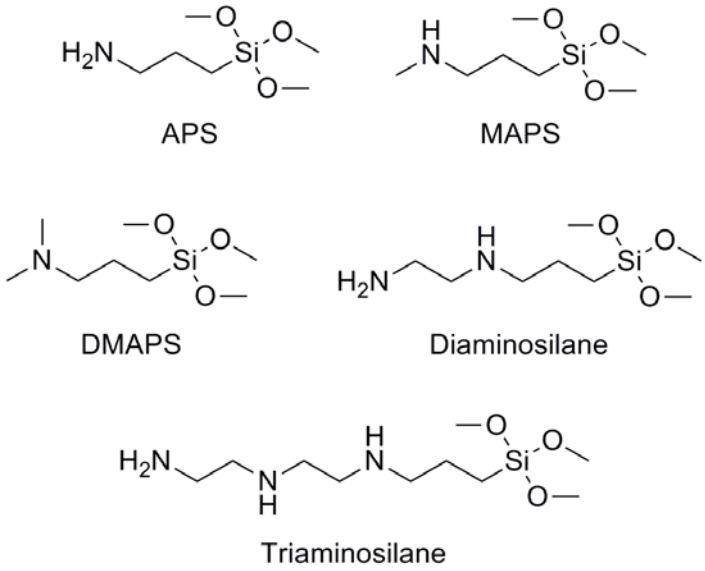

Figure 3.1. Chemical structures of common aminosilanes used in previous works as well as the aminosilanes used for this study (APS, MAPS, DMAPS).

Table 3.1. Silanes used to prepare adsorbent materials.

Silane	Amine Type	Sample Name
3-aminopropyl-trimethoxysilane	Primary - APS	MCF-APS-low, MCF-APS-high
(N-methylaminopropyl)-trimethoxysilane	Secondary - MAPS	MCF-MAPS
(N,N-dimethylaminopropyl)-trimethoxysilane	Tertiary - DMAPS	MCF-DMAPS

Upon functionalization, the silica materials were characterized via nitrogen physisorption, elemental analysis (EA), thermogravimetric analysis (TGA), Fourier transform infrared spectroscopy (FTIR), and ^{13}C cross-polarization magic angle spinning (CP-MAS) nuclear magnetic resonance (NMR) spectroscopy (see supplementary information). The nitrogen adsorption/desorption isotherms are displayed in Figure 3.2 and show a dramatic decrease in pore volume upon incorporation of the amine functionalities on the silica support. The pore size distributions as well as pore volumes of the adsorbents were calculated from physisorption data using the Broekhoff-de Boer-Frankel Halsey Hill (BdB-FHH) method[43] and are presented in Table 3.2 along with the amine loading of materials as determined by EA. Primary, secondary and tertiary materials were synthesized with similar amine loadings so that direct comparisons could be made between adsorption characteristics. A material with a higher loading of primary amine was also synthesized so that the influence of loading on amine efficiency could be assessed. It should be noted that the primary amine impurity discussed by Sayari et al.[47] was studied and found to have negligible effect on CO_2 adsorption after purification and

functionalization of the secondary aminosilane. (Purification method and CO_2 adsorption performance presented in appendix B.)

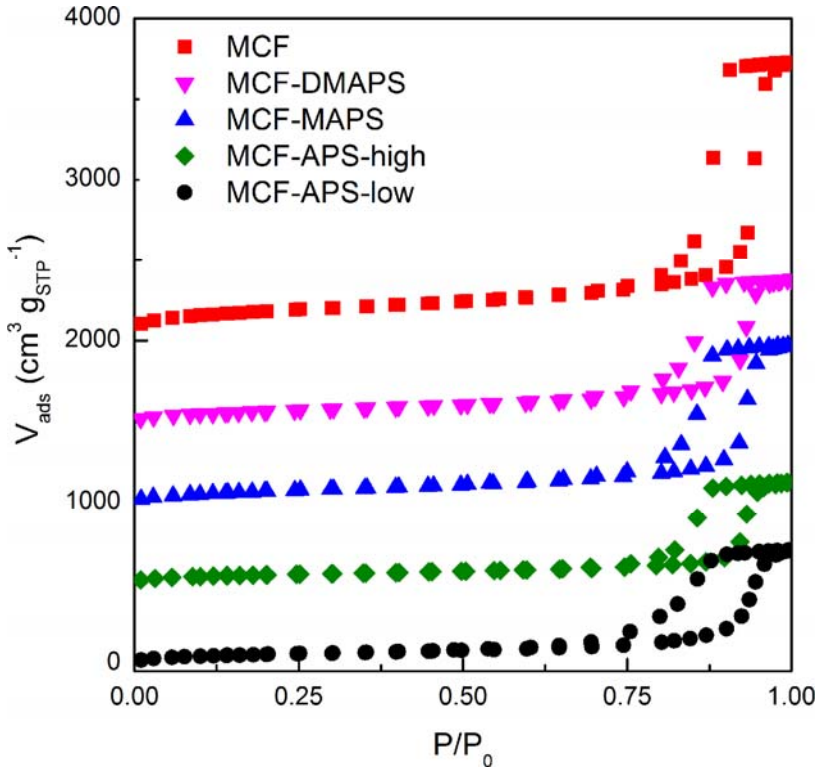

Figure 3.2. Nitrogen adsorption/desorption isotherms of bare and amine functionalized silica with 500 cm^3 g_{STP}^{-1} offset between isotherms.

Table 3.2. Physical properties of adsorbent materials.

Material	Material Abbreviation	BET SA ($m^2\ g_{SiO2}^{-1}$)	V_{pore} ($cm^3\ g_{SiO2}^{-1}$)	Amine Loading (mmol N g^{-1})
Bare silica support 1	MCF1	648	2.72	-
Bare silica support 2	MCF2	563	2.17	-
Silica with primary amines, low loading	MCF-APS-low	237	1.40	2.70
Silica with primary amines, high loading	MCF-APS-high	230	1.35	3.75
Silica with secondary amines	MCF-MAPS	344	2.01	2.41
Silica with tertiary amines	MCF-DMAPS	317	1.81	2.20

^{13}C CP MAS NMR spectra for the three amine types are presented in Figure 3.3. The 3 shifts at 11.51, 23.37 and 44.39 ppm for MCF-APS-high correspond to the 3 carbons in the propyl chain. Shifts at 10.97, 21.75 and 53.55 ppm for MCF-MAPS and 11.51, 22.29 and 63.26 ppm for MCF-DMAPS also indicate the presence of the propyl carbon group and have an additional shift at 34.69 and 44.39 ppm, respectively, which corresponds to the methyl group bonded to the amine. The shift at 165.14 ppm for both MCF-APS-high and MCF-MAPS is from CO_2 adsorption from the ambient air.

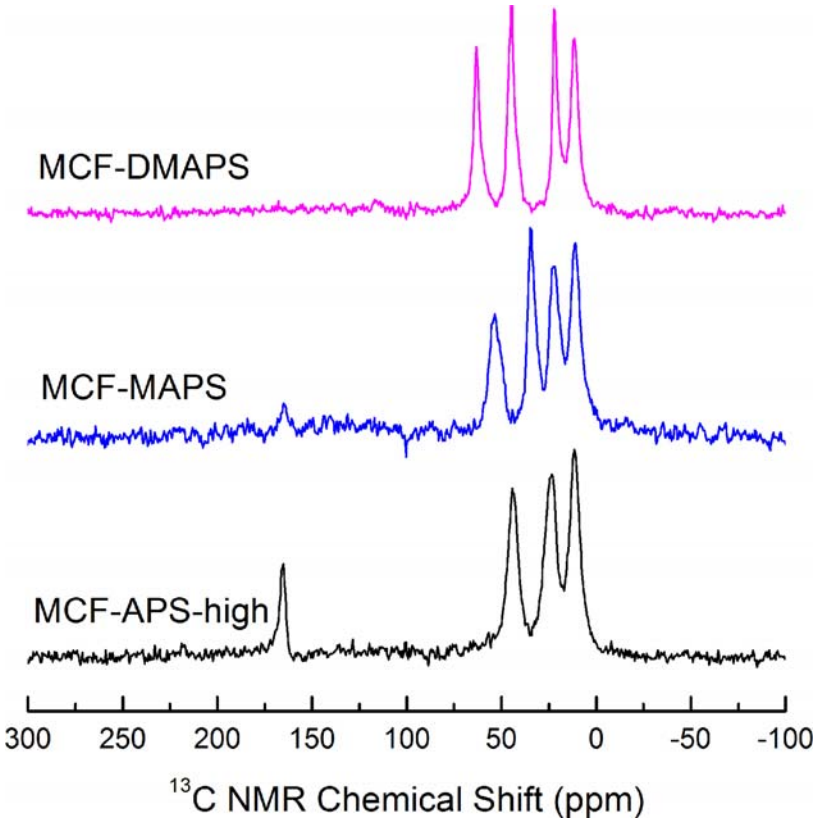

Figure 3.3. ^{13}C CP MAS NMR spectra for amine functionalized materials.

3.3.2 Carbon Dioxide Adsorption

Adsorption isotherms were approximated by measuring CO_2 adsorption capacities at multiple gas concentrations using a TGA. Figure 3.4 shows the adsorption results for CO_2 with primary, secondary and tertiary amines under dry conditions at multiple temperatures. As expected, adsorption capacity is highest at ambient temperature, 25 °C, and decreases as the temperature increases to 45 and then 65 °C. Primary amines exhibit the highest adsorption capacities at all CO_2 partial pressures and possess dramatically higher capacities at air capture conditions than materials constructed of secondary amines. Tertiary amines have negligible CO_2 adsorption even at 25 °C, as predicted, due

to the different adsorption mechanism for tertiary amines with CO_2. Therefore, the minimal uptake observed can be attributed to physisorption of CO_2 on the silica support. It should also be noted that even at the lowest partial pressure of CO_2, roughly 100 ppm, highly loaded primary amines exhibited adsorption capacities close to 1 mmol CO_2 $g_{sorbent}^{-1}$ at ambient temperature and are therefore already outside of the Henry's law regime of adsorption.

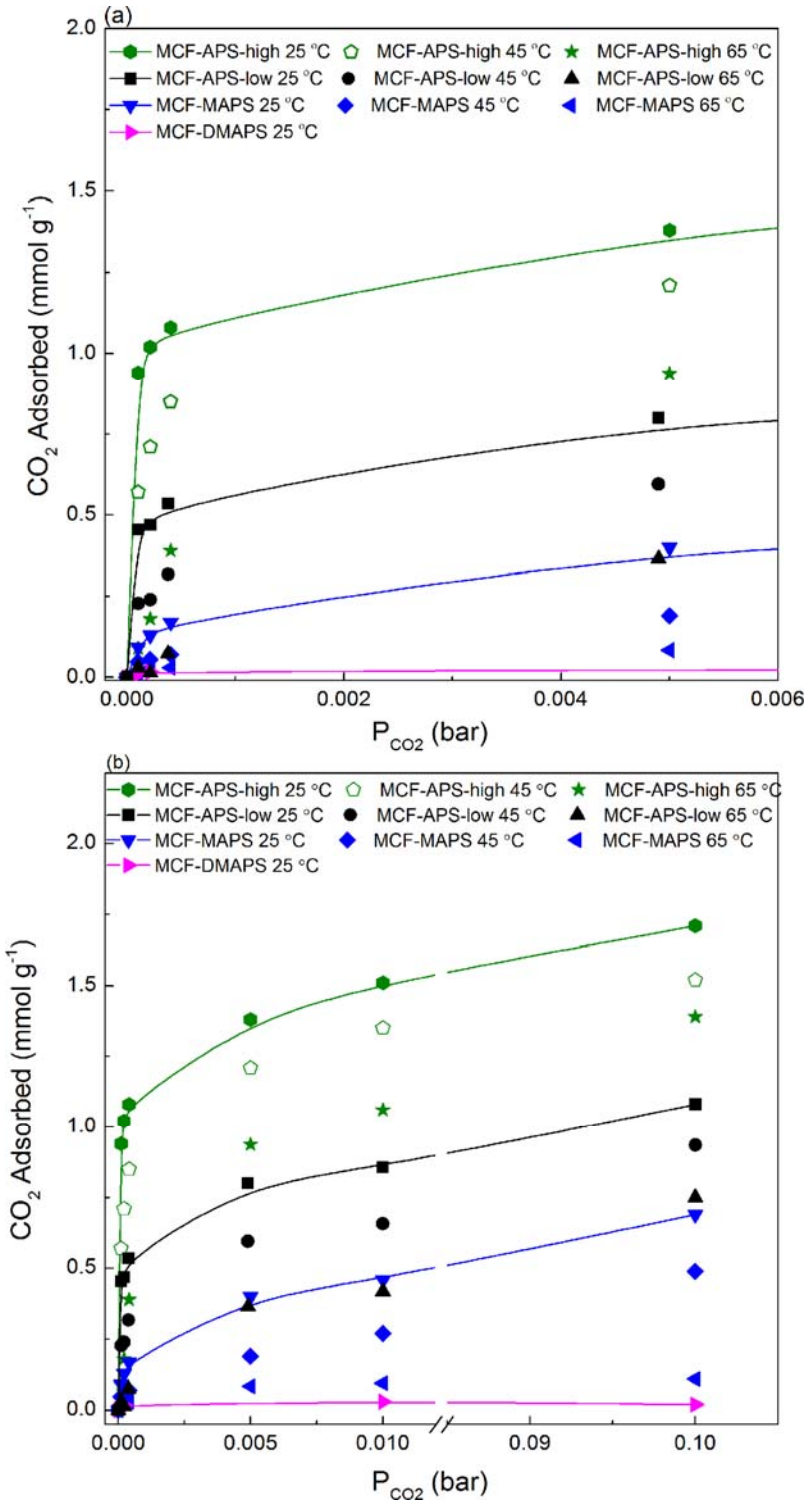

Figure 3.4. (a) Expanded, low partial pressure region CO_2 adsorption isotherms for primary, secondary and tertiary amine materials at multiple temperatures and (b) Full scale adsorption isotherms. Materials functionalized with MAPS (DMAPS) are shown with blue (pink) symbols. Materials functionalized with APS at high (low) loadings are shown with green (black) symbols.

Comparing amine efficiencies of primary and secondary amines in Figure 3.5, it can be seen that at 400 ppm, primary amines possess efficiencies more than twice that of secondary amines with efficiency values of 0.20 and 0.07 mmol CO_2 mmol N^{-1} for MCF-APS-low and MCF-MAPS, respectively, at 25 °C. Tertiary amines have no efficiency reported because their CO_2 adsorption is negligible. The difference between MCF-APS-high and MCF-APS-low demonstrates that primary amine efficiency can be increased to an extent with increased loading. This is not unexpected, as the loadings are not excessive (for example causing significant pore blocking or filling) and, under the dry conditions used here, two amines are expected to participate in the adsorption of one CO_2 molecule, based on the existing mechanistic knowledge of CO_2 adsorption under wet and dry conditions.[38,39] Our data shows that for highly loaded primary amines, efficiency closer to 0.30 mmol CO_2 mmol N^{-1} can be achieved, even under dry air capture conditions. By comparison, Ko et al. found that primary and secondary amines possessed comparable amine efficiencies under pure CO_2 adsorption conditions, with reported values of 0.28 and 0.24 mmol N^{-1}, respectively.[44] Thus, these ultra-dilute conditions significantly decrease the ability for secondary amines to adsorb CO_2 but have more limited effect on the primary amines. It is apparent that primary amines are strong chemisorbers and can obtain efficiencies close to the theoretical maximum (0.5, in this case, under dry conditions) even at the dilute CO_2 concentrations associated with air capture. This dramatic difference in amine efficiency provides strong motivation for the use of primary amine materials in dilute CO_2 capture processes if such processes are to be practically relevant. Secondary and tertiary amines are of limited use as air capture adsorbents since they provide little interaction with the CO_2 during an adsorption process. Additionally,

primary amines exhibit fast adsorption kinetics even at ultra-dilute CO_2 concentrations, indicating that capture processes can operate with relatively fast cycle times (see appendix C for kinetic plots).

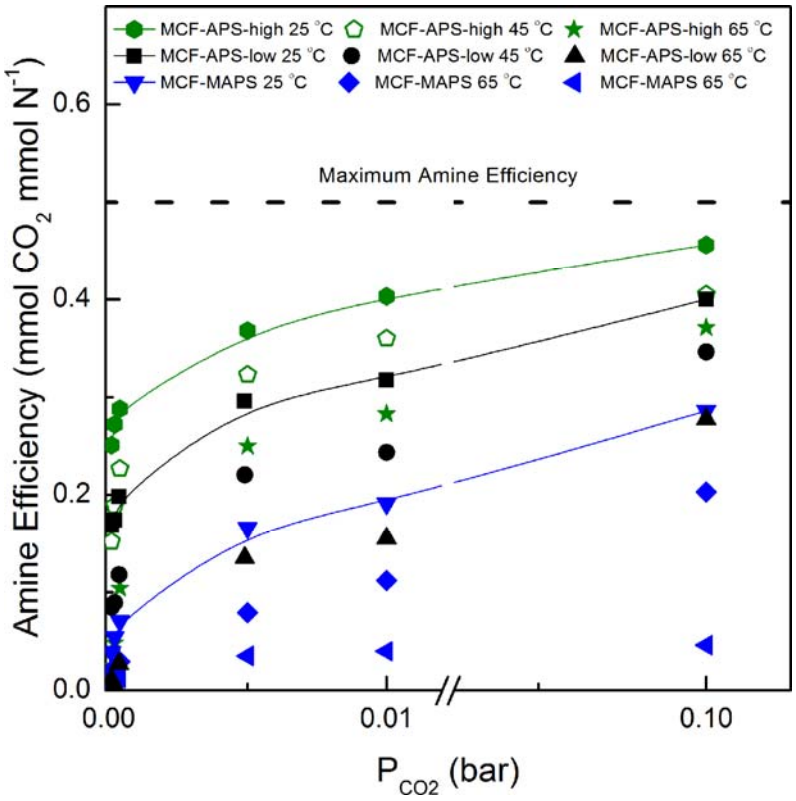

Figure 3.5. Amine efficiency of primary and secondary amines at multiple temperatures. Materials functionalized with MAPS are shown with blue symbols. Materials functionalized with APS at high (low) loadings are shown with green (black) symbols.

The experimental data from isotherm measurements of primary and secondary amines were used to calculate isosteric heats of adsorption using the temperature dependent Toth isotherm model. This model has been used previously for isosteric heat of adsorption measurements and is a good approximation for adsorption of CO_2 onto supported amines.[48] The isosteric heat of adsorption as a function of CO_2 coverage is

presented in Figure 3.6 and shows that primary amines possess a higher heat of adsorption at low loadings than secondary amines. This can explain the increased amine efficiency at ultra-low partial pressures of CO_2 in comparison to secondary amines. From the isotherm model, zero coverage heat of adsorption values were found to be 130 and 88 kJ/mol for primary and secondary amines, respectively. These results for primary and secondary amines are comparable to previously reported trends for APS, MAPS and triamine on mesoporous silica.[48–50]

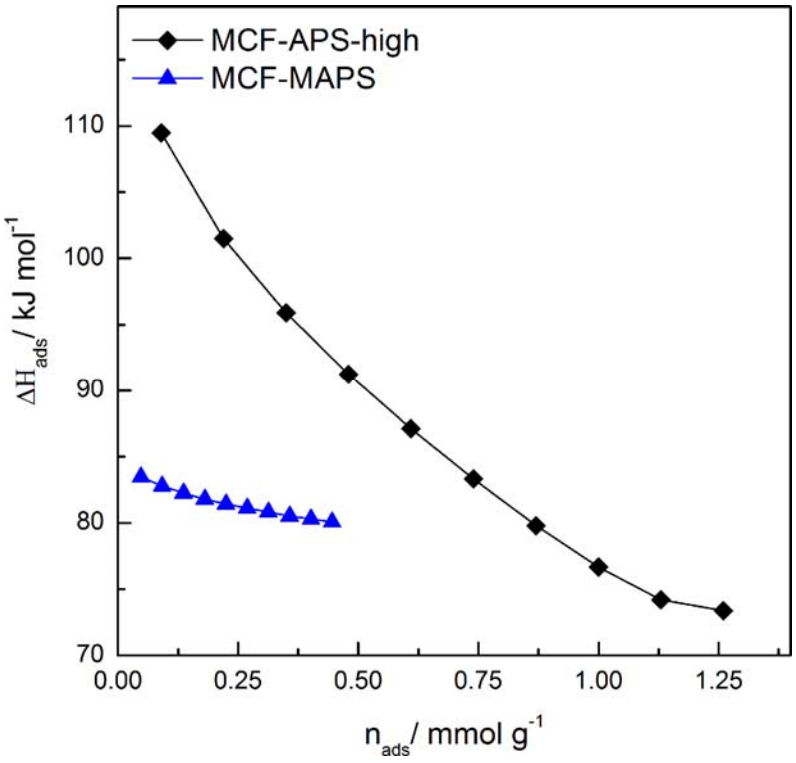

Figure 3.6. Isosteric heat of adsorption for CO_2 on the primary and secondary amine functionalized silica materials as determined using the temperature dependent Toth isotherm model.

3.3.3 Water Adsorption

Understanding water interaction with different amine groups is another key component to finding a practical adsorbent for CO_2 capture, as both air capture and flue gas capture streams typically contain significant amounts of humidity. Assessing the hydrophilic/hydrophobic nature of materials is essential to understand what materials will be best suited to adsorption in humid environments. Hydrophilic materials can facilitate higher CO_2 adsorption efficiencies by attracting water that can act as the free base for deprotonation of the zwitterionic intermediate during CO_2 adsorption, thereby increasing amine efficiency.[51,52] However, an excess of humidity or extreme hydrophillicity could negatively impact adsorption if the water condenses in the pores and blocks access of CO_2 to adsorption sites. Similarly, in a cyclic temperature swing adsorption process, any adsorbed water is likely desorbed under regeneration conditions, potentially incurring an energy penalty associated with removal of the water. It should be noted that the ability of supported amine materials to work as effective air-capture adsorbents under any humidity conditions may offer an advantage over other adsorbents reported for air capture that require precise humidity control such as the ammonium resin studied by Wang and Lackner.[15]

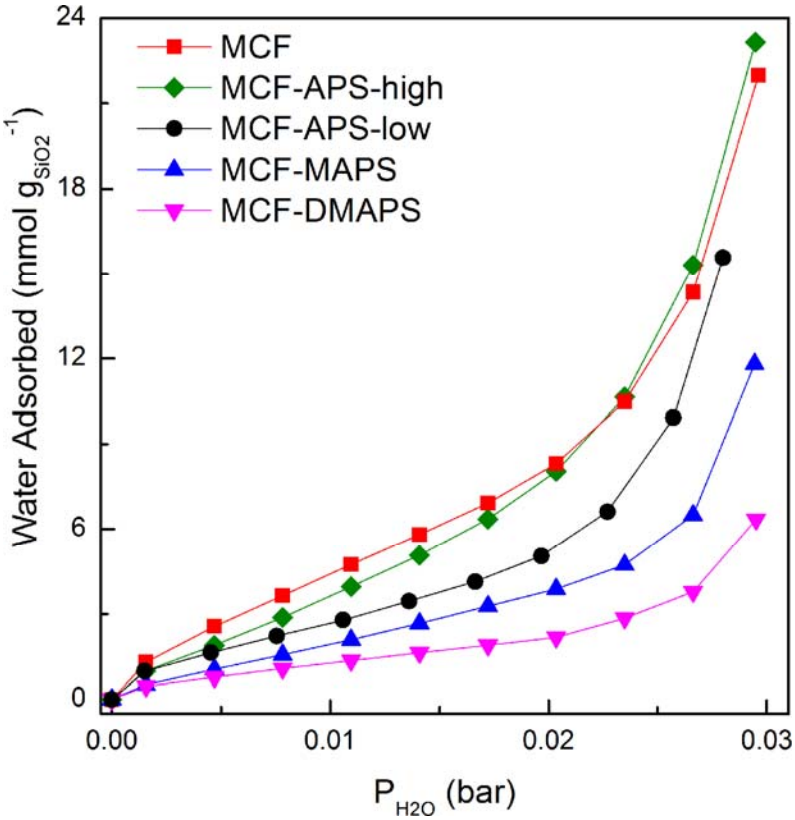

Figure 3.7. Water adsorption isotherms for bare silica and amine functionalized silica at 25 °C.

Based on the hypothesis that water adsorption is dominated by physisorption of water onto surface silanol groups, it may be expected that water adsorption will be maximized on the bare support. Water vapor adsorption isotherms were measured for all the materials at multiple temperatures and it was found that the silica materials functionalized with primary amines have the highest water uptake per gram of silica at all relative humidities, as can be seen in Figure 3.7 (water adsorption isotherms for these materials normalized by surface area are presented in appendix D). Furthermore, MCF-APS-high displayed higher water uptake values than MCF-APS-low, demonstrating a positive correlation between primary amine loading and water uptake. As expected, water

uptake decreases with increasing temperatures, as displayed in Figure 3.8. It is apparent that primary amines enhance hydrophilicity of the adsorbent, whereas secondary or tertiary amines make the material less hydrophillic than the bare support. This characteristic of primary amines coupled with high amine efficiencies at ultra-dilute CO_2 concentrations suggests that an enhanced cooperativity between CO_2, water and the amine would occur upon humid adsorption processes, thus leading to potentially highly efficient adsorbents.

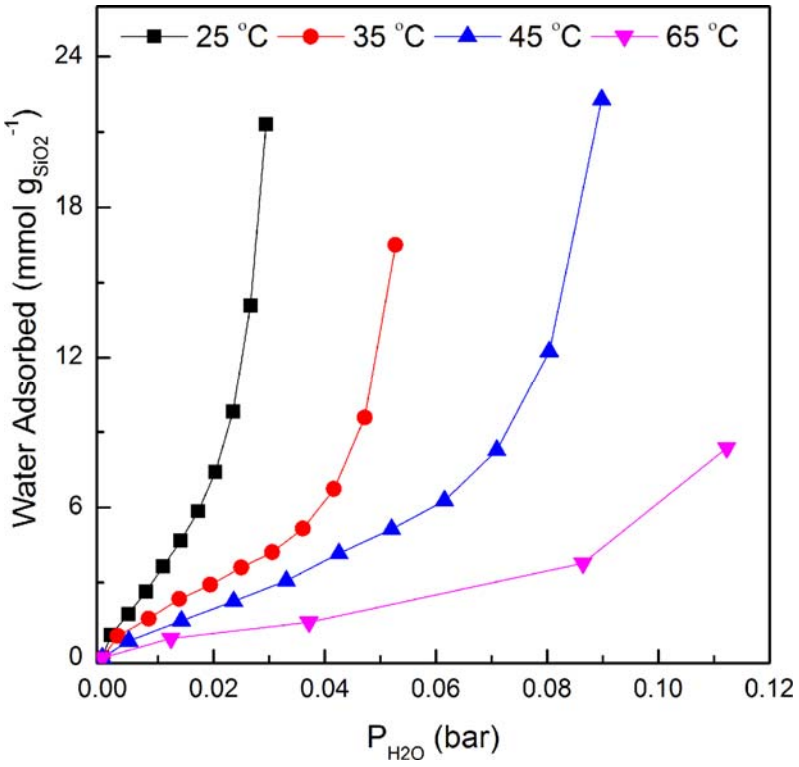

Figure 3.8. Water adsorption isotherms at multiple temperatures for the high loading primary amine material (MCF-APS-high).

3.4 Conclusions

A fundamental study of primary, secondary and tertiary class 2 amine-functionalized materials was performed to evaluate adsorption characteristics of different amine structures as they relate to air capture conditions. It was found that primary amines exhibit significantly higher adsorption capacities and amine efficiencies than secondary and tertiary amines with respect to CO_2 adsorption. Additionally, water vapor adsorption isotherms for bare silica as well as amine functionalized silica materials showed that primary amines enhance the water affinity of the solids. This could lead to significant enhancements in amine efficiency for air capture processes, as co-adsorbed water has been shown to enhance CO_2 adsorption in previous studies focused on CO_2 capture from flue gas.[38,39] These results indicate that future studies on supported amines for air capture should focus on the design and stability assessment of all primary amine or mostly primary amine materials for air capture processes.

3.5 References

(1) Lackner, K. S.; Ziock, H.; Grimes, P. Carbon Dioxide Extraction from Air: Is It an Option? In *24th International Conference on Coal Utilization & Fuel Systems*; Clearwater, FL, 1999.

(2) Zeman, F.; Lackner, K. S. Capturing Carbon Dioxide Directly from the Atmosphere. *World Res. Rev.* **2004**, *16*, 157–172.

(3) Zeman, F. Energy and Material Balance of CO_2 Capture from Ambient Air. *Environ. Sci. Technol.* **2007**, *41*, 7558–7563.

(4) Nikulshina, V.; Hirsch, D.; Mazzotti, M.; Steinfeld, A. CO_2 Capture from Air and Co-Production of H_2 via the $Ca(OH)_2$–$CaCO_3$ Cycle Using Concentrated Solar power–Thermodynamic Analysis. *Energy* **2006**, *31*, 1715–1725.

(5) Baciocchi, R.; Storti, G.; Mazzotti, M. Process Design and Energy Requirements for the Capture of Carbon Dioxide from Air. *Chem. Eng. Proces.* **2006**, *45*, 1047–1058.

(6) Stolaroff, J. K.; Keith, D. W.; Lowry, G. V. Carbon Dioxide Capture from Atmospheric Air Using Sodium Hydroxide Spray. *Environ. Sci. Technol.* **2008**, *42*, 2728–2735.

(7) Sherman, S. R. Nuclear Powered CO_2 Capture from the Atmosphere. *Environ. Prog. Sustain. Energy* **2009**, *28*, 52–59.

(8) Mahmoudkhani, M.; Keith, D. W. Low-Energy Sodium Hydroxide Recovery for CO_2 Capture from Atmospheric air—Thermodynamic Analysis. *Int. J. Greenh. Gas Control* **2009**, *3*, 376–384.

(9) Tepe, J. B.; Dodge, B. F. Absorption of Carbon Dioxide by Sodium Hydroxide Solutions in a Packed Column. *Trans. Am. Inst. Chem. Eng.* **1943**, *39*, 255–276.

(10) Spector, N. A.; Dodge, B. F. Removal of Carbon Dioxide from Atmospheric Air. *Trans. Am. Inst. Chem. Eng.* **1946**, *42*, 827–848.

(11) Blum, H. A.; Stutzman, L. F.; Dodds, W. S. Gas Absorption - Absorption of Carbon Dioxide from Air by Sodium and Potassium Hydroxides. *Ind. Eng. Chem. Res.* **1952**, *44*, 2969–2974.

(12) Nikulshina, V.; Ayesa, N.; Gálvez, M. E.; Steinfeld, A. Feasibility of Na-Based Thermochemical Cycles for the Capture of CO_2 from air—Thermodynamic and Thermogravimetric Analyses. *Chem. Eng. J.* **2008**, *140*, 62–70.

(13) Nikulshina, V.; Gebald, C.; Steinfeld, A. CO_2 Capture from Atmospheric Air via Consecutive CaO-Carbonation and $CaCO_3$-Calcination Cycles in a Fluidized-Bed Solar Reactor. *Chem. Eng. J.* **2009**, *146*, 244–248.

(14) Lackner, K. S. Capture of Carbon Dioxide from Ambient Air. *Eur. Phys. J. Spec. Top.* **2009**, *176*, 93–106.

(15) Wang, T.; Lackner, K. S. A Moisture Swing Sorbent for Carbon Dioxide Capture from Ambient Air. *Environ. Sci. Technol.* **2011**, *45*, 6670–6675.

(16) Choi, S.; Drese, J. H.; Eisenberger, P. M.; Jones, C. W. A New Paradigm of Anthropogenic CO_2 Reduction: Adsorptive Fixation of CO_2 from the Ambient Air as a Carbon Negative Technology. In *AIChE Annual Meeting*; Nashville, 2009.

(17) Choi, S.; Drese, J. H.; Eisenberger, P. M.; Jones, C. W. Application of Amine-Tethered Solid Sorbents for Direct CO_2 Capture from the Ambient Air. *Environ. Sci. Technol.* **2011**, *45*, 2420–2427.

(18) Choi, S.; Gray, M. L.; Jones, C. W. Amine-Tethered Solid Adsorbents Coupling High Adsorption Capacity and Regenerability for CO_2 Capture from Ambient Air. *ChemSusChem* **2011**, *4*, 628–635.

(19) Belmabkhout, Y.; Serna-Guerrero, R.; Sayari, A. Amine-Bearing Mesoporous Silica for CO_2 Removal from Dry and Humid Air. *Chem. Eng. Sci.* **2010**, *65*, 3695–3698.

(20) Chaikittisilp, W.; Lunn, J. D.; Shantz, D. F.; Jones, C. W. Poly(L-Lysine) Brush-Mesoporous Silica Hybrid Material as a Biomolecule-Based Adsorbent for CO_2 Capture from Simulated Flue Gas and Air. *Chem. Eur. J.* **2011**, *17*, 10556–10561.

(21) Chaikittisilp, W.; Khunsupat, R.; Chen, T. T.; Jones, C. W. Poly(allylamine)-Mesoporous Silica Composite Materials for CO_2 Capture from Simulated Flue Gas or Ambient Air. *Ind. Eng. Chem. Res.* **2011**, *50*, 14203–14210.

(22) Chaikittisilp, W.; Kim, H.; Jones, C. W. Mesoporous Alumina-Supported Amines as Potential Steam-Stable Adsorbents for Capturing CO_2 from Simulated Flue Gas and Ambient Air. *Energy Fuels* **2011**, *25*, 5528–5537.

(23) Gebald, C.; Wurzbacher, J. A.; Tingaut, P.; Zimmermann, T.; Steinfeld, A. Amine-Based Nanofibrillated Cellulose as Adsorbent for CO_2 Capture from Air. *Environ. Sci. Technol.* **2011**, *45*, 9101–9208.

(24) Wurzbacher, J. A.; Gebald, C.; Steinfeld, A. Separation of CO_2 from Air by Temperature-Vacuum Swing Adsorption Using Diamine-Functionalized Silica Gel. *Energy Environ. Sci.* **2011**, *4*, 3584–3592.

(25) Stuckert, N. R.; Yang, R. T. CO_2 Capture from the Atmosphere and Simultaneous Concentration Using Zeolites and Amine-Grafted SBA-15. *Environ. Sci. Technol.* **2011**, *45*, 10257–10264.

(26) Wang, X.; Ma, X.; Schwartz, V.; Clark, J. C.; Overbury, S. H.; Zhao, S.; Xu, X.; Song, C. A Solid Molecular Basket Sorbent for CO_2 Capture from Gas Streams with Low CO2 Concentration under Ambient Conditions. *Phys. Chem. Chem. Phys.* **2012**, *14*, 1485–1492.

(27) Goeppert, A.; Czaun, M.; May, R. B.; Prakash, G. K. S.; Olah, G. A.; Narayanan, S. R. Carbon Dioxide Capture from the Air Using a Polyamine Based Regenerable Solid Adsorbent. *J. Am. Chem. Soc.* **2011**.

(28) He, L.; Fan, M.; Dutcher, B.; Cui, S.; Shen, X.; Kong, Y.; Russell, A. G.; McCurdy, P. Dynamic Separation of Ultradilute CO_2 with a Nanoporous Amine-Based Sorbent. *Chem. Eng. J.* **2012**, *189-190*, 13–23.

(29) Kulkarni, A. R.; Sholl, D. S. Analysis of Equilibrium-Based TSA Processes for Direct Capture of CO_2 from Air. *Ind. Eng. Chem. Res.* **2012**, *51*, 8631–8645.

(30) Rahaman, M. S. A.; Zhang, L.; Cheng, L.-H.; Xu, X.-H.; Chen, H.-L. Capturing Carbon Dioxide from Air Using a Fixed Carrier Facilitated Transport Membrane. *RSC Adv.* **2012**, *2*, 9165–9172.

(31) Goldberg, D. S.; Lackner, K. S.; Han, P.; Slagle, A. L.; Wang, T. Co-Location of Air Capture, Subseafloor CO_2 Sequestration, and Energy Production on the Kerguelen Plateau. *Environ. Sci. Technol.* **2013**, *47*, 7521–7529.

(32) Gebald, C.; Wurzbacher, J. A.; Tingaut, P.; Steinfeld, A. Stability of Amine-Functionalized Cellulose during Temperature-Vacuum-Swing Cycling for CO_2 Capture from Air. *Environ. Sci. Technol.* **2013**, *47*, 10063–10070.

(33) Lu, W.; Sculley, J. P.; Yuan, D.; Krishna, R.; Zhou, H.-C. Carbon Dioxide Capture from Air Using Amine-Grafted Porous Polymer Networks. *J. Phys. Chem. C* **2013**, *117*, 4057–4061.

(34) He, H.; Zhong, M.; Konkolewicz, D.; Yacatto, K.; Rappold, T.; Sugar, G.; David, N. E.; Matyjaszewski, K. Carbon Black Functionalized with Hyperbranched Polymers: Synthesis, Characterization, and Application in Reversible CO_2 Capture. *J. Mater. Chem. A* **2013**, *1*, 6810–6821.

(35) He, H.; Li, W.; Zhong, M.; Konkolewicz, D.; Wu, D.; Yaccato, K.; Rappold, T.; Sugar, G.; David, N. E.; Matyjaszewski, K. Reversible CO_2 Capture with Porous Polymers Using the Humidity Swing. *Energy Environ. Sci.* **2013**, *6*, 488–493.

(36) Wörmeyer, K.; Smirnova, I. Adsorption of CO_2, Moisture and Ethanol at Low Partial Pressure Using Aminofunctionalised Silica Aerogels. *Chem. Eng. J.* **2013**, *225*, 350–357.

(37) Gebald, C.; Wurzbacher, J. a; Borgschulte, A.; Zimmermann, T.; Steinfeld, A. Single-Component and Binary CO_2 and H_2O Adsorption of Amine-Functionalized Cellulose. *Environ. Sci. Technol.* **2014**, *48*, 2497–2504.

(38) Choi, S.; Drese, J. H.; Jones, C. W. Adsorbent Materials for Carbon Dioxide Capture from Large Anthropogenic Point Sources. *ChemSusChem* **2009**, *2*, 796–854.

(39) Bollini, P.; Didas, S. A.; Jones, C. W. Amine-Oxide Hybrid Materials for Acid Gas Separations. *J. Mater. Chem.* **2011**, *21*, 15100–15120.

(40) Ping, E. W.; Wallace, R.; Pierson, J.; Fuller, T. F.; Jones, C. W. Highly Dispersed Palladium Nanoparticles on Ultra-Porous Silica Mesocellular Foam for the Catalytic Decarboxylation of Stearic Acid. *Microporous Mesoporous Mater.* **2010**, *132*, 174–180.

(41) Harlick, P. J. E.; Sayari, A. Applications of Pore-Expanded Mesoporous Silica. 5. Triamine Grafted Material with Exceptional CO_2 Dynamic and Equilibrium Adsorption Performance. *Ind. Eng. Chem. Res.* **2007**, *46*, 446–458.

(42) Sing, K. S. W.; Everett, D. H.; Haul, R. A. W.; Moscou, L.; Pierotti, R. A.; Rouquerol, J.; Siemieniewska, T. Reporting Physisorption Data for Gas Solid Systems with Special Reference to the Determination of Surface-Area and Porosity (Recommendations 1984). *Pure Appl. Chem* **1985**, *57*, 603–619.

(43) Lukens Jr, W. W.; Schmidt-Winkel, P.; Zhao, D.; Feng, J.; Stucky, G. D. Evaluating Pore Sizes in Mesoporous Materials: A Simplified Standard Adsorption Method and a Simplified Broekhoff-de Boer Method. *Langmuir* **1999**, *15*, 5403–5409.

(44) Ko, Y. G.; Shin, S. S.; Choi, U. S. Primary, Secondary, and Tertiary Amines for CO_2 Capture: Designing for Mesoporous CO2 Adsorbents. *J. Colloid Interface Sci.* **2011**, *361*, 594–602.

(45) Bollini, P.; Choi, S.; Drese, J. H.; Jones, C. W. Oxidative Degradation of Aminosilica Adsorbents Relevant to Post-Combustion CO_2 Capture. *Energy Fuels* **2011**, *25*, 2416–2425.

(46) Heydari-Gorji, A.; Belmabkhout, Y.; Sayari, A. Degradation of Amine-Supported CO_2 Adsorbents in the Presence of Oxygen-Containing Gases. *Microporous Mesoporous Mater.* **2011**, *145*, 146–149.

(47) Sayari, A.; Belmabkhout, Y.; Da'na, E. CO_2 Deactivation of Supported Amines: Does the Nature of Amine Matter? *Langmuir* **2012**, *28*, 4241–4247.

(48) Serna-Guerrero, R.; Belmabkhout, Y.; Sayari, A. Modeling CO_2 Adsorption on Amine-Functionalized Mesoporous Silica: 1. A Semi-Empirical Equilibrium Model. *Chem. Eng. J.* **2010**, *161*, 173–181.

(49) Knofel, C.; Martin, C.; Hornebecq, V.; Llewellyn, P. L. Study of Carbon Dioxide Adsorption on Mesoporous Aminopropylsilane-Functionalized Silica and Titania Combining Microcalorimetry and in Situ Infrared Spectroscopy. *J. Phys. Chem. C* **2009**, *113*, 21726–21734.

(50) Mello, M. R.; Phanon, D.; Silveira, G. Q.; Llewellyn, P. L.; Ronconi, C. M. Amine-Modified MCM-41 Mesoporous Silica for Carbon Dioxide Capture. *Microporous Mesoporous Mater.* **2011**, *143*, 174–179.

(51) Caplow, M. Kinetics of Carbamate Formation and Breakdown. *J. Am. Chem. Soc.* **1968**, *90*, 6795–6803.

(52) Donaldson, T. L.; Nguyen, Y. N. Carbon Dioxide Reaction Kinetics and Transport in Aqueous Amine Membranes. *Ind. Eng. Chem. Fundam.* **1980**, *19*, 260–266.

Chapter 4

AN ADSORPTION APPARATUS TO STUDY BINARY ADSORPTION OF CO_2 AND WATER ON SUPPORTED AMINE ADSORBENTS

4.1 Background

It is known that the presence of water vapor will have an impact on the adsorption capacities of CO_2 on supported amine adsorbents.[1] However, the degree of enhancement varies between materials and operating conditions used. Nevertheless, because water vapor is present both in flue gas streams and ambient air, it is necessary to obtain a qualitative and quantitative understanding of the kinetic and thermodynamic behavior of water and CO_2 co-adsorption on potential CO_2 capture sorbents. The former can be achieved with a packed bed-mass spectrometer flow system set up whereby the gas lines entering the fixed bed can be pre-humidified with water spargers and the breakthrough of both CO_2 and water can be monitored via mass spectroscopy.[2,3] The latter requires an instrument that will yield binary adsorption isotherms.

Traditionally, single component adsorption isotherms are evaluated in one of two ways: gravimetrically with a TGA or volumetrically with a pressure decay cell (PDC). TGA is the easiest measurement to perform as it simply consists of measuring the increase in weight of a candidate sorbent as CO_2 flows past it. The downside to TGA is that it is not equipped for humid measurements unless significant modifications are made

to the system, as has been done by Sayari's group.[4] A PDC measures adsorption through the change in pressure in a sample cell containing adsorbent material followed by a mole balance to determine the amount of gas adsorbed. Pressure decay cells are excellent for measuring single component adsorption isotherms in the ambient to high pressure range. However, they cannot measure multicomponent isotherms, as the adsorption from CO_2 and water cannot be deconvoluted into individual contributions. Both of these techniques work well for single component adsorption studies. However, they are less practical to use if one wants to consider the additional component of water vapor.

To address the need for binary equilibrium adsorption data, I chose to build a custom volumetric adsorption system that is similar to other systems traditionally used for multicomponent analysis of organics with solid sorbents like zeolites and activated carbons.[5–7] This system is akin to a PDC but has a GC sampling valve connected to the closed loop system so that both CO_2 and water adsorption can be monitored. The following chapter discusses the design, operational procedure and validation of an adsorption apparatus constructed to obtain this critical data.

4.2 Experiments

4.2.1 Apparatus

The design for the volumetric system was inspired by Qi and LeVan's system for binary organic-water vapor sorption analysis.[7,8] The basic premise of the system is to place a known amount of sorbent material into a closed, fixed volume (55.7 cm^3), circulating system where known amounts of CO_2 and water vapor can be injected periodically. Adsorption of the two components is monitored via a gas chromatograph (GC) and a mole balance is used for calculating the amount of adsorbed species. A

schematic of the system is shown in Figure 4.1. The system is comprised of a stainless steel closed loop that connects a fixed bed (0.5" VCR bulkhead union with fritted gasket), water injection port (Swagelok type SS-42GVCR4, one end fitted with GC injector septa Restek type 06-802-771), CO_2 dose valve (Swagelok type SS-42GXVCR4), GC sampling valve (VICI type DC6UWE), pressure transducers (Swagelok type PTU-S-AC3-31AD-C) and a circulation pump (Ruska type 2330-802). The system is contained within an environmental chamber (Russells RB-4-03-03) that controls the temperature and can operate at temperatures of -50 to 150 ºC. Two mass flow controllers (MKS type 1480A00111CR1BM, 1480A00151CR1BM) are used to mix CO_2 and helium gas to desired concentrations that are then dosed into the closed loop system from the gas reservoir (282 cm^3). National Instrument LabView software is used to read and record system and reservoir pressures. Gas concentrations in the system are sampled with a 250 µL sample loop (VICI type SL250NW) that are then analyzed via GC (Agilent 7890A Series Custom). A flame ionization detector (FID) is used to analyze CO_2 concentration while a thermal conductivity detector (TCD) is used for water. The GC is equipped with a custom designed nickel catalyst bed used to methanize CO_2 at 375 ºC during GC analysis so that FID can be used. This provides a higher degree of resolution for CO_2 detection as opposed to TCD (ppb levels versus ppm level detection limit). A HP-Plot U capillary column (30 m×530 µm ID×20 µm) is used to separate CO_2 and water.

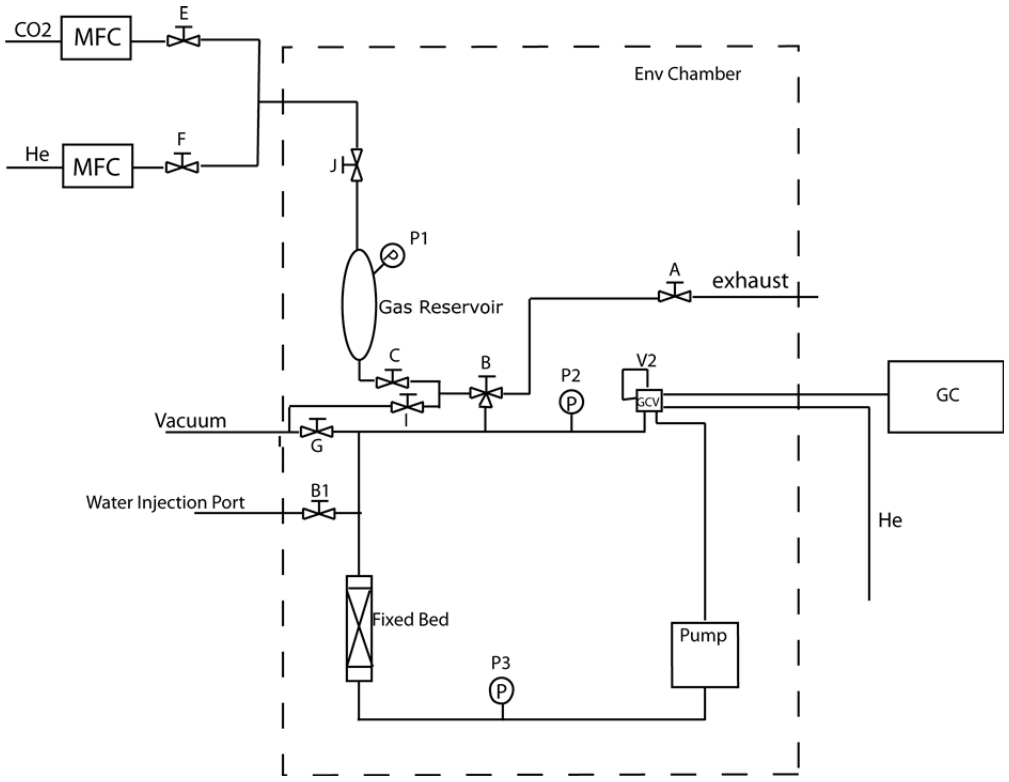

Figure 4.1. Schematic of volumetric system designed for binary CO_2-H_2O adsorption.

4.2.2 Operation Procedure

Before experiments were conducted, the GC signal responses to a wide range of CO_2 and water concentrations were recorded to calibrate the instrument. Dilute mixture cylinders of CO_2 in helium were used for CO_2 calibration. The gas cylinders were directly connected to the GC sampling valve and allowed to flow for several hours before sampling. At least three GC measurements were taken and then averaged to obtain one calibration point. For water calibration, a helium cylinder was connected to a Setaram WetSys humidity generator. This instrument allows for precise setting of gas relative humidity, temperature and flow rate. The outlet gas line from the WetSys was connected to the GC sampling valve directly and at least three GC measurements were averaged to obtain one calibration point.

Before an adsorption experiment, powder adsorbent material was first pressed into pellets under a pressure of 1000 psi and then crushed and sieved in a size range of 355-850 μm. Next, between 50-80 mg of sample was loaded into the fixed bed, sitting on top of a 0.5 μm fritted gasket with glass wool on top. The fixed bed was then connected to the volumetric system (Note: Fresh VCR gaskets were used every time the fixed bed unit was reattached to the apparatus). Prior to each adsorption experiment, the system was leak checked by charging with helium gas up to 1 bar gauge at 30 °C and monitoring pressure for 1 h. A pressure loss less than -1×10^{-5} mbar s^{-1} was deemed acceptable since that was within the noise of the pressure transducers. After leak testing the system, heat tape was wrapped around the fixed bed unit and heated to 120 ºC for regeneration of the sorbent. To regenerate the sorbent, a series of vacuum-helium flush cycles was performed to remove CO_2 and water previously bound to the adsorbent. The concentration of CO_2 and water in the system was monitored with the GC and regeneration was complete when no CO_2 or water was detected coming off the adsorbent during the helium purge step. After regeneration, the heating tape was removed and the fixed bed unit was allowed to cool at room temperature before closing the environmental chamber and setting it to the desired temperature of operation.

To generate binary isotherms, water was first injected into the system under an inert helium environment followed by successive CO_2 doses to obtain data for a fixed water loading. A custom designed, gas tight syringe with 10 μL capacity from Hamilton Company was used so that the point of entrance for the water was directly in line with circulation flow of the system to ensure faster dispersion of the water vapor. At the time of water injection, the water injection port was heated with heat tape to approximately

100 ºC as an additional measure to ensure that the liquid water evaporated within the system. After water injection, the heating tape was turned off and the water vapor was allowed to circulate in the system for at least 12 h before introduction of CO_2. The system was monitored with the GC to determine when equilibrium had been reached and the concentration of remaining gas species. Equilibrium was defined as a molar adsorption rate less than 1×10^{-9} mmol s^{-1}. This translates to an adsorption rate of approximately 8×10^{-5} mmol day^{-1} and was therefore deemed an acceptable criterion for pseudoequilibrium. Typically, equilibrium was achieved within 24 h, except for highly loaded materials that took much longer. A material balance was applied to determine the amount of adsorbed CO_2 and water by subtracting the amount of each component circulating in the system by the amount that was injected/dosed.

4.2.3 Validation Procedures

To ensure that the system was operating properly for both CO_2 and water adsorption measurements, materials were tested on the volumetric system and then compared to values obtained with other commercially available single component adsorption instruments. The methods for validating both CO_2 and water operation for the volumetric system are discussed below.

4.2.3.1 CO_2 Validation

Two external instruments were used to validate the volumetric system for CO_2 adsorption capabilities, one being a gravimetric technique and the other volumetric. A TA instruments TGA was used as the gravimetric apparatus. Standard operating procedures for this instrument are discussed in previous chapters. A PDC was used for the

volumetric apparatus. For PDC operation, between 30-50 mg of adsorbent was loaded into the sample cell and regenerated at 120 ºC under vacuum for 3 h. The sample was then cooled down to the adsorption temperature; in this case 30 ºC was used for all validation experiments. After the sample cooled completely, the vacuum connection was closed and the adsorption measurement was started. The material used for these experiments was pelletized silica supported primary amine adsorbent, SBA-APS. Synthesis and functionalization for this type of material was discussed in chapter 2.

4.2.3.2 Water Validation

A gravimetric technique was used to validate the volumetric system for water adsorption capabilities. A Hiden IGASorp was used to measure single component water vapor isotherms that could be compared to water adsorption values obtained with the volumetric system. Operation procedures for this instrument were discussed in chapter 3. However, for these experiments regeneration was performed for 3 h at 120 ºC under flowing nitrogen. The material used for these experiments was pelletized un-functionalized silica, MCF. Synthesis for this type of material was discussed in chapter 3.

4.3 Results & Discussion

4.3.1 Validation

To ensure that the volumetric system was operating properly after construction, single component water and CO_2 adsorption isotherms were obtained using adsorbent materials that had been evaluated on other instrumentation as well so that it could be verified that accurate values can be obtained with the newly developed system. Figure 4.2 and Figure 4.3 show the data that was obtained for this purpose. It can be seen that for

both CO_2 and water adsorption there is good agreement between values obtained with the volumetric system (VS) and other adsorption apparatuses.

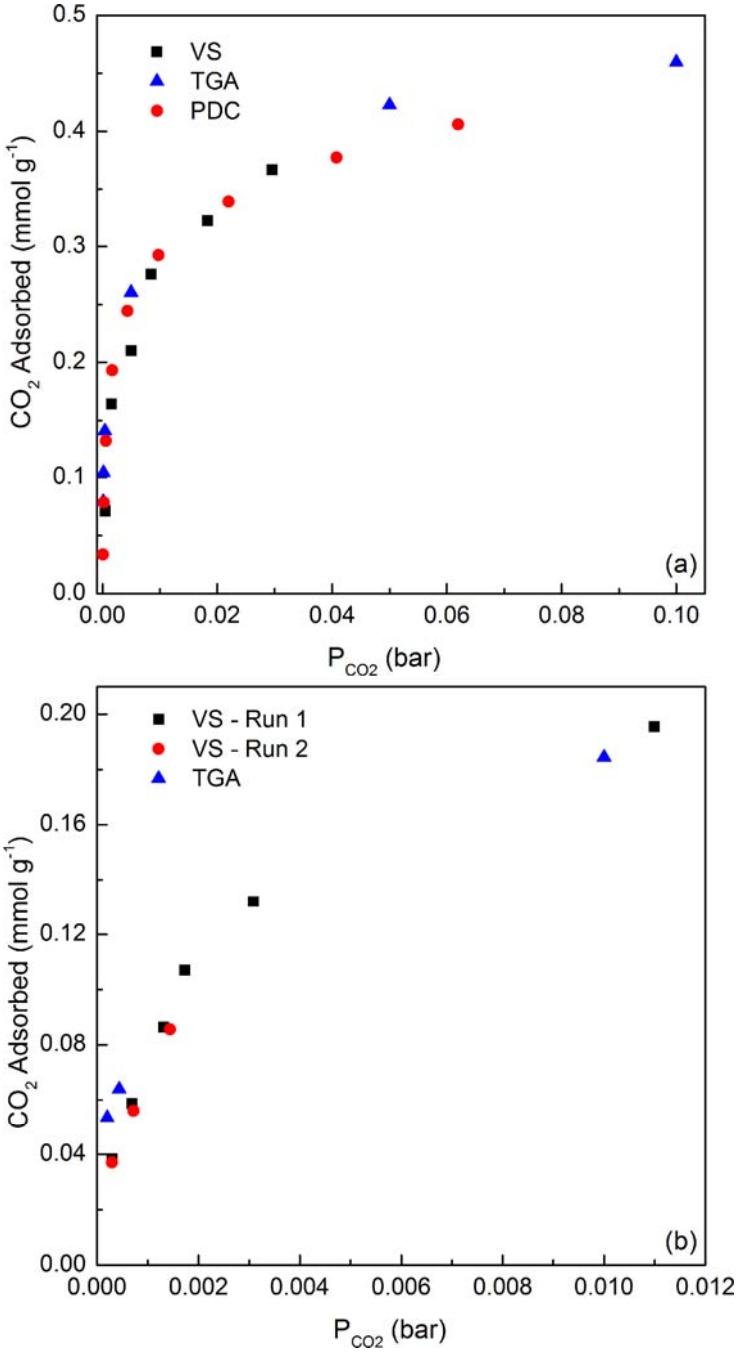

Figure 4.2. Comparison of CO_2 isotherms (a) obtained with the volumetric system and two other adsorption equipment and (b) measured in duplicate on the volumetric system. All measurements are done at 30 ºC. Note: a different SBA-APS material was used for the measurements in plot (a) vs plot (b).

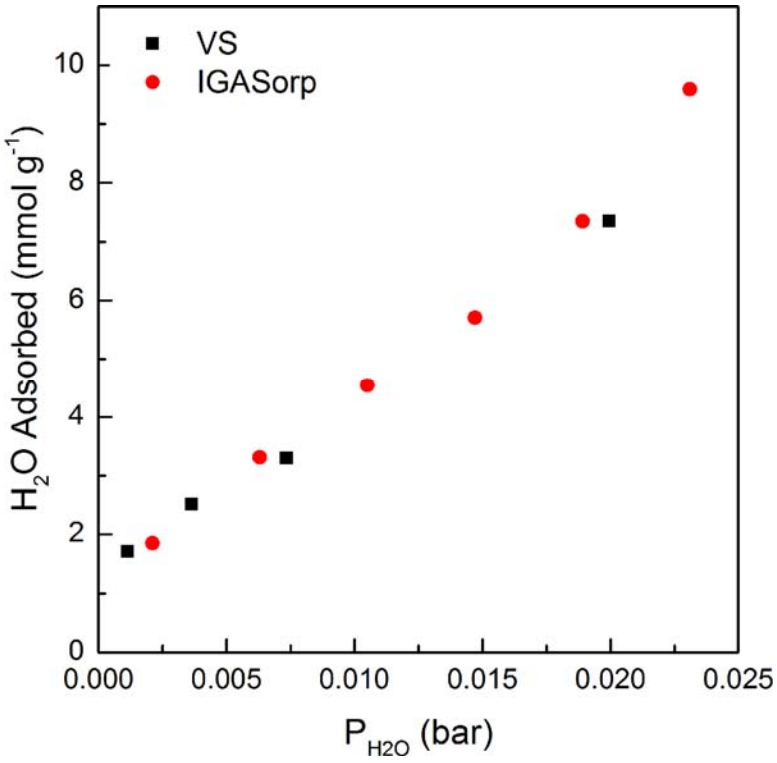

Figure 4.3. Comparison of water isotherms obtained with volumetric system and another adsorption apparatus for the same adsorbent material at 30ºC.

4.3.2 Error Estimation

It is important to understand the potential sources of error for this system to get an idea of the accuracy that can be achieved when operating. There are five major sources of error that could have an impact on the isotherms measured: (1) the GC calibration, (2) variation in the GC measurement, (3) the CO_2 dose, (4) the water dose, and (5) uncertainty in reaching equilibrium. Each of these and their potential impact on measurement accuracy are discussed below.

4.3.2.1 GC calibration

As mentioned in the experimental section, the GC was calibrated for both CO_2 and water responses to known gas compositions so that a calibration curve could be obtained to determine the concentration of unknown gas mixtures. Figure 4.4 shows the

calibration curves obtained for CO_2 and water that are used to interpret co-adsorption GC measurements. The calibration equations obtained are as follows:

CO_2 Concentration [ng μL^{-1}] = 6.582×10^{-3} × GC Area – 0.0134

H_2O Concentration [ng μL^{-1}] = 0.0654 × GC Area + 0.437

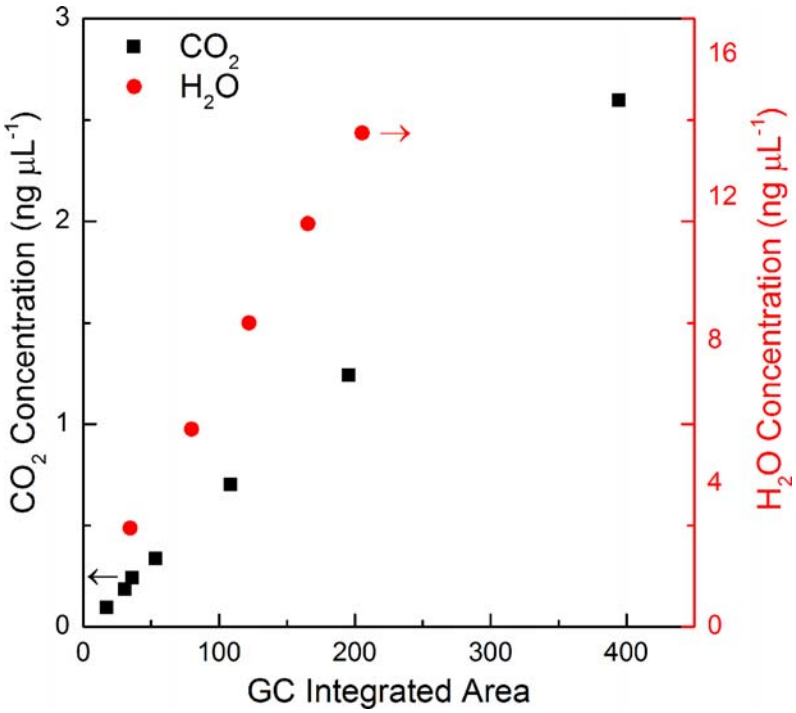

Figure 4.4. GC response areas to known CO_2 and H_2O concentrations. Data used to obtain calibration equation for both gas components.

If the fit of the calibration curve is not good enough, inaccurate predictions of gas concentrations will result during adsorption experiments. This would lead to incorrect mass balances that could affect measured adsorption capacities. However, the R^2 values for both the water and CO_2 data fits are greater than 0.999. Therefore, the calibration is

considered quite good and will not have a significant impact on operation of the volumetric system.

4.3.2.2 Variation of GC measurement

Variability that exists with both the FID and TCD detectors must be evaluated to determine what the effects will be on low partial pressure measurements for both CO_2 and water. Therefore the precision of repeated measurements for both detectors with a constant gas concentration was evaluated. The result of these measurements for both the FID and TCD are shown in Figure 4.5. To evaluate the FID, a helium-CO_2 gas mixture with a concentration representing a partial pressure of roughly 4×10^{-4} bar CO_2 was circulated in the system with no adsorbent. A low concentration was used as this represents the region where absolute error is the highest with respect to the calibration of the GC and is also where variability in the detector would have the greatest impact on measurements. Five measurements were made throughout the course of 21 hours. The variation between measurements averaged a 1.7% error. To evaluate the TCD, a helium-water vapor gas mixture with a concentration representing a partial pressure of roughly 5.6×10^{-3} bar H_2O was circulated in the system with no adsorbent. Ten measurements were made throughout the course of six days. The variation between measurements averaged a 2.4% error. Therefore, it can be assumed that the GC will give consistent results, even in the lower limits of the detectors' capabilities.

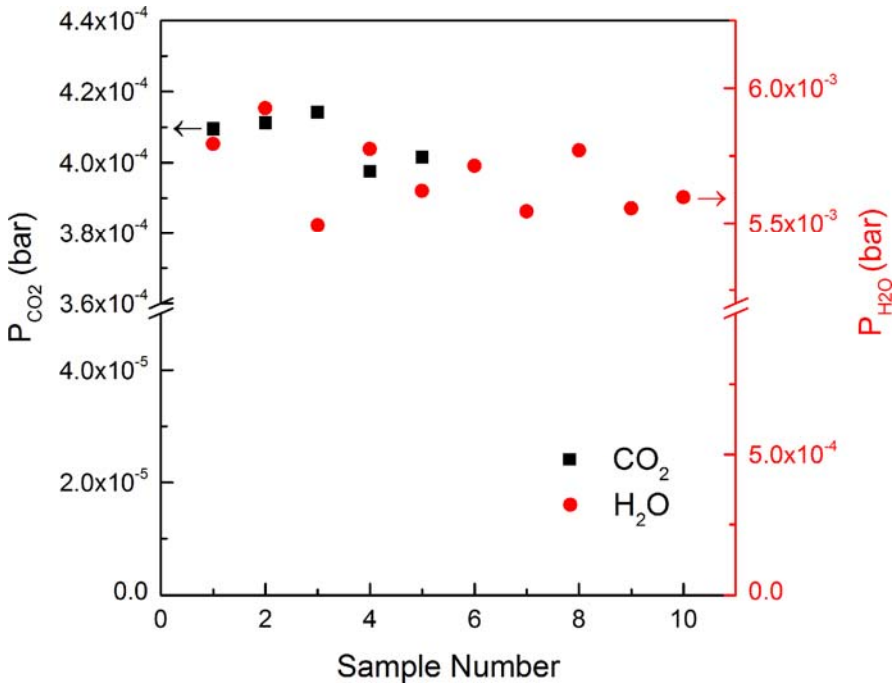

Figure 4.5. GC variation in FID (squares, CO_2) and TCD (circles, H_2O) measurements for a single component gas circulated with no adsorbent over multiple samples.

4.3.2.3 CO_2 dose

An error in the estimation of how much CO_2 is dosed into the system will affect the CO_2 mass balance and therefore the calculation of how much CO_2 has been adsorbed by the adsorbent. The amount of CO_2 dosed into the system is calculated by measuring the change in pressure of the gas reservoir and then applying the ideal gas law to determine the number of moles of CO_2 that have been introduced into the system. Therefore, inaccuracies in operation of the mass flow controllers and pressure transducers are the biggest contributors to error in this scenario. The uncertainty in the pressure transducers and mass flow controllers are 0.065% and 1% of the set point, respectively. To demonstrate the impact this would have on an adsorption experiment, the upper and lower bounds of a CO_2 dose were calculated for an adsorption experiment considering

these uncertainties. For a sample size of roughly 75 mg, a $\pm 1.4\times10^{-3}$ mmol g^{-1} error is introduced for a material with an equilibrium adsorption capacity of 0.038 mmol g^{-1} at 295 ppm CO_2 partial pressure. Therefore it can be concluded that error contributions from the aspect of CO_2 dosing will be negligible.

4.3.2.4 Water dose

Similar to the CO_2 dose, an error in estimating the amount of water injected will affect the calculation of how much water has been adsorbed by the material. The amount of water injected into the system is determined visually by markings on the syringe. The syringe used has a maximum capacity of 10 μL with indicator markings at every tenth of a microliter. Therefore, the uncertainty in measurement will be ±0.05 μL.[9] To demonstrate the impact this would have on an adsorption experiment, the upper and lower bounds of a water dose were calculated for an adsorption experiment using this uncertainty. For a sample size of roughly 75 mg, a ±0.036 mmol g^{-1} error is introduced for a material with an equilibrium adsorption capacity of 1.94 mmol g^{-1} at a water partial pressure of 7.09×10^{-3} bar. Therefore, the uncertainty in water capacities is greater than that for CO_2 adsorption capacities, but is still relatively low.

4.3.2.5 Uncertainty in reaching equilibrium

Because the GC will never reach an exact equilibrium where there is precisely no variation in GC measurements, a reasonable criteria for equilibrium must be established. Therefore it is possible that reported adsorption capacities are lower than the true equilibrium amount that would be adsorbed for an infinite amount of measurement time. As mentioned in the experimental part of this chapter, equilibrium is defined for this

system's operation as the point where the molar adsorption rate of a gas species is less than 1×10^{-9} mmol s^{-1}. For an experiment using 80 mg of adsorbent, if a measurement was allowed to go for 20 days past this equilibrium criterion, it would result in an increase of adsorption capacity of 0.02 mmol g^{-1}. As diffusionally resistant materials are the most likely candidates to suffer from underpredictions of adsorption capacity, and those materials possess higher adsorption capacities due to high amine content, it can be concluded that this would be a minor fraction of the overall capacity measured.

4.4 Conclusions

Binary adsorption isotherms for supported amine adsorbents can potentially enhance the fundamental knowledge of CO_2-H_2O-amine interactions during various adsorption processes. This chapter described the design, operational procedure and validation of an adsorption apparatus that will allow for such studies to take place. After consideration of potential sources of error to this experimental method it can be concluded that sufficiently accurate and consistent dual component isotherms can be measured using this system, thus enabling for new fundamental information to be obtained in the field of supported amine adsorbents for CO_2 capture. The application of this system to a series of supported amine adsorbents is discussed in the following chapter.

4.5 References

(1) Bollini, P.; Didas, S. A.; Jones, C. W. Amine-Oxide Hybrid Materials for Acid Gas Separations. *J. Mater. Chem.* **2011**, *21*, 15100–15120.

(2) Bollini, P.; Brunelli, N. A.; Didas, S. A.; Jones, C. W. Dynamics of CO_2 Adsorption on Amine Adsorbents. 1. Impact of Heat Effects. *Ind. Eng. Chem. Res.* **2012**, *51*, 15145–15152.

(3) Fan, Y.; Lively, R. P.; Labreche, Y.; Rezaei, F.; Koros, W. J.; Jones, C. W. Evaluation of CO_2 Adsorption Dynamics of Polymer/silica Supported Poly(ethylenimine) Hollow Fiber Sorbents in Rapid Temperature Swing Adsorption. *Int. J. Greenh. Gas Control* **2014**, *21*, 61–71.

(4) Serna-Guerrero, R.; Da'na, E.; Sayari, A. New Insights into the Interactions of CO_2 with Amine-Functionalized Silica. *Ind. Eng. Chem. Res.* **2008**, *47*, 9406–9412.

(5) Abdul-Rehman, H.; Hasanain, M.; Loughlin, K. Quaternary, Ternary, Binary, and Pure Component Sorption on Zeolites. 1. Light Alkanes on Linde S-115 Silicalite at Moderate to High Pressures. *Ind. Eng. Chem. Res.* **1990**, *29*, 1525–1535.

(6) Rudisill, E. N.; Hacskaylo, J. J.; LeVan, M. D. Coadsorption of Hydrocarbons and Water on BPL Activated Carbon. *Ind. Eng. Chem. Res.* **1992**, *31*, 1122–1130.

(7) Qi, N.; LeVan, M. D. Coadsorption of Organic Compounds and Water Vapor on BPL Activated Carbon . 5 . Methyl Ethyl Ketone , Methyl Isobutyl Ketone , Toluene , and Modeling. *Ind. Eng. Chem. Res.* **2005**, *44*, 3733–3741.

(8) Qi, N. Adsorption of Organic Compounds and Water Vapor on Activated Carbon: Equilibria and Fixed-Bed Humidity Steps. *Dissertation*, Vanderbilt University, 2003.

(9) Harris, D. C. *Quantitative Chemical Analysis*; 6th ed.; W.H. Freeman and Company: New York, 1982.

Chapter 5

BINARY ADSORPTION STUDIES AT DILUTE CONDITIONS FOR PRIMARY AMINE ADSORBENTS: EFFECT OF AMINE LOADING

5.1 Background

As discussed in chapter 4, a binary adsorption system was built so that supported amine adsorbents could be evaluated at ultra-dilute CO_2 conditions in humid environments. Based on the results from chapter 3, primary amines were identified as the ideal amine type to investigate in this study, as they display the highest amine efficiency in dry, low pressure CO_2 environments and are also the most hydrophilic amine type. Thus, it is believed that primary amines have the potential to display significantly enhanced CO_2 uptake when co-adsorbing water. This is due to the fact that a different adsorption mechanism is postulated to be possible in the presence of humidity, where it has previously been shown that water can promote the formation of bicarbonate and increase amine efficiency to a maximum stoichiometric ratio of 1 CO_2:1 NH_2 in aqueous liquid systems, as discussed in chapter 1. Because it was also observed in chapter 3 that the loading of the primary amine materials affected both CO_2 and water adsorption properties, it would be useful to examine how that same variation in surface coverage would affect adsorption in a humid CO_2 environment. Therefore, the aim of this study was to examine a set of primary amine materials with different amine loadings and to observe how dilute CO_2 adsorption was affected when water co-adsorbed on the material.

5.2 Experiments

5.2.1 Materials Synthesis

Amine functionalized SBA-15 materials were used for this study. The synthesis for SBA-15 is described in chapter 2. The procedure for amine functionalization is as follows: 2 g calcined SBA-15 was dried overnight at 120 ºC on a Schlenk line. After drying, 200 mL of toluene was added to the round bottom flask and stirred at room temperature for 3 h. Next, 3-aminopropyltrimethoxysilane (APS) was added in varying ratios. For SBA-APS-low and SBA-APS-medium, 2 g and 8 g of APS were added, respectively. The solutions were allowed to stir for 24 h at room temperature. For the high loading material, the following alterations were made to the synthesis procedure to achieve organosilane polymerization:[1] 0.6 mL DI water was added to the SBA-15 in toluene solution after 30 min of stirring, then after 3 h of stirring, 4 g APS was added and the solution was then quickly heated to 85 ºC and stirred for 24 h. The resulting solids of all three syntheses were separately filtered and washed with copious amounts of toluene, hexane and methanol. They were then dried overnight on a Schlenk line at 50 °C.

5.2.2 Materials Characterization

Nitrogen physisorption was evaluated with a Micromeritics Tristar II. Nitrogen content of functionalized materials was determined via elemental analysis from Atlantic Microlabs (Norcross, GA, USA).

5.2.3 Adsorption Measurements

The volumetric adsorption system described in chapter 4 was used to obtain single component CO_2 adsorption isotherms as well as binary CO_2-H_2O adsorption isotherms.

Single component water isotherms were measured using a Hiden IGASorp. Operation procedures for both apparatuses are described in chapter 4. For binary adsorption, the amount of water injected was adjusted so that the quantity of adsorbed water on all materials would be approximately equivalent. The amount of water to be injected was estimated from the single component water isotherms. All adsorption experiments were performed at 30 °C.

5.2.4 In-Situ FTIR

FTIR spectroscopy was performed on a Nicolet 8700 FTIR spectrometer with a MCT/A detector. Each spectrum was recorded with 64 scans at a resolution of 4 cm^{-1}. For the *in-situ* FTIR spectroscopy of CO_2 adsorption and desorption, the sample was pressed into a self-supported wafer and loaded into a high-vacuum transmission FTIR cell. The wafer was activated at 110 °C under vacuum (less than 10^{-6} mbar) for 3 h, cooled down to room temperature, and a spectrum was collected. Under dry conditions, the cell was dosed with 10 mbar of CO_2 and then allowed to equilibrate for 10 h. A spectrum was collected every 5 min. Under humid conditions, the cell was dosed with 5 mbar of H_2O vapor and then equilibrated for 1 h, followed by dosing 1.5 mbar of CO_2 and then equilibrating for 10 h. A spectrum was collected every 5 min. After 10 h of adsorption under each condition, the cell was evacuated for 3 h and a spectrum was collected every 2 min. Thermo Fischer Scientific Inc Grams 9.1 software was used to process the difference spectra. The difference spectra that are presented use the activated spectrum before addition of CO_2 as the subtrahend for dry adsorption, desorption and humid desorption. The spectrum equilibrated with water for 1 h is used as the subtrahend for the difference spectra presented for humid CO_2 adsorption.

5.3 Results & Discussion

5.3.1 Materials Synthesis & Characterization

As mentioned previously, the aim of this study was to explore the effect of amine surface coverage on CO_2 adsorption properties in a humid environment for supported amine adsorbents. To achieve this, adsorbent materials were prepared using a primary aminosilane (APS) that was grafted to silica SBA-15 with varying degrees of surface coverage. Three materials were prepared as depicted in Figure 5.1. The first material, SBA-APS-low, possesses a sub-monolayer surface coverage of amines. This is supported by the fact that free OH groups are observable in the IR spectra (see appendix E) and that the addition of more silane to the reaction mixture in anhydrous synthesis conditions yields a material with higher surface coverage, SBA-APS-medium. It is believed that this material is close to monolayer coverage since four times the amount of silane was used as compared to the synthesis of SBA-APS-low. The third material has a dense, multi-layer surface of amines (SBA-APS-high), and was synthesized using a technique that involves the addition of water to the reaction mixture during functionalization to polymerize the aminosilane.[1]

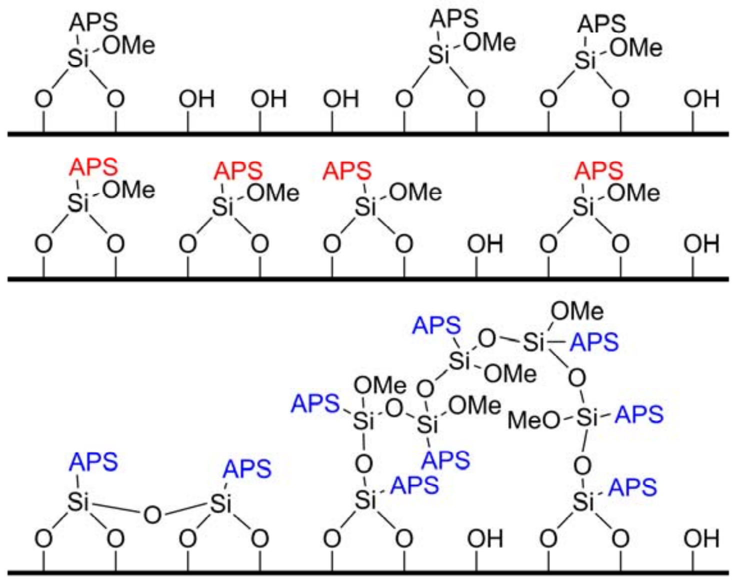

Figure 5.1. Hypothetical representation of the materials used in this study: SBA-APS-low with sub-monolayer surface coverage (top), SBA-APS-medium (middle) and SBA-APS-high with multi-layer coverage (bottom).

Results from elemental analysis and nitrogen physisorption are summarized in Figure 5.2 and Table 5.1. The nitrogen physisorption isotherms in Figure 5.2 show that SBA-APS-low and SBA-APS-medium retain their mesoporosity while the mesopores of SBA-APS-high become completely blocked with grafted amines, as evidenced by the minimal uptake of nitrogen and loss of hysteresis. Elemental analysis shows that SBA-APS-high has more than twice the loading as SBA-APS-medium. This coupled with the loss of porosity suggest that SBA-APS-high is a densely loaded material with multi-layer coverage. Thus, this set of materials is a good candidate for evaluation of the effects of amine surface coverage on CO_2 adsorption in the presence of water vapor.

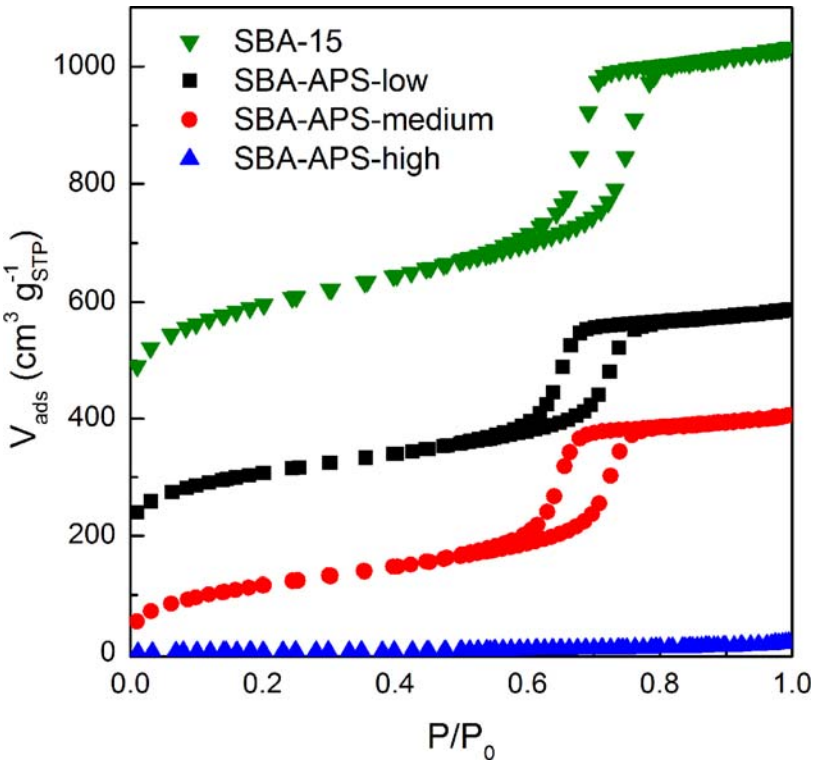

Figure 5.2. Nitrogen physisorption isotherms for bare and APS functionalized materials. Isotherms are vertically offset by 175 (SBA-APS-medium), 350 (SBA-APS-low) and 525 (SBA-15) cm^3 g_{STP}^{-1}.

Table 5.1. Physical properties of bare support and amine functionalized materials.

Material	BET SA (m^2 g_{SiO2}^{-1})	V_p (cm^3 g_{SiO2}^{-1})	Nitrogen Content (mmol N g^{-1})
SBA-15	887	1.02	-
SBA-APS-low	551	0.75	1.65
SBA-APS-medium	501	0.78	2.03
SBA-APS-high	21	0.04	4.33

5.3.2 Single Component Adsorption

Pure CO_2 and water adsorption isotherms were obtained for all materials at 30 °C to observe the differences in adsorption capacities between the materials and to serve as a benchmark for comparison with the humid adsorption experiments. Adsorption isotherms for CO_2 are shown in Figure 5.3. The measured data were fit to a single-site Toth isotherm model, which is also depicted in Figure 5.3. As expected, CO_2 adsorption capacity increases with (i) increasing partial pressure of CO_2 and (ii) increasing surface coverage of amines. It is interesting to note that while the difference in loading between SBA-APS-low and SBA-APS-medium is relatively small (roughly a factor of 1.2), the adsorption capacity has a correspondingly larger increase between the two materials, thus indicating that within this relatively small range of amine loadings a change in the behavior of the material to loading and CO_2 uptake occurs. This has previously been observed by Young and Notestein.[2]

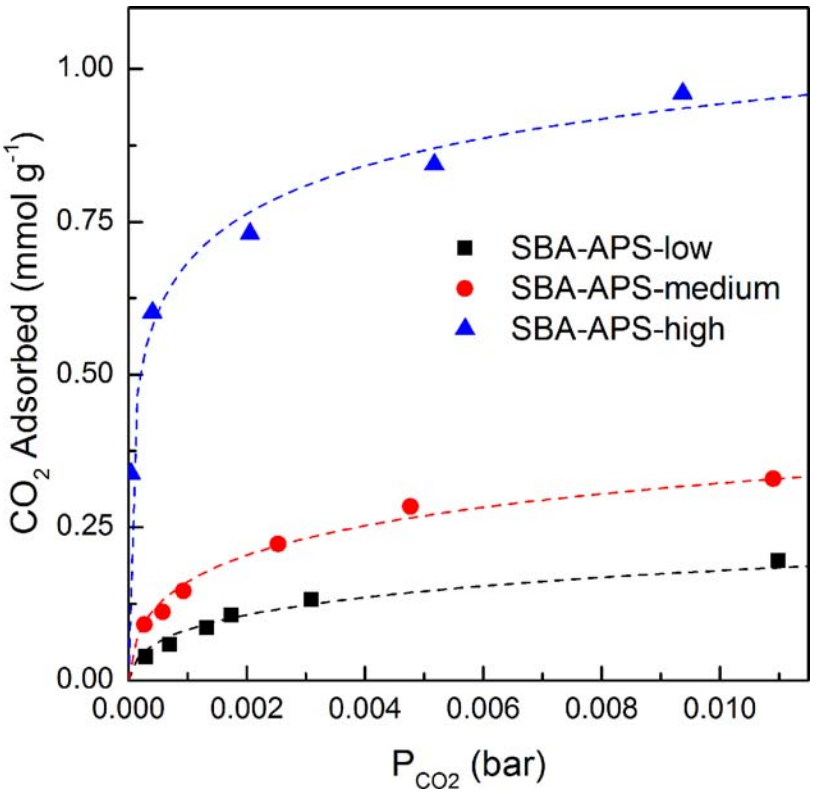

Figure 5.3. CO_2 adsorption isotherms at 30 °C for APS adsorbents with different amine loadings. Dashed lines through data points are from numerical fitting using the single site Toth model.

Water adsorption isotherms in Figure 5.4 reveal that SBA-APS-high possesses a higher water adsorption capacity in the low partial pressure (or relative humidity) regime compared to the less densely grafted materials, but a lower capacity at higher partial pressures where capillary condensation occurs. This is likely the result of a combination of two factors, the first being that the absence of mesoporosity in the SBA-APS-high material results in no capillary condensation of water within the highly loaded material, a phenomena that greatly increases water adsorption for both SBA-APS-low and SBA-APS-medium at higher water partial pressures since both materials retain mesoporosity. A second potential contribution to the lower uptakes at high partial pressures of water for

SBA-APS-high could be due to an experimental constraint, where a maximum equilibration time of 5 h was permitted during these adsorption measurements. Due to the high loading and diffusional resistance that is known to occur in these materials, it is possible that the equilibrium capacities are slightly underrepresented.

The focus of this study was to examine binary adsorption at fixed water loading in the pre-capillary condensation regime for these materials. Using the information from the dry water isotherms, the required amount of water to inject was determined for each material so that all materials had similar water adsorption capacities during binary experiments.

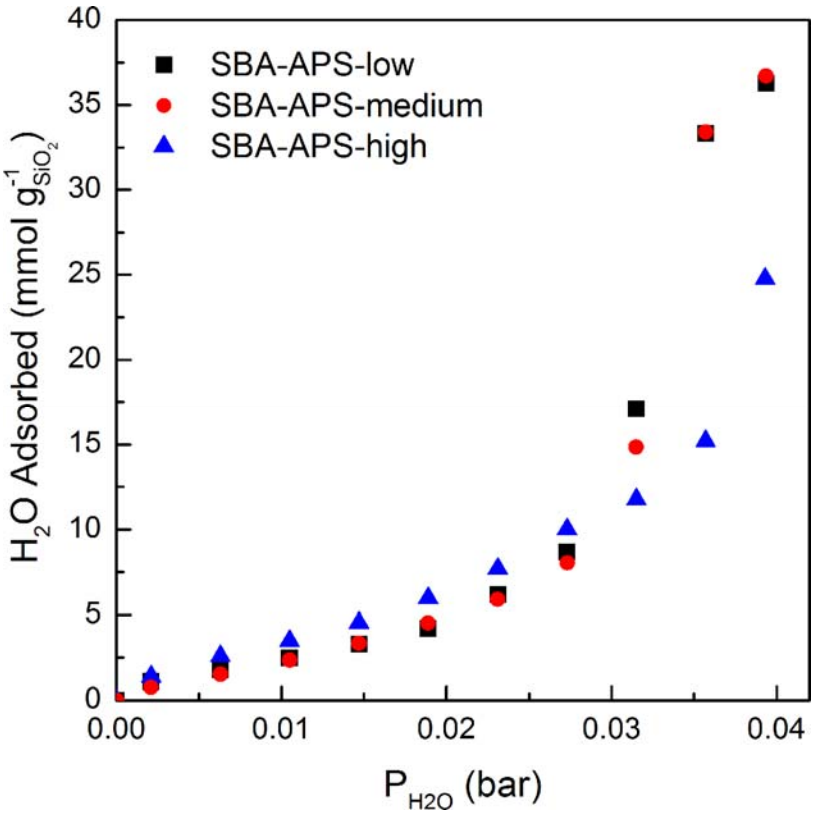

Figure 5.4. Water adsorption isotherms at 30 °C for APS adsorbents with different amine loadings.

5.3.3 Binary Adsorption

As mentioned previously, binary CO_2 isotherms were collected for a fixed loading of water. By holding the water loading constant for humid studies, the effect of surface coverage of amines can be more clearly observed with respect to CO_2 uptake. This type of measurement can only work if the adsorption of water onto the amine adsorbent is independent of CO_2 partial pressure and CO_2 adsorption. This is verified in Figure 5.5 below. It can be seen that for all experiments conducted, the water loading stayed constant within the margin of error previously discussed in chapter 4. This phenomena was previously observed by Gebald et al. for an amine functionalized nanofibrillated cellulose.[3]

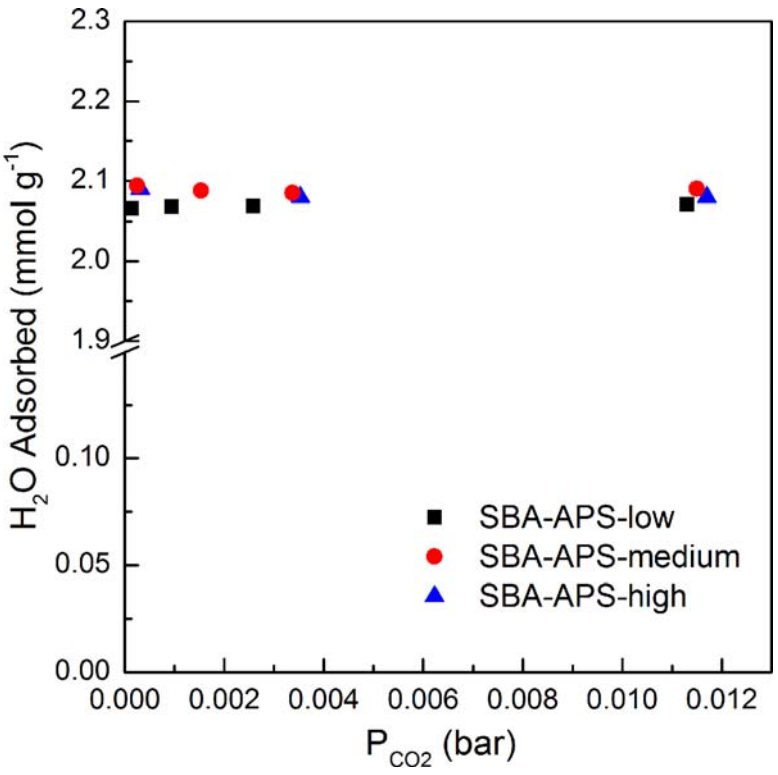

Figure 5.5. Measured water uptake for SBA-APS materials during humid CO_2 adsorption isotherm measurements at 30 °C. Note that water loading remains constant as CO_2 partial pressure increases.

The water loading that was chosen for these binary adsorption experiments is such that adsorption occurs in the low water coverage region of the water adsorption isotherm. This was done to explore the effects of water on CO_2 adsorption capacities when water is not condensing in the pores, as this could potentially result in a more aqueous *absorption* behavior for the material than a gas-solid interaction. The measured binary adsorption isotherms for the amine adsorbents are displayed in Figure 5.6 along with the corresponding dry CO_2 adsorption data.

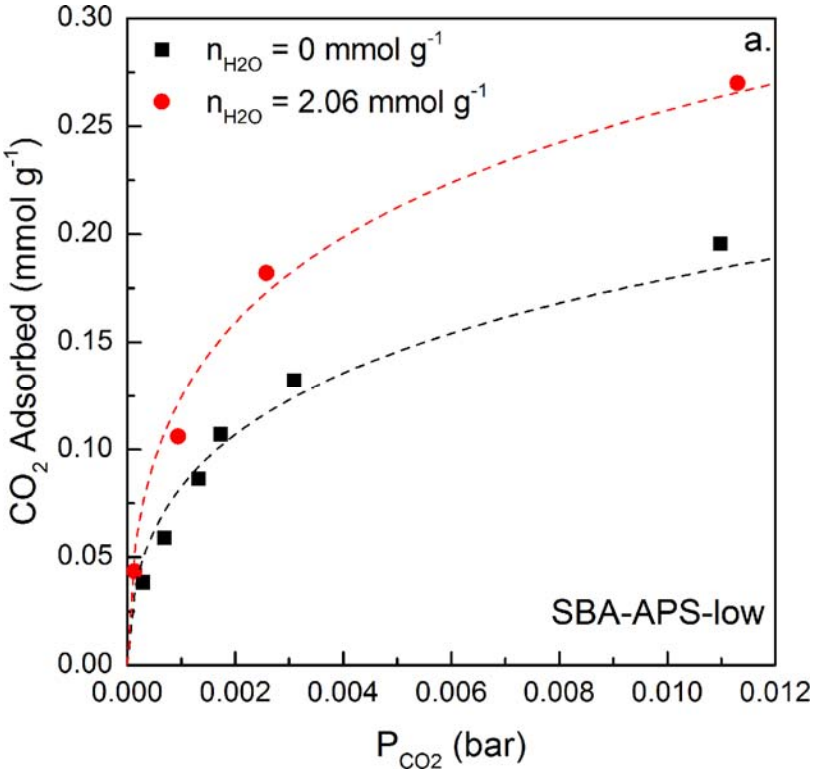

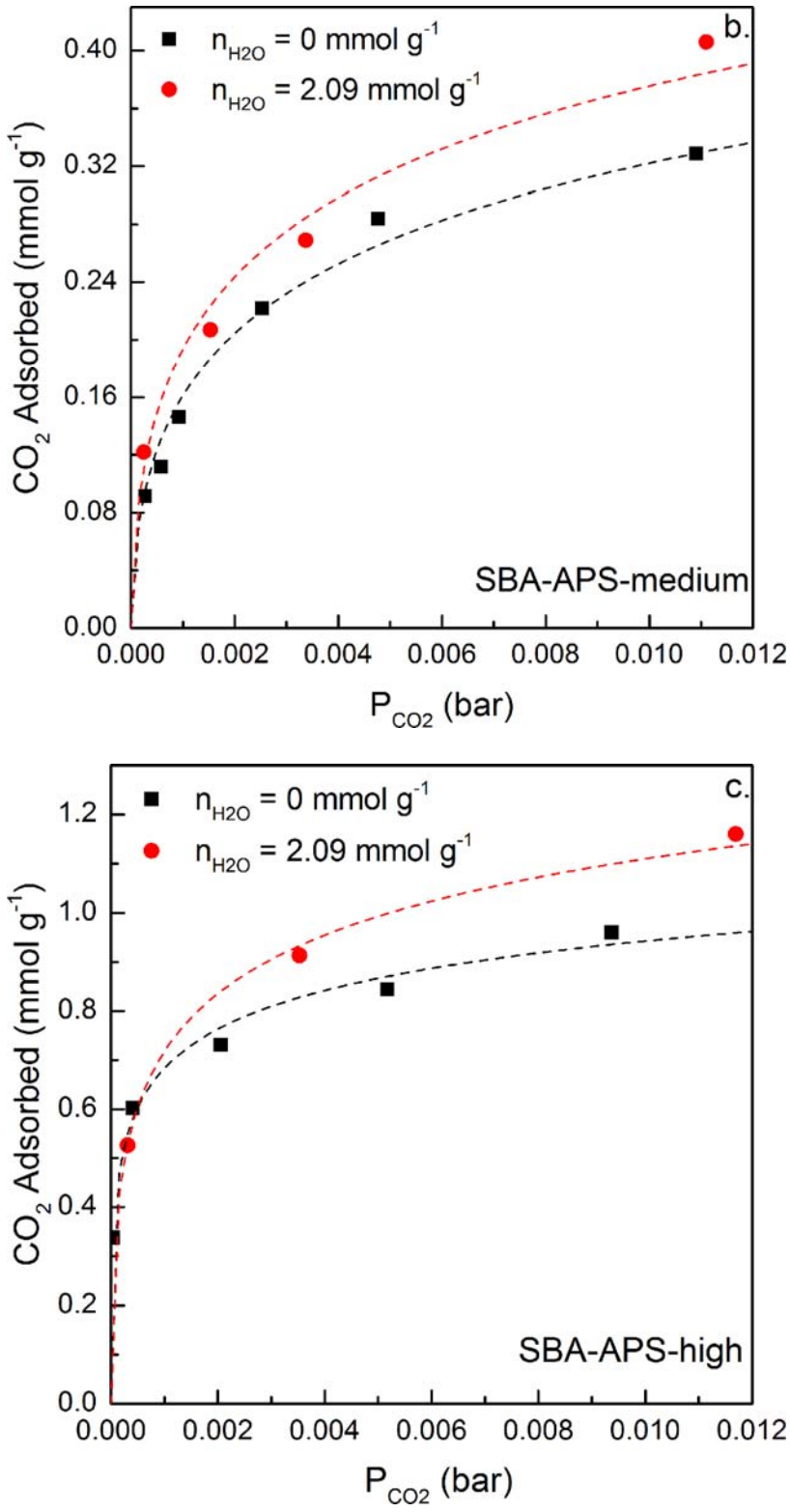

Figure 5.6. Binary adsorption isotherms of CO_2 at 30 °C and constant water loading for (a) SBA-APS-low (b) SBA-APS-medium and (c) SBA-APS-high. Dashed lines through the data points are from numerical fitting using the single site Toth model.

From the binary adsorption isotherms, it can be seen that water has the most beneficial impact on the adsorption of CO_2 for SBA-APS-low, followed by SBA-APS-medium and then SBA-APS-high, especially in the ultra-low pressure region that corresponds to air capture conditions. This could suggest that monolayer to multi-layer coverage of amines on the surface in some way hinders the ability of CO_2 to interact with water as favorably in the adsorption process, or that the presence of surface silanols on SBA-APS-low offers an additional route to CO_2 adsorption with water that does not occur with the other materials. This concept can be further examined by comparing the amine efficiency of each material between dry and humid adsorption conditions. To do so, the efficiency enhancement was calculated for each material and compared as a function of CO_2 partial pressure using the numerical fits obtained from measured isotherms. Efficiency enhancement is defined as follows:

$$Efficiency\ Enhancement = \frac{Amine\ Efficiency|_{nH2O>0}}{Amine\ Efficiency|_{nH2O=0}}$$

The efficiency enhancement for the amine adsorbents is shown in Figure 5.7. This figure demonstrates the effect of amine surface coverage with respect to humid adsorption in low RH conditions, where the greatest degree of enhancement is observed for the material with the lowest amine loading. It is interesting to note that while the low and medium loading materials show favorable enhancement throughout the adsorption isotherm range when water is co-adsorbed, the high loading material initially displays slightly lower amine efficiencies compared to dry adsorption and then surpasses dry conditions at higher partial pressures of CO_2. Reduced humid CO_2 uptake for air capture

conditions was also observed by Goeppert et al. when evaluating a fumed silica material impregnated with 52 wt% PEI for dry and humid air capture (400 ppm CO_2, 67% RH).[4] A more drastic reduction in CO_2 uptake was seen for that material, where the humid adsorption resulted in an 18% decrease in amine efficiency. Their explanation for this behavior was that the adsorbed water could block access to some of the more difficult to reach amine groups, thereby reducing capacity. Higher partial pressures of CO_2 were not evaluated in that study to see if the behavior continued. Subagyono et al. also observed a similar trend, where CO_2 isotherms measured with 2.8% RH only started to surpass dry adsorption capacities in the range of 5-30% CO_2 for highly loaded (~70 wt%) branched and linear PEI adsorbents.[5] Those experiments were performed in a higher partial pressure range, from 2.5-50% CO_2 at an adsorption temperature of 75 °C. However, the general consensus is that the presence of water aids CO_2 adsorption, especially for highly loaded materials, as the adsorbed water can act as a diffusive intermediate to transport CO_2.[6] It is not clear why these differences are observed.

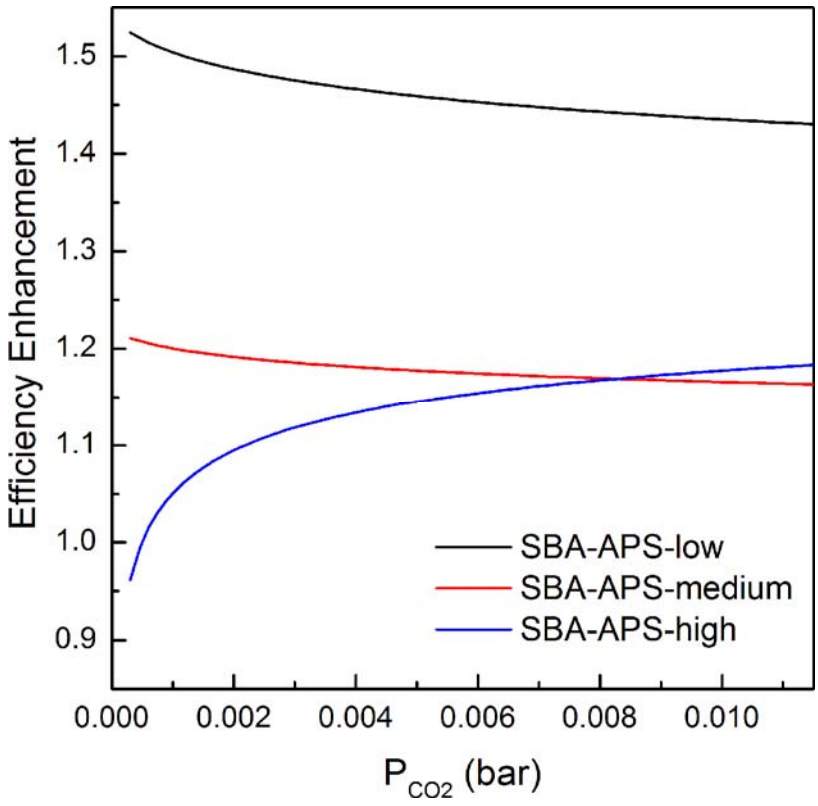

Figure 5.7. Enhancement of amine efficiency between dry CO_2 adsorption and humid CO2 adsorption for SBA-APS materials with varied surface loading.

5.3.4 In-Situ FTIR

The findings from the binary adsorption studies show a difference in humid adsorption behavior for SBA-APS-low and SBA-APS-high. One possible cause for these differences could be the result of a different adsorption mechanism occurring with the two materials. To investigate this, *in-situ* FTIR spectroscopy was employed for both materials in dry and humid CO_2 adsorption conditions. As discussed in chapter 1, it is currently believed that the dominant adsorbed species of CO_2 are in the form of ammonium carbamate ion pairs, carbamic acid, and surface bound carbamate (dry CO_2, low amine surface coverage conditions only). The most recent literature suggests that

bicarbonates and carbonates do not form upon humid CO_2 adsorption, and that any increase in amine efficiency is the result of (i) more carbamate ion pairs forming (ii) formation of hydrogen bond stabilized carbamic acid and/or (iii) the release of additional hydrogen bonded amines.[7,8] Despite this general consensus, there is still some debate over specific band assignments observed in the IR spectrum for supported amine materials exposed to CO_2. For example, the band evolved at 1480-1495 cm^{-1} during CO_2 adsorption is attributed to carbamate formation. However, some references ascribe this to a symmetric COO^- stretch of the carbamate[9–11] while others say it is the result of the symmetric deformation of NH_3^+.[7,12,13] As a result, general conclusions about the nature of the adsorbed species can be made, but more in depth analysis of the assignment of certain bands is still needed. A summary of various band assignments from the literature is presented in Table 5.2 for reference.

Table 5.2. IR band assignments from recent literature for species observed upon contacting CO_2 with amine adsorbents. Note there is some disagreement between assignments of species.

Wavenumber (cm^{-1})	Assignment	Species	Ref.
1715-1710	C=O stretch	Bound carbamate	[7,13,14]
1715	C=O stretch	Carbamic acid	[7,11]
1700-1680	C=O stretch	Carbamic acid	[7,9,11,12,15,16]
1635-1625	NH_3^+ asym def	NH_3^+	[7,9,10,12,13,16–23]
1601-1590	N-H deformation	NH_2	[7,11,13]
1570-1545	COO^- asym stretch	Carbamate	[7,9,11–21,24,25]
1550-1485	NH_3^+ sym def	NH_3^+	[7,9,12–16,22]
1520-1510	NH def/C-N stretch	Bound carbamate	[7,13,14]
1490-1480	COO^- sym stretch	Carbamate	[9,11,19,24]
~1430	COO^- sym stretch	Carbamate	[7,9,12–14,16,21,24,26]
~1380	COO^- sym stretch	Carbamate	[12–14,16,21,26]
1360-1350	C-O sym stretch	Bicarbonate	[10,27,28]
1320	$NCOO^{-1}$ skeletal vibration	Carbamate	[9,11,19,24]

The *in-situ* IR experiments were conducted at a fixed CO_2 or CO_2/H_2O pressure and examined over time. The purpose of this was to examine if the nature of the adsorbed species changed during the course of adsorption, especially in the presence of water, since the formation of different species has been shown to occur over varying timescales.[29] The dry and humid adsorption difference spectra for SBA-APS-low and SBA-APS-high are presented in Figure 5.8 and Figure 5.9, respectively. It should be

restated that the difference spectrum for humid adsorption is normalized differently than that for dry. In the case of dry adsorption, the difference is between the adsorbed amount after a given time of adsorption and the activated spectra, whereas for humid adsorption, the difference is between the adsorbed amount after a given time of adsorption and the water adsorption spectra just before introduction of CO_2. In this way, contributions from CO_2 adsorption can be more clearly observed.

For the most part, the IR results are fairly consistent with what has been observed previously in the literature. SBA-APS-low appears to form carbamate, carbamic acid and bound carbamate in dry CO_2 conditions (further evidence for bound carbamate is discussed later), while SBA-APS-high only forms carbamate in dry conditions. It is clear that SBA-APS-high would not form bound carbamate during adsorption since there are no to relatively few surface silanols. However, carbamic acid could still form for the high loading material. The absence of this formation suggests that carbamate ion pairs are the dominant species for adsorbed CO_2 when amines are clustered. Also noteworthy is the apparent slower equilibration time of SBA-APS-high compared to SBA-APS-low. It is evident that after 10 h, equilibrium has been achieved for the low loading material, as the 9 and 10 h spectra overlap. However, the absorbance intensity of SBA-APS-high appears to be still increasing after 10 h. This is consistent with what was observed during binary adsorption experiments, and can be explained by diffusional resistance that has been observed for highly loaded materials.[30]

The humid adsorption spectrum for SBA-APS-low appears very similar to that of humid SBA-APS-high with one key exception. It appears that both materials form only ammonium carbamate ion pairs, as bands due to bound carbamate and carbamic acid are

no longer observed for the low loading material. However, the intensity of the asymmetric deformation of NH_3^+ at 1626 cm^{-1} gradually decreases with time and redshifts to 1616 cm^{-1}, as can be seen from the inset of Figure 5.9a. Additionally, the adsorbed water band at 1658 cm^{-1} emerges in the shoulder. It is unclear whether this is the result of (i) a blueshift in the adsorbed water band at 1651 cm^{-1} due to interaction with some other species (see Appendix E for pure water adsorption spectrum) or (ii) the evolution of more adsorbed water, since the pre-equilibration time for water before introduction of CO_2 was only 1 h.

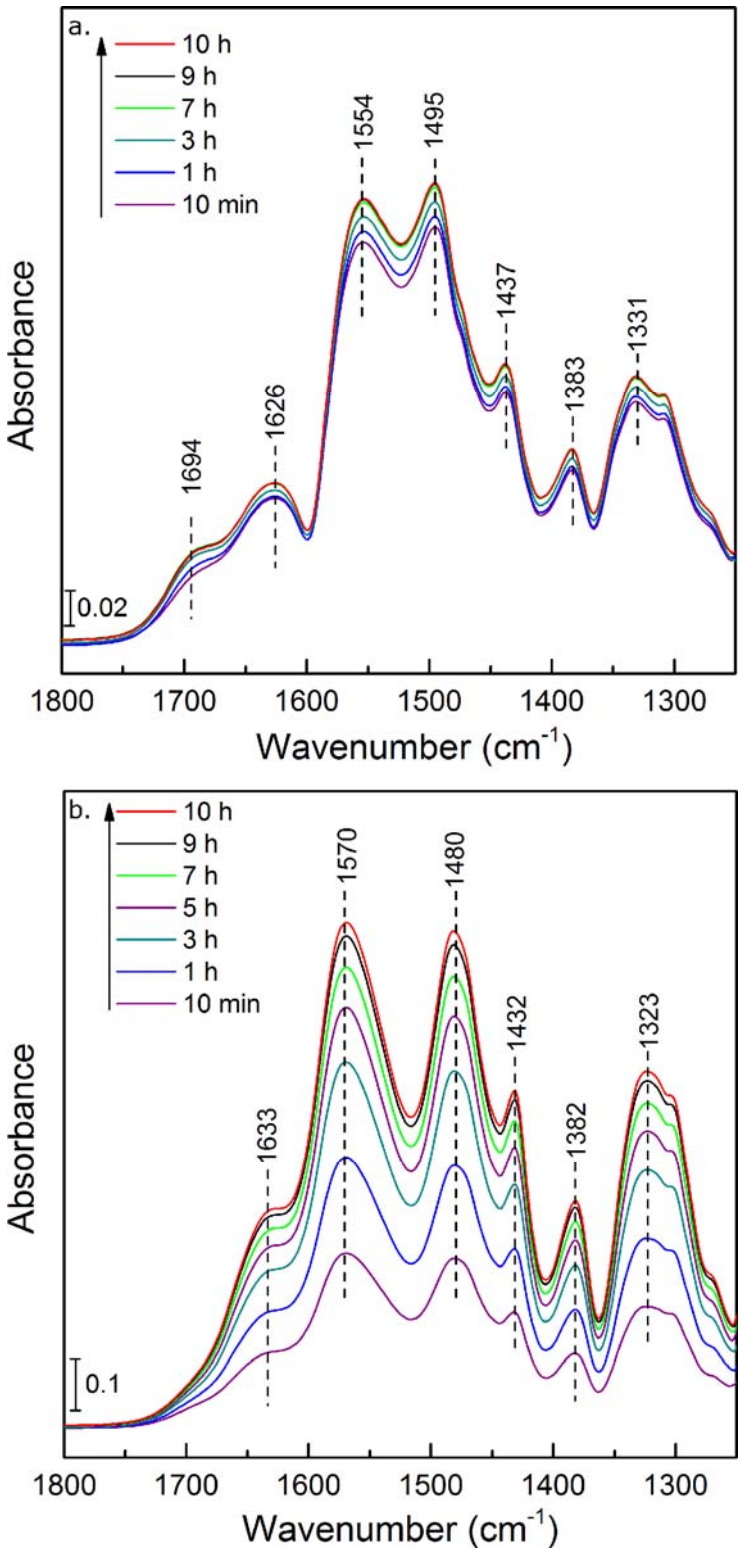

Figure 5.8. *In-situ* FTIR difference spectra of (a) SBA-APS-low and (b) SBA-APS-high contacted with 10 mbar CO_2 as a function of adsorption time. Sample spectra were collected at room temperature. Assignments can be found in Table 5.2.

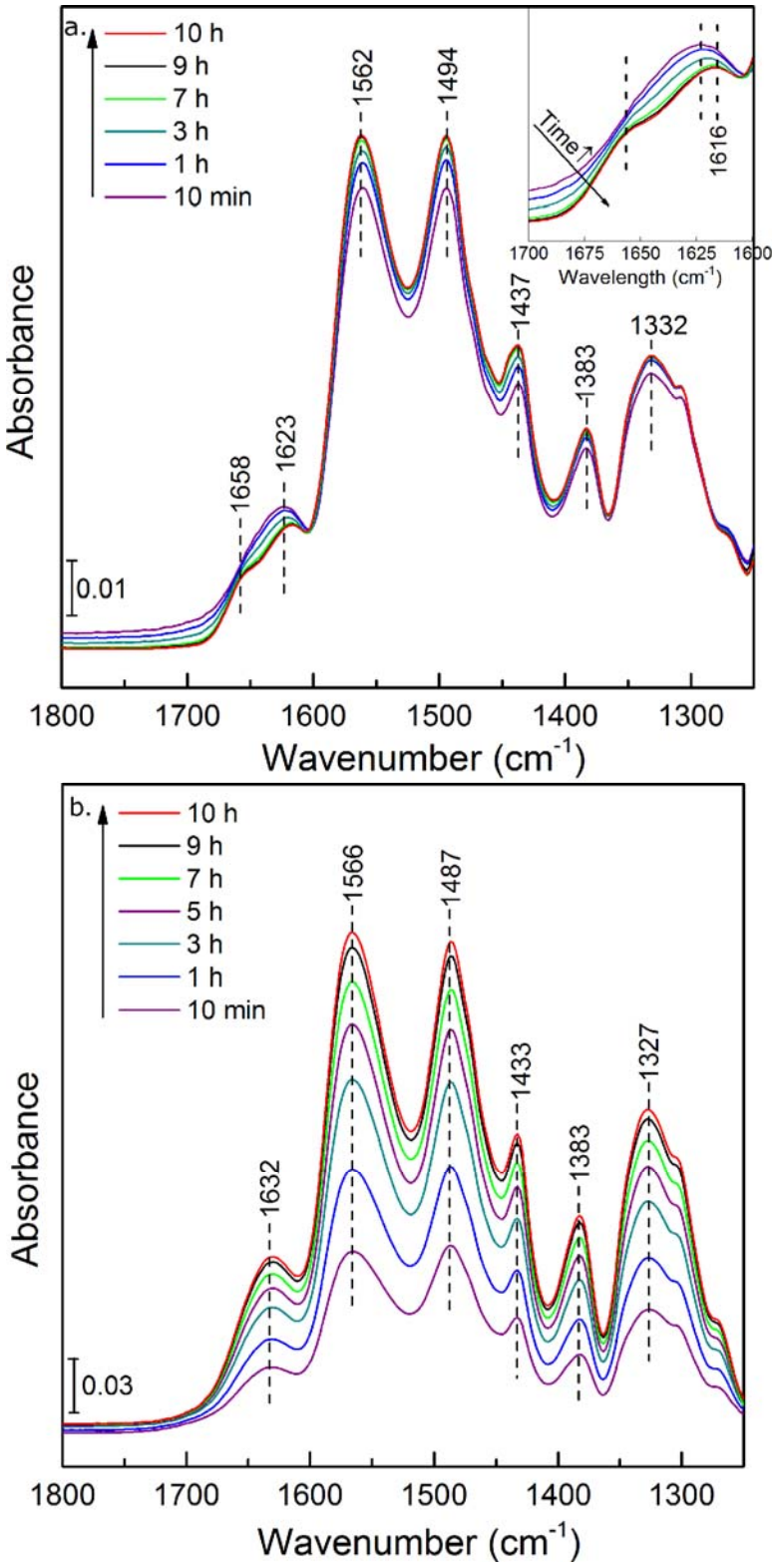

Figure 5.9. *In-situ* FTIR difference spectra of (a) SBA-APS-low and (b) SBA-APS-high contacted with 1.5 mbar CO_2 and 5 mbar H_2O as a function of adsorption time. Sample spectra were collected at room temperature. Assignments can be found in Table 5.2.

Due to the redshift that was observed in the spectrum for humid SBA-APS-low in Figure 5.9a, a more detailed analysis of the dynamics of adsorption was performed. To do so, the difference in adsorbed species at different time segments was examined. This method allows for the observation of species forming at different timescales and was used by Bacsik et al. to deconvolute rapidly forming carbamic acid from slower forming silylpropylcarbamate during CO_2 adsorption on silica supported APS.[7] The results of this analysis can be seen in Figure 5.10 and Figure 5.11. For dry CO_2 adsorption on SBA-APS-low, similar behavior as has been reported elsewhere is observed, where bands for bound carbamate are more clearly resolved after subtracting out the initial 10 min of adsorption.[7,13] The humid spectrum of SBA-APS-low looks very different from its dry counterpart as well as what is observed for dry and humid SBA-APS-high spectra. A blueshift in the band at 1562 cm^{-1} is likely due to overlap with a newly evolved band at 1595 cm^{-1} that corresponds with the liberation of amines from surface hydrogen bonds with silanols or silypropylcarbamate in the presence of humidity.[7] It can also be seen that a new stretch starts to evolve at 1350 cm^{-1} after the first several hours of adsorption and is most clearly seen in the "10h-1h" spectrum. This cannot be seen in Figure 5.9a, because it overlaps with the $NCOO^-$ skeletal vibration around 1330 cm^{-1}. However, by removing the contribution from the rapidly forming carbamate ion pairs in the initial hour of adsorption it can clearly be seen that, on longer timescales, a different type of adsorption occurs that has not been widely discussed in the supported amine literature. In aqueous amine absorption literature, the evolution of a band in the range of 1360-1350 cm^{-1} is attributed to the symmetric C-O stretch of HCO_3^-.[10,27,28] Therefore, it is suggested that the observed band at 1350 cm^{-1}, coupled with the redshift and decrease in intensity of the

band at 1623 cm^{-1}, could indicate formation of bicarbonate, as this matches well with what is observed for aqueous amines. This band is not observed for humid adsorption of SBA-APS-high. In fact, no difference in adsorbed species during later stages of adsorption can be observed for this material. It is possible that this is the result of the longer equilibration time observed for the densely loaded material, and the fact that bicarbonate is a slow forming product. Nevertheless, on these timescales it appears that the low surface coverage of SBA-APS-low allows for the adsorption of CO_2 via a bicarbonate mechanism under humid conditions. This most likely occurs with isolated amines that cannot form the more favorable carbamate species. While bicarbonate formation for this material is observed, it is not believed that this is the sole contribution to increased amine efficiency under humid conditions, as other studies have shown that humid CO_2 adsorption can increase efficiency through the formation of more ammonium carbamate ion pairs as well as through the liberation of hydrogen bonded amines.[7,8]

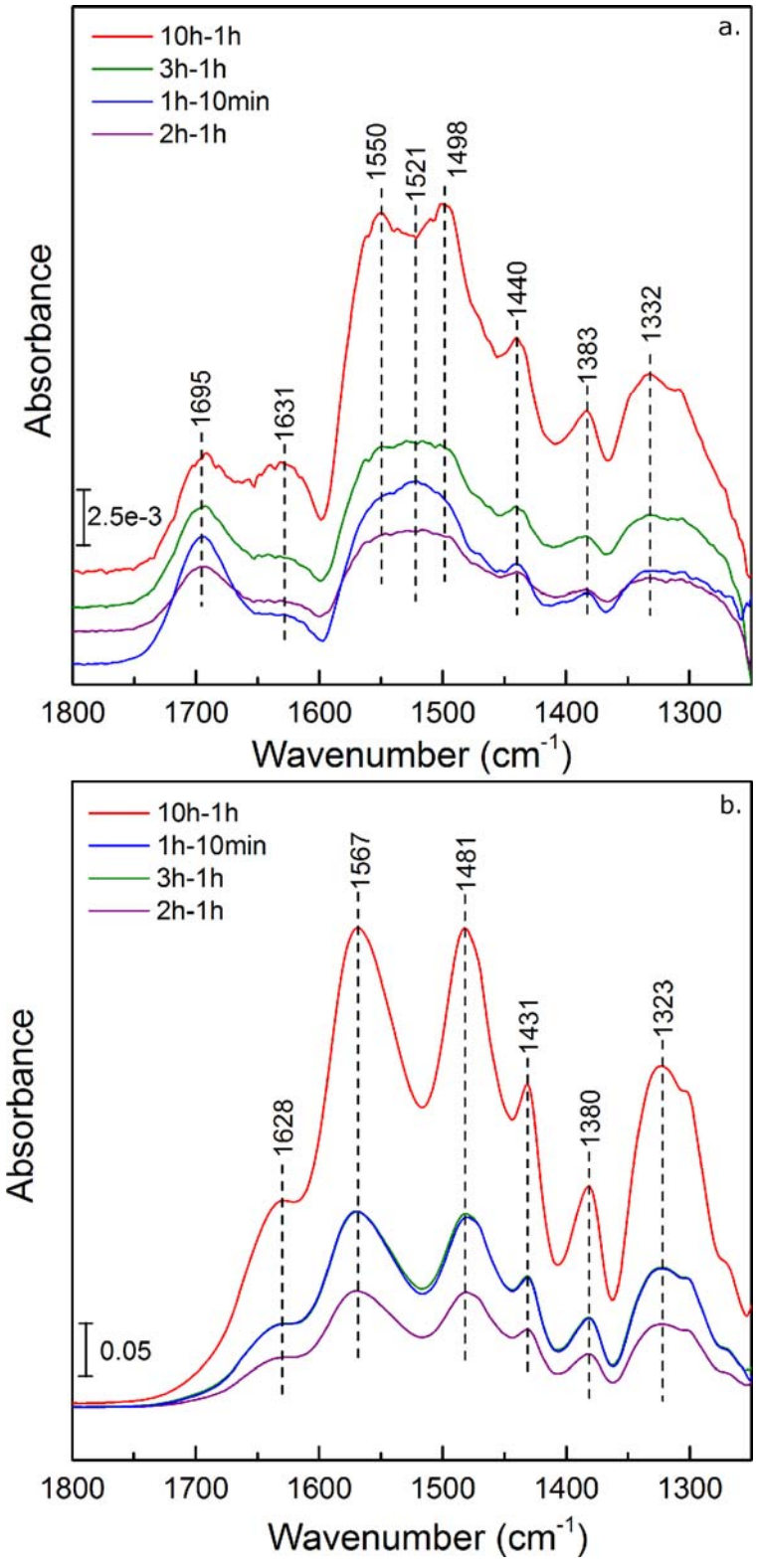

Figure 5.10. Time evolved FTIR spectra at varying time intervals to display slow and rapid forming species for (a) SBA-APS-low and (b) SBA-APS-high in dry CO_2 conditions.

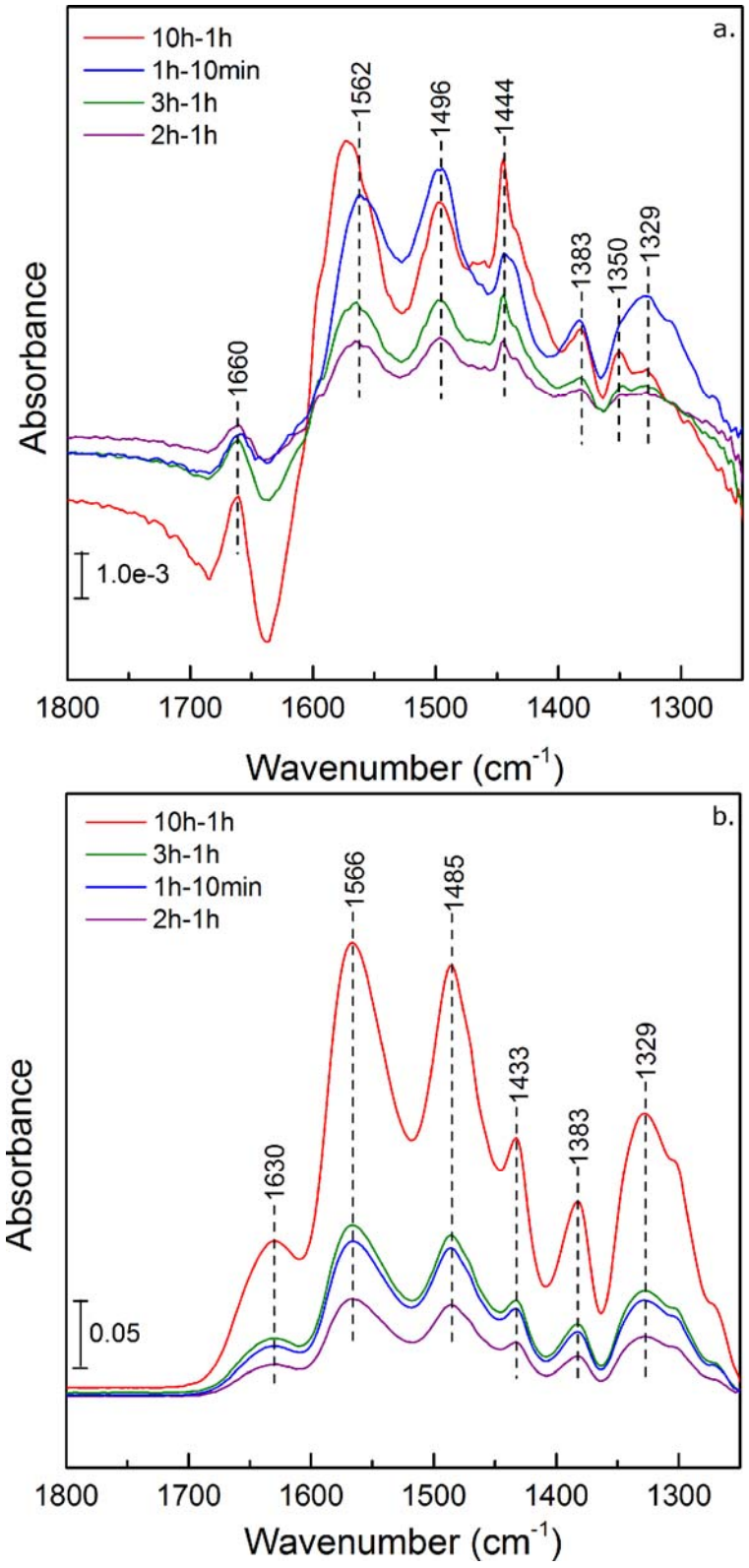

Figure 5.11. Time evolved FTIR spectra at varying time intervals to display slow and rapid forming species for (a) SBA-APS-low and (b) SBA-APS-high in humid CO_2 conditions.

5.4 Conclusions

A study on the effect of amine loading towards CO_2-H_2O interactions in the low coverage region of both CO_2 and water was conducted for silica supported primary amine materials by measuring binary adsorption isotherms. It was found that amine materials with low surface coverage displayed the most improvement in adsorption efficiency during co-adsorption with water. Adsorbents with multi-layer amine coverage displayed the least amount of improvement upon humid adsorption. This is different than what is generally observed in higher relative humidity conditions of CO_2 adsorption, and could be due to the fact that these experiments were done at very low water coverage. *In-situ* FTIR spectra of low and high surface coverage amine adsorbents suggests one possible reason for the difference in amine efficiency between materials is a difference in the adsorbed species for humid CO_2 conditions. Bicarbonate along with ammonium carbamate ion pairs are observed for humid CO_2 adsorption on amines with low surface coverage, whereas adsorbents with multi-layers of amines produce only ammonium carbamate species upon humid adsorption at the timescales investigated. The results of these studies indicate that the effect of water co-adsorption with CO_2 is dependent on the choice of amine material and adsorption conditions. This further demonstrates the need to explore different operating conditions for adsorption so that an optimum in terms of operating costs and adsorption efficiency can be found.

5.5 References

(1) Harlick, P. J. E.; Sayari, A. Applications of Pore-Expanded Mesoporous Silica. 5. Triamine Grafted Material with Exceptional CO_2 Dynamic and Equilibrium Adsorption Performance. *Ind. Eng. Chem. Res.* **2007**, *46*, 446–458.

(2) Young, P. D.; Notestein, J. M. The Role of Amine Surface Density in Carbon Dioxide Adsorption on Functionalized Mixed Oxide Surfaces. *ChemSusChem* **2011**, 1–9.

(3) Gebald, C.; Wurzbacher, J. A.; Borgschulte, A.; Zimmermann, T.; Steinfeld, A. Single-Component and Binary CO_2 and H_2O Adsorption of Amine-Functionalized Cellulose. *Environ. Sci. Technol.* **2014**, *48*, 2497–2504.

(4) Goeppert, A.; Czaun, M.; May, R. B.; Prakash, G. K. S.; Olah, G. A.; Narayanan, S. R. Carbon Dioxide Capture from the Air Using a Polyamine Based Regenerable Solid Adsorbent. *J. Am. Chem. Soc.* **2011**, *133*, 20164–20167.

(5) Subagyono, D. J. N.; Marshall, M.; Knowles, G. P.; Chaffee, A. L. CO_2 Adsorption by Amine Modified Siliceous Mesostructured Cellular Foam (MCF) in Humidified Gas. *Microporous Mesoporous Mater.* **2014**, *186*, 84–93.

(6) Mebane, D. S.; Kress, J. D.; Storlie, C. B.; Fauth, D. J.; Gray, M. L.; Li, K. Transport, Zwitterions, and the Role of Water for CO_2 Adsorption in Mesoporous Silica-Supported Amine Sorbents. *J. Phys. Chem. C* **2013**, *117*, 26617–26627.

(7) Bacsik, Z.; Ahlsten, N.; Ziadi, A.; Zhao, G.; Garcia-Bennett, A. E.; Martín-Matute, B.; Hedin, N. Mechanisms and Kinetics for Sorption of CO_2 on Bicontinuous Mesoporous Silica Modified with N-Propylamine. *Langmuir* **2011**, *27*, 11118–11128.

(8) Aziz, B.; Hedin, N.; Bacsik, Z. Quantification of Chemisorption and Physisorption of Carbon Dioxide on Porous Silica Modified by Propylamines : Effect of Amine Density. *Microporous Mesoporous Mater.* **2012**, *159*, 42–49.

(9) Bacsik, Z.; Atluri, R.; Garcia-Bennett, A. E.; Hedin, N. Temperature-Induced Uptake of CO_2 and Formation of Carbamates in Mesocaged Silica Modified with N-Propylamines. *Langmuir* **2010**, *26*, 10013–10024.

(10) Richner, G.; Puxty, G. Assessing the Chemical Speciation during CO_2 Absorption by Aqueous Amines Using in Situ FTIR. *Ind. Eng. Chem. Res.* **2012**, *51*, 14317–14324.

(11) Srikanth, C. S.; Chuang, S. S. C. Infrared Study of Strongly and Weakly Adsorbed CO_2 on Fresh and Oxidatively Degraded Amine Sorbents. *J. Phys. Chem. C* **2013**, *117*, 9196–9205.

(12) Knofel, C.; Martin, C.; Hornebecq, V.; Llewellyn, P. L. Study of Carbon Dioxide Adsorption on Mesoporous Aminopropylsilane-Functionalized Silica and Titania Combining Microcalorimetry and in Situ Infrared Spectroscopy. *J. Phys. Chem. C* **2009**, *113*, 21726–21734.

(13) Danon, A.; Stair, P. C.; Weitz, E. FTIR Study of CO_2 Adsorption on Amine-Grafted SBA-15: Elucidation of Adsorbed Species. *J. Phys. Chem. C* **2011**, *115*, 11540–11549.

(14) Socrates, G. *Infrared and Raman Characteristic Group Frequencies: Tables and Charts*; 3rd ed.; Wiley: Chichester, New York, 2001.

(15) Bossa, J.-B.; Borget, F.; Duvernay, F.; Theulé, P.; Chiavassa, T. Formation of Neutral Methylcarbamic Acid ($CH_3NHCOOH$) and Methylammonium Methylcarbamate [$CH_3NH_3^+$][CH_3NHCO_2-] at Low Temperature. *J. Phys. Chem. A* **2008**, *112*, 5113–5120.

(16) Bossa, J. B.; Theulé, P.; Duvernay, F.; Borget, F.; Chiavassa, T. Carbamic Acid and Carbamate Formation in NH_3 : CO_2 Ices – UV Irradiation versus Thermal Processes. *Astron. Astrophys.* **2008**, *492*, 719–724.

(17) Huang, H. Y.; Yang, R. T.; Chinn, D.; Munson, C. L. Amine-Grafted MCM-48 and Silica Xerogel as Superior Sorbents for Acidic Gas Removal from Natural Gas. *Ind. Eng. Chem. Res.* **2003**, *42*, 2427–2433.

(18) Hiyoshi, N.; Yogo, K.; Yashima, T. Adsorption Characteristics of Carbon Dioxide on Organically Functionalized SBA-15. *Microporous Mesoporous Mater.* **2005**, *84*, 357–365.

(19) Kim, S.; Ida, J.; Guliants, V. V; Lin, J. Y. S. Tailoring Pore Properties of MCM-48 Silica for Selective Adsorption of CO_2. *J. Phys. Chem. B* **2005**, *109*, 6287–6293.

(20) Wang, X. X.; Schwartz, V.; Clark, J. C.; Ma, X. L.; Overbury, S. H.; Xu, X. C.; Song, C. Infrared Study of CO_2 Sorption over "Molecular Basket" Sorbent Consisting of Polyethylenimine-Modified Mesoporous Molecular Sieve. *J. Phys. Chem. C* **2009**, *113*, 7260–7268.

(21) Roeges, N. P. G. *A Guide to the Complete Interpretation of Infrared Spectra of Organic Structures*; Wiley: New York, 1994; pp. 83–87.

(22) Frasco, D. L. Infrared Spectra of Ammonium Carbamate and Deuteroammonium Carbamate. *J. Chem. Phys.* **1964**, *41*, 2134.

(23) Belli Dell'Amico, D.; Calderazzo, F.; Labella, L.; Marchetti, F.; Pampaloni, G. Converting Carbon Dioxide into Carbamato Derivatives. *Chem. Rev.* **2003**, *103*, 3857–3897.

(24) Aresta, M.; Quaranta, E. Role of the Macrocyclic Polyether in the Synthesis of N-Alkylcarbamate Esters from Primary Amines , CO_2 and Alkyl Halides in the Presence of Crown-Ethers. *Tetrahedron* **1992**, *48*, 1515–1530.

(25) Aresta, M.; Ballivet-Tkatchenko, D.; Belli Dell'Amico, D.; Bonnest, M. C.; Boschi, D.; Calderazzo, F.; Faure, R.; Labella, L.; Marchetti, F. Isolation and Structural Determination of Two Derivatives of the Elusive Carbamic Acid. *Chem. Commun.* **2000**, *8*, 1099–1100.

(26) Colthup, N. B.; Daly, L. H.; Wiberley, S. E. *Introduction to Infrared and Raman Spectroscopy*; 3rd ed.; Academic Press: New York, 1990.

(27) Robinson, K.; McCluskey, A.; Attalla, M. I. An FTIR Spectroscopic Study on the Effect of Molecular Structural Variations on the CO_2 Absorption Characteristics of Heterocyclic Amines. *ChemPhysChem* **2011**, *12*, 1088–1099.

(28) Robinson, K.; McCluskey, A.; Attalla, M. I. An ATR-FTIR Study on the Effect of Molecular Structural Variations on the CO_2 Absorption Characteristics of Heterocyclic Amines, Part II. *ChemPhysChem* **2012**, *13*, 2331–2341.

(29) Bollini, P.; Didas, S. A.; Jones, C. W. Amine-Oxide Hybrid Materials for Acid Gas Separations. *J. Mater. Chem.* **2011**, *21*, 15100–15120.

(30) Bollini, P.; Brunelli, N. A.; Didas, S. A.; Jones, C. W. Dynamics of CO_2 Adsorption on Amine Adsorbents. 2. Insights into Adsorbent Design. *Ind. Eng. Chem. Res.* **2012**, *51*, 15153–15162.

Chapter 6

SUMMARY & FUTURE DIRECTIONS

6.1 Summary

A summary of this dissertation with the main conclusions is broken down by chapters and presented below:

Chapter 1

An introduction was given to organic-inorganic hybrid materials used for CO_2 capture from flue gas and ambient air. Key areas were identified that need to be addressed for application of these materials in commercial technologies.

Chapter 2

Differences in stability were observed for primary amine materials with methyl, ethyl and propyl alkyl linkers. Amine surface coverage was also shown to affect the extent of CO_2-induced deactivation. Propyl amine materials with higher surface coverage were found to undergo the most deactivation in extreme CO_2 environments. It was suggested that this resulted from the higher amine efficiency and flexibility of this material, as DFT calculations showed that the most energetically favored pathway to urea formation involved amine or silanol assisted reactions.

Chapter 3

Primary amines were identified as the most favorable amine type over secondary and tertiary amines for air capture applications. This is due to the materials' display of high CO_2 adsorption efficiency along with increased hydrophilic nature compared to the other amine types.

Chapter 4

The motivation for, design and validation of a volumetric adsorption system for measuring binary adsorption of CO_2 and water on adsorbent materials were discussed. Estimation of system error confirms the system can get reliable data for typical operating conditions of dilute CO_2 adsorption analysis.

Chapter 5

Differences in CO_2 adsorption efficiency were observed in low humidity environments for primary amine materials with surface coverages ranging from sub-monolayer to multi-layer. The greatest enhancement for CO2 adsorption with low-level humidity was seen for sub-monolayer materials. *In-situ* FTIR suggests one reason for this behavior is the result of a different adsorption mechanism, whereby isolated amines adsorb CO_2 as bicarbonate over the traditionally observed ammonium carbamate. This was the first

compelling demonstration of the formation of bicarbonate for supported amine materials in the presence of water.

6.2 Future Directions

There still exists work that must be done before supported amine adsorbents can be implemented as a practical solution to CO_2 capture, either for flue gas or air capture applications. Several possibilities for future investigation are discussed below:

6.2.1 Synthesis of Low Molecular Weight Poly(allylamine)

Results from this dissertation suggest that design focus for new adsorbent materials should focus on primary or mostly primary amine containing materials as they are oxidatively stable, have high amine efficiencies and are hydrophilic. Poly(allylamine) (PAA) is a linear, all primary aminopolymer that was introduced by our group as a candidate material for CO_2 capture from flue gas and ambient air. This polymer has been shown to possess improved oxidative stability and comparable amine efficiencies to branched PEI adsorbents, which are considered the benchmark material for commercial implementation.[1–3] However, the molecular weight for PEI is 800 Da while the molecular weight for PAA was estimated to be roughly 2200 Da.[3] It is hypothesized that a smaller PAA polymer would further improve the amine efficiency of this material, as the smaller size would likely improve diffusional limitations and bulky interactions inherent in the larger polymer network.

6.2.2 Further Investigation of Low RH Adsorption Conditions

The findings in chapter 5 with respect to humid dilute CO_2 adsorption in the highly loaded amine adsorbent (SBA-APS-high) were quite interesting. In general, most groups study wet CO_2 adsorption in much higher relative humidity regimes (typically 100% RH). Additionally, the conclusions that have been made with respect to water decreasing diffusional limitations have been observed in high humidity systems as well.[4,5] Therefore, a more thorough investigation in the low RH region for dilute CO_2 capture of highly loaded amine adsorbents could provide novel insight into the adsorption behavior of these materials.

6.3 References

(1) Chaikittisilp, W.; Khunsupat, R.; Chen, T. T.; Jones, C. W. Poly(allylamine)-Mesoporous Silica Composite Materials for CO_2 Capture from Simulated Flue Gas or Ambient Air. *Ind. Eng. Chem. Res.* **2011**, *50*, 14203–14210.

(2) Bali, S.; Chen, T. T.; Chaikittisilp, W.; Jones, C. W. Oxidative Stability of Amino Polymer–Alumina Hybrid Adsorbents for Carbon Dioxide Capture. *Energy Fuels* **2013**, *27*, 1547–1554.

(3) Alkhabbaz, M. A.; Khunsupat, R.; Jones, C. W. Guanidinylated Poly(allylamine) Supported on Mesoporous Silica for CO_2 Capture from Flue Gas. *Fuel* **2014**, *121*, 79–85.

(4) Mebane, D. S.; Kress, J. D.; Storlie, C. B.; Fauth, D. J.; Gray, M. L.; Li, K. Transport, Zwitterions, and the Role of Water for CO_2 Adsorption in Mesoporous Silica-Supported Amine Sorbents. *J. Phys. Chem. C* **2013**, *117*, 26617–26627.

(5) Fan, Y.; Lively, R. P.; Labreche, Y.; Rezaei, F.; Koros, W. J.; Jones, C. W. Evaluation of CO_2 Adsorption Dynamics of Polymer/silica Supported Poly(ethylenimine) Hollow Fiber Sorbents in Rapid Temperature Swing Adsorption. *Int. J. Greenh. Gas Control* **2014**, *21*, 61–71.

Appendix A

TRANSITION STATE STRUCTURES FOR DENSITY FUNCTIONAL THEORY CALCULATIONS

The transition state structures discussed in chapter 2 of the first step in the deactivation pathway (carbamic acid formation) interacting with different primary amine types are reproduced in this appendix and shown in the figure below. Calculations are done at the B3LYP/6-31+G** Level.

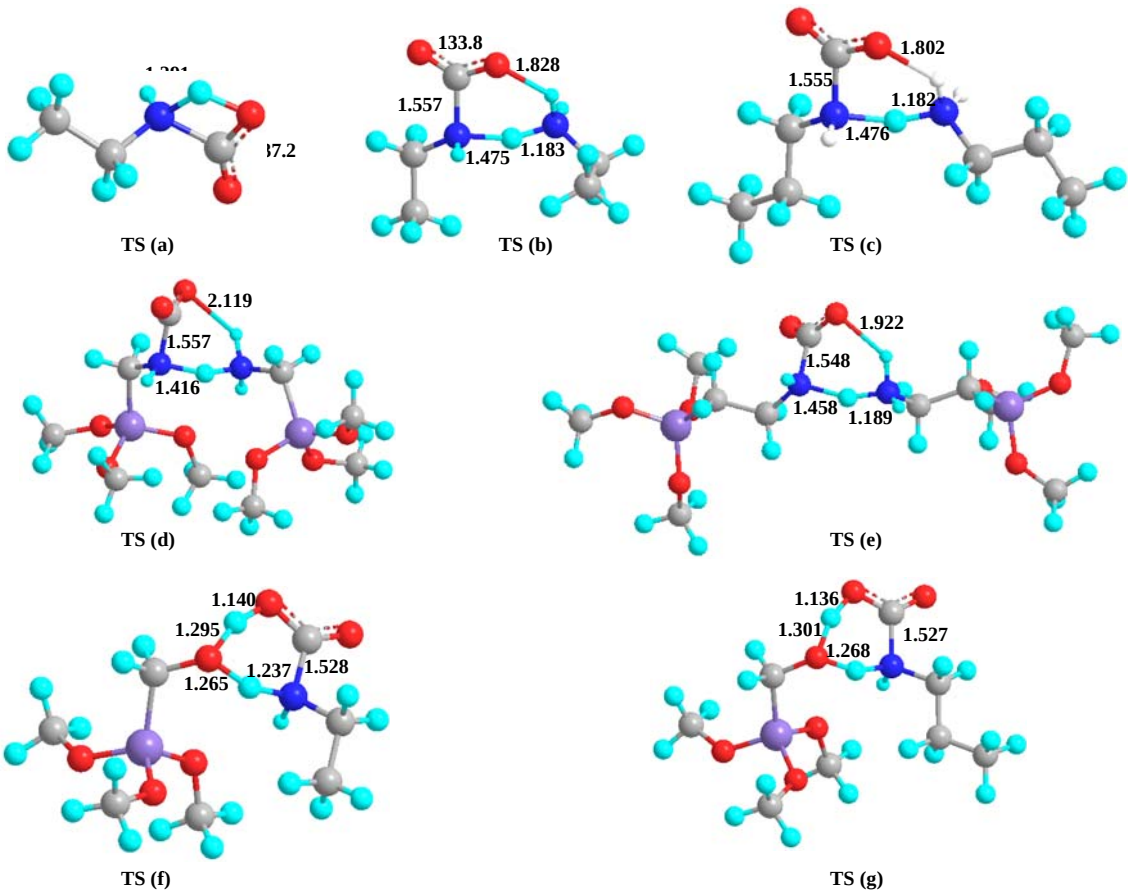

Figure A.1 Transition state structures for different primary amines forming carbamic acid.

Appendix B

PURIFICATION PROCEDURE FOR (N-METHYLAMINOPROPYL)-TRIMETHOXYSILANE

Primary amine impurities have been observed in the secondary aminosilane, MAPS. These impurities were removed from MAPS through reaction with polymer bound 4-benzyloxybenzaldehyde to form a benzyliminosilane that can be separated from the purified secondary aminosilane through filtration followed by roto-evaporation to remove solvent. The purified silane, MCF-MAPS-Purified, was then functionalized onto MCF using typical synthesis methods discussed in chapter 3. Adsorption measurements at multiple temperatures with 400 ppm CO_2 in inert were then carried out to assess the potential effect of impurities on adsorption studies. As Figure B.1 shows, there is no appreciable difference in amine efficiencies for the as-is and purified silanes. Therefore the experiments done using non-purified silanes can still be considered to represent adsorption behavior for that amine type.

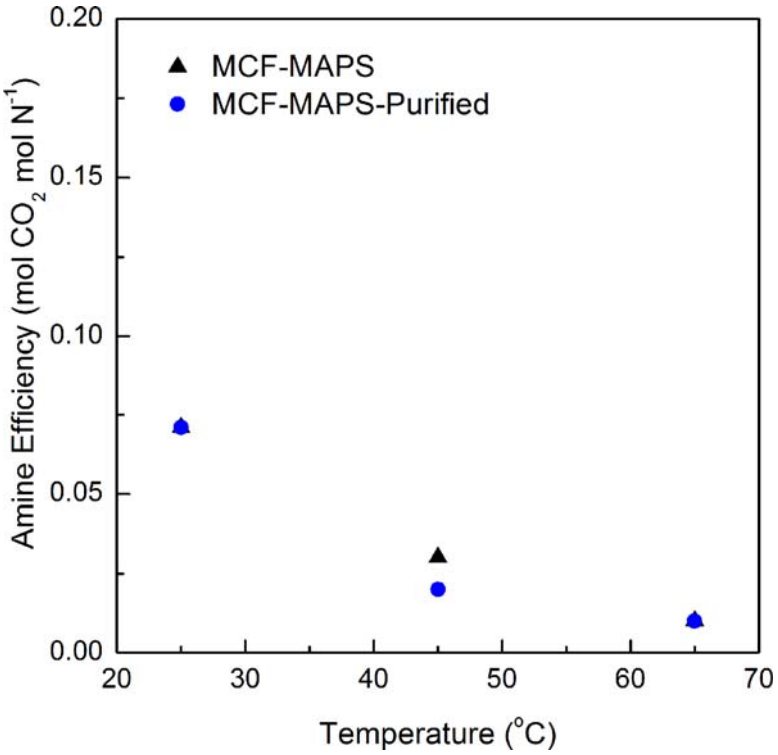

Figure B.1. Amine efficiency comparison of purified and as made MAPS functionalized silicas using 400 ppm CO_2 measured at 3 temperatures.

Appendix C

CARBON DIOXIDE KINETIC UPTAKE FOR PRIMARY AND SECONDARY AMINE MATERIALS

Kinetic rates for low pressure CO_2 adsorption are of interest for commercial processes. It can be seen in Figure C.1 that primary amines exhibit fast adsorption kinetics even at ultra-dilute CO_2 concentrations, indicating that capture processes can operate with relatively fast cycle times. From the inset of Figure C.1 it can be seen that the initial uptake rates are the same for both primary and secondary amine materials at varying temperatures. However, the length of time that the material remains at that initial rate is dependent on primary vs. secondary amines, and to a lesser degree, the adsorption temperature. A quick tailing out is observed for secondary amines while primary amines adsorb at a faster initial rate for a longer period of time.

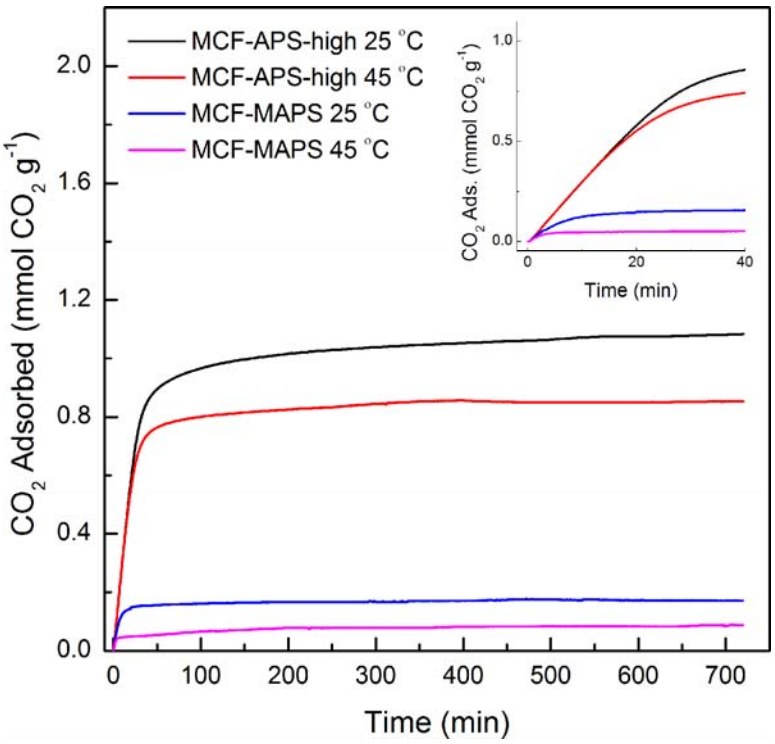

Figure C.1. CO_2 mass uptake for primary and secondary amines at 25 and 45 C at 400 ppm CO_2 adsorption conditions.

Appendix D

SURFACE AREA NORMALIZED WATER ADSORPTION ISOTHERMS FOR DIFFERENT AMINE TYPES

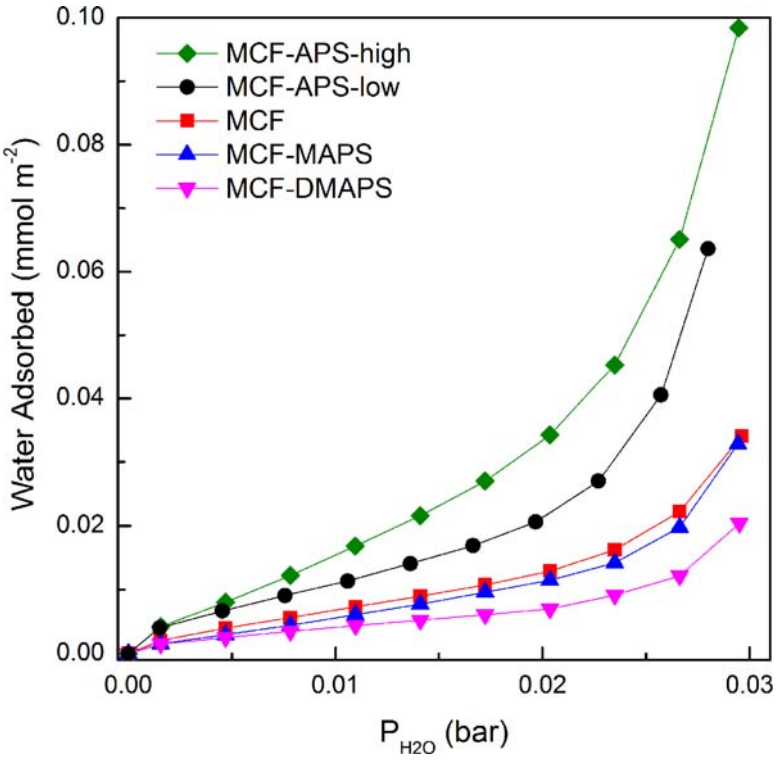

Figure D.1. Water adsorption isotherms at 25 °C for bare and amine functionalized silica normalized by surface area.

Appendix E

ADDITIONAL FTIR SPECTRA FOR SBA-APS-LOW AND SBA-APS-HIGH: ACTIVATED, PURE WATER ADSORPTION AND DESORPTION SPECTRA

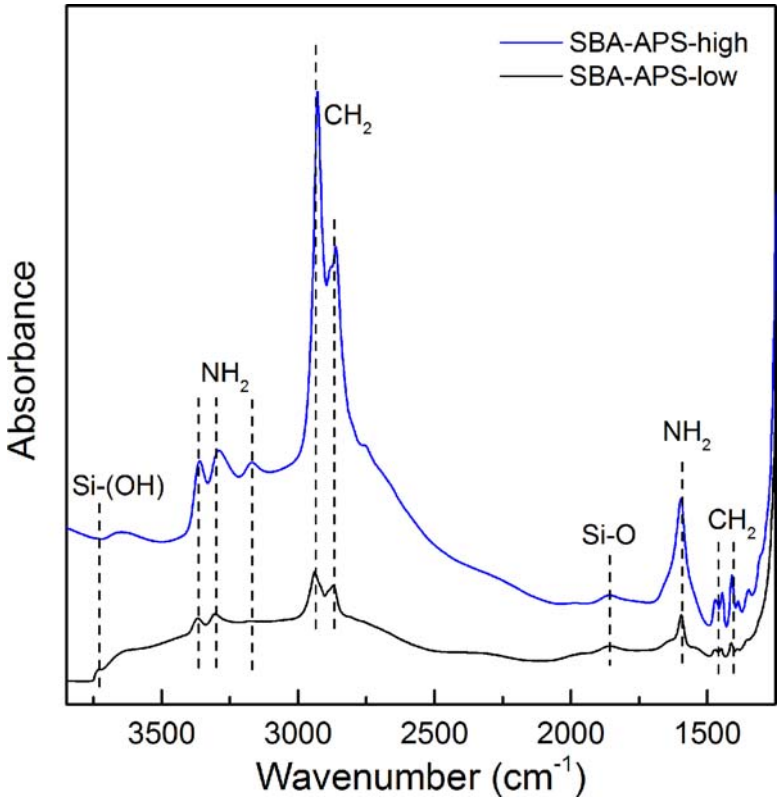

Figure E.1. FTIR spectra for SBA-APS-low and SBA-APS-high after activation by heating for 3 h at 110 °C under vacuum to remove pre-adsorbed CO_2 and water.

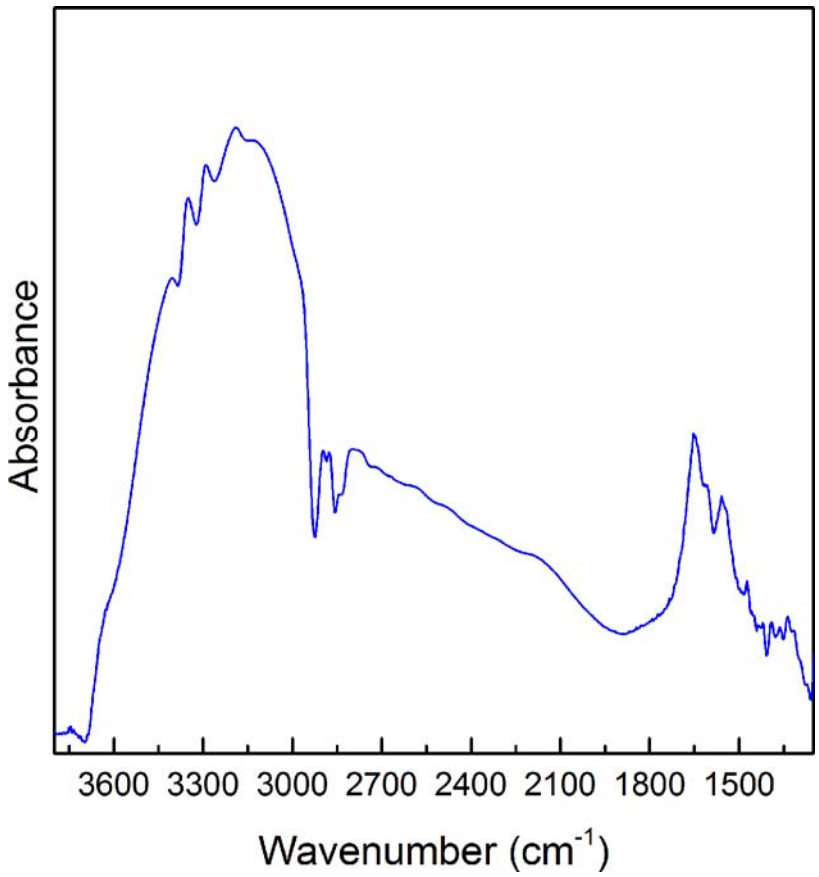

Figure E.2. FTIR spectrum of SBA-APS-high contacted with 5 mbar H_2O at room temperature before introduction of CO_2.

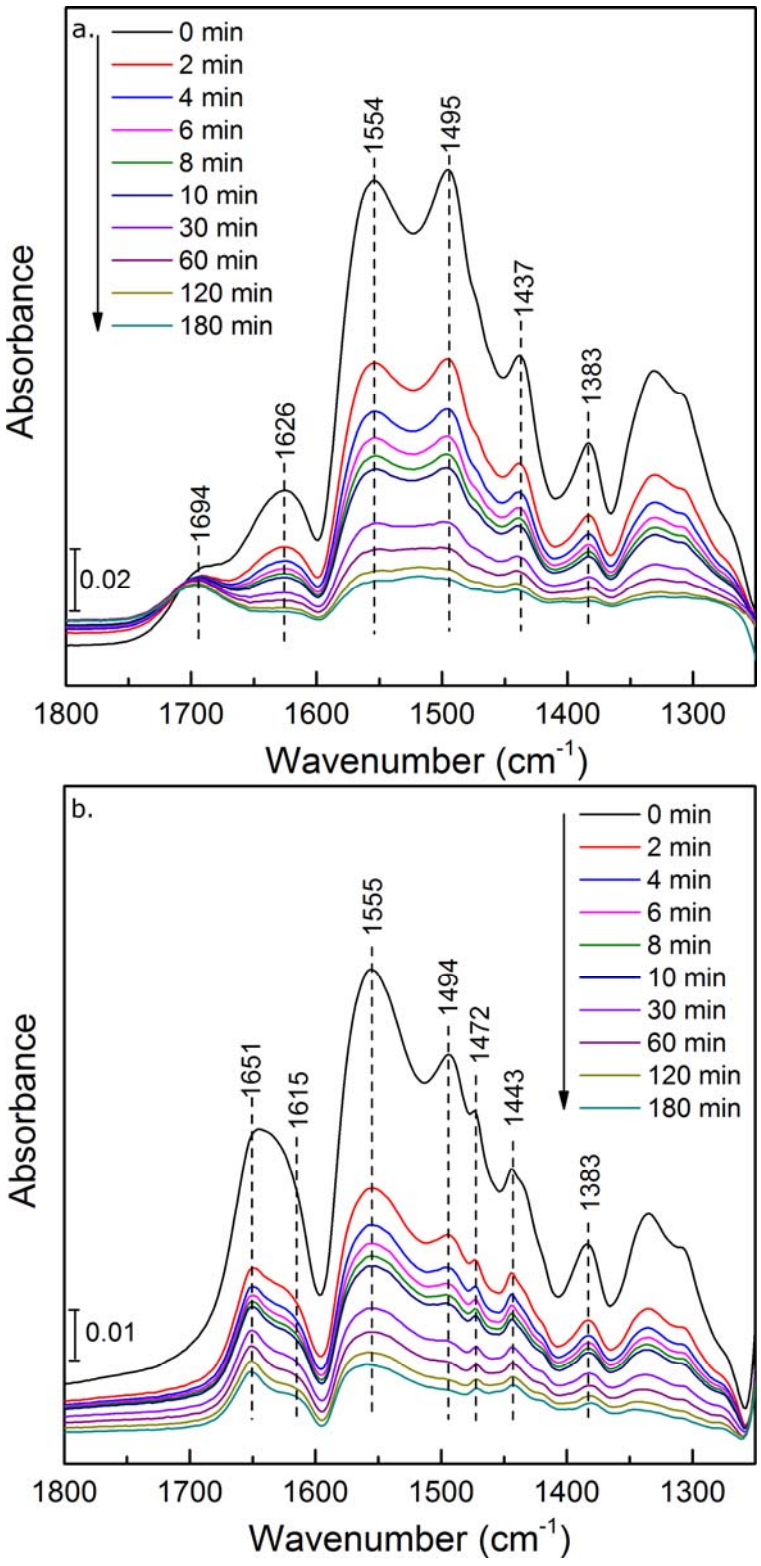

Figure E.3. *In-situ* FTIR difference spectra of SBA-APS-low as a function of vacuum time after exposure to (a) 10 mbar CO_2 and (b) at 1.5 mbar CO_2 and 5 mbar H_2O. Sample spectra were collected at room temperature.

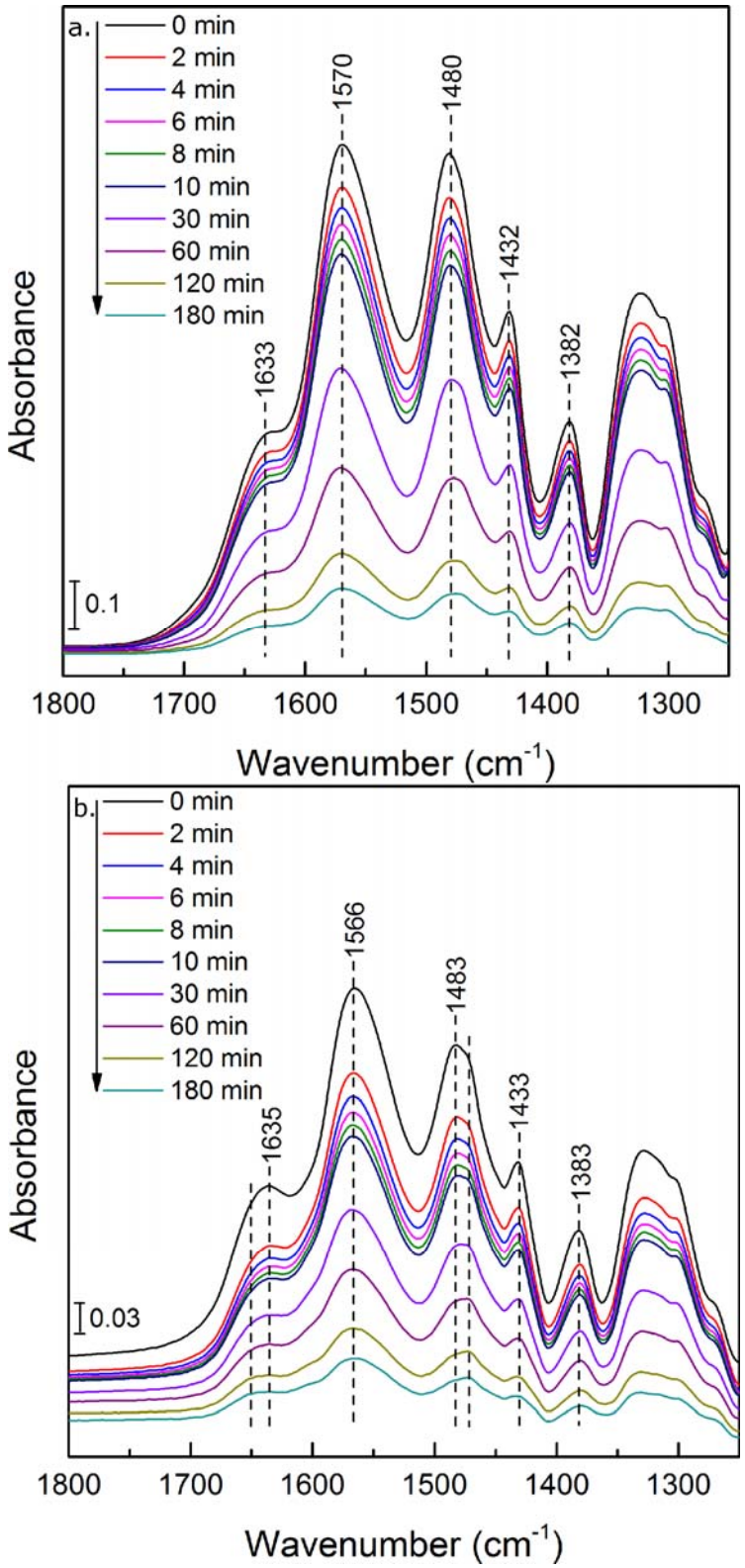

Figure E.4. *In-situ* FTIR difference spectra of SBA-APS-high as a function of vacuum time after exposure to (a) 10 mbar CO_2 and (b) at 1.5 mbar CO_2 and 5 mbar H_2O. Sample spectra were collected at room temperature.